Biotechnology Advances 57 (2022) 107948

Contents lists available at ScienceDirect

Biotechnology Advances

journal homepage: www.elsevier.com/locate/biotechadv

Research review paper

Nanoantibiotics to fight multidrug resistant infections by Gram-positive bacteria: hope or reality?

Francesca Berini *, Viviana Orlandi, Rosalba Gornati, Giovanni Bernardini, Flavia Marinelli

Department of Biotechnology and Life Sciences, University of Insubria, via JH Dunant 3, 21100 Varese, Italy

ARTICLE INFO

Keywords:
Glycopeptide antibiotics
Vancomycin
Teicoplanin
Daptomycin
Nanoparticles
Nanomaterials
Nanoantibiotics
Drug delivery
Antimicrobial activity
Biofilms

ABSTRACT

The spread of antimicrobial resistance in Gram-positive pathogens represents a threat to human health. To counteract the current lack of novel antibiotics, alternative antibacterial treatments have been increasingly investigated. This review covers the last decade's developments in using nanoparticles as carriers for the two classes of frontline antibiotics active on multidrug-resistant Gram-positive pathogens, i.e., glycopeptide antibiotics and daptomycin. Most of the reviewed papers deal with vancomycin nanoformulations, being teicoplanin- and daptomycin-carrying nanosystems much less investigated. Special attention is addressed to nanoantibiotics used for contrasting biofilm-associated infections. The status of the art related to nanoantibiotic toxicity is critically reviewed.

1. Introduction

Antimicrobial resistance (AMR) in pathogenic bacteria represents one of the greatest threats to human health, causing morbidity and mortality worldwide and determining an increasing economic burden for the healthcare systems (Cassini et al., 2019). The seriousness of the problem forced experts to state that we are currently on the edge of a 'post-antibiotic' era, in which common infections and small injuries may become once again lethal. A recent report estimated that infections by drug-resistant bacteria caused in 2019 the death of 1.27 million people (Antimicrobial Resistance Collaborators, 2022). If specific actions to address AMR are not urgently taken, this number is projected to increase to ten million by 2050, thus overcoming the deaths caused by road accidents, diabetes, or cancer (Cassini et al., 2019; *Interagency Coordination Group on Antimicrobial Resistance*, 2019).

AMR is a natural phenomenon by which bacteria have adapted to survive environmental threats. Common mechanisms of self-protection include: (i) the production of enzymes that modify and inactivate the antimicrobial molecules (as in the case of bacteria resistant to β-lactams thanks to β-lactamase production (Mora-Ochomogo and Lohans, 2021)), (ii) alterations of the cellular antibiotic target that prevent binding (as in pathogens resistant to glycopeptide antibiotics, which synthesize a modified resistant cell wall (Binda et al., 2014)), (iii) expression of multidrug efflux pumps against many different classes of antibiotics (for instance tigecycline or imipenem resistance in *Acinetobacter baumannii* (Breijyeh et al., 2020)), and (iv) reduction of cell permeability to

Abbreviations: AMR, Antimicrobial resistance; BSA, bovine serum albumin; CLSI, Clinical and Laboratory Standard Institute; D-Ala-D-Ala, D-alanine-D-alanine; DMBA, didodecyldimethylammonium bromide; MTT, 3-(4,5-dimethylthiazol-2-yl-2,5-diphenyltetrazolium bromide; FDA, Food and Drug Administration; FIC, fractional inhibiting concentration; GPA, glycopeptide antibiotic; LPDH, linear polymer-dendrimer hybrid; LDHN, lipid-dendrimer hybrid nanoparticle; LPHN, lipid-polymer hybrid nanoparticle; MSN, mesoporous silica nanoparticle; ZIF-8, metal-organic zeolitic imidazole framework-8; MRSA, methicillin-resistant *Staphylococcus aureus*; MSSA, methicillin-sensitive *Staphylococcus aureus*; MBEC, minimum biofilm eradication concentration; MBIC, minimum biofilm inhibitory concentration; MIC, minimum inhibitory concentration; MDR, multidrug resistant; NM, nanomaterial; NP, nanoparticle; NIR, near-infrared; DMPEI, N,N-dodecyl,methyl-poly-ethylenimine; PG, phosphatidylglycerol; PAMAM, 4-poly amidoamine; PCL, polycaprolactone; PEG, poly(ethylene glycol; PHVB, poly(3-hydroxybutyrate-co-3-6% hydroxyvalerate; PLGA, polylactic acid-co-glycolic acid; PMMA, polymethyl methacrylate; PVA, poly (vinyl alcohol); ROS, reactive oxygen species; SLN, solid lipid nanoparticle; VISA, vancomycin intermediate *Staphylococcus aureus*; VRE, vancomycin-resistant *Enterococcus faecium*; VRSA, vancomycin-resistant *Staphylococcus aureus*; VSE, vancomycin sensitive enterococci; VSSA, vancomycin sensitive *Staphylococcus aureus*; WHO, World Health Organization.

* Corresponding author.
E-mail addresses: f.berini@uninsubria.it (F. Berini), viviana.orlandi@uninsubria.it (V. Orlandi), rosalba.gornati@uninsubria.it (R. Gornati), giovanni.bernardini@uninsubria.it (G. Bernardini), flavia.marinelli@uninsubria.it (F. Marinelli).

https://doi.org/10.1016/j.biotechadv.2022.107948
Received 30 September 2021; Received in revised form 15 March 2022; Accepted 17 March 2022
Available online 23 March 2022

preclude antibiotics reaching their target (particularly in Gram-negatives as *A. baumannii* and *Pseudomonas aeruginosa* due to down-regulation or elimination of transmembrane porins (Breijyeh et al., 2020)).

The current alarming level of AMR is, however, mainly the result of human behaviour. The misuse and/or overuse of antimicrobials for human pathologies, as well as for growth promotion in farms and aquaculture, have triggered and accelerated the transmission via horizontal transfer of resistance-conferring genes (Siriam et al., 2021). Global antibiotic consumption has increased by 65 % between 2000 and 2015 in both low- and middle-income countries (Klein et al., 2018). Following the adoption of the Global Action Plan on Antimicrobial Resistance in 2015 (World Health Organization, 2015), posing boundaries to antibiotic indiscriminate use, a reduction in total antibiotic consumption has been registered in a few countries (Robertson et al., 2021), but still increasing levels of resistance are being reported globally, being particularly alarming for immunocompromised and/or hospitalized patients (Cassini et al., 2019). Particularly in the elder population, the frequent use of indwelling urinary catheters, cardiac valves, and protheses facilitates the colonization of pathogens forming antibiotic-resistant biofilms, which are actually considered the cause of 65-to-80 % of hospital-acquired infections (Bowler et al., 2020). Sessile bacterial cells residing in biofilms are from 10- to 1000-times less susceptible to antimicrobial treatments than their free-floating planktonic counterparts (Bowler et al., 2020). In addition, among these cells living in close proximity, horizontal transmission of resistance genes is reported to be 700-times more efficient than among planktonic bacterial cells (Flemming et al., 2016), significantly contributing to AMR spread. Finally, the recent health crisis caused by SARS-CoV-2 has worsen this scenario, promoting a further increase in antibiotic consumption: a recent report estimated that 71 % of Covid-19 patients received at least one dose of a broad-spectrum antibiotic, despite the occurrence of bacterial co-infections was only 3.6 % (Nori et al., 2021).

As a consequence of AMR spread, we are assisting at an increasing medical need for novel antimicrobials active either versus Gram-negative bacteria, which are more impermeable to the commonly used drugs (Breijyeh et al., 2020; May and Grabowicz, 2018), or towards multidrug-resistant (MDR) Gram-positive pathogens. These last have become resistant to different classes of traditionally used antibiotics. World Health Organization (WHO) has recently included the Gram-positive vancomycin-resistant *Enterococcus faecium* (VRE) and the methicillin- and vancomycin-resistant *Staphylococcus aureus* (MRSA and VRSA, respectively) in the list of the twelve priority pathogens for which new antimicrobial treatments are urgently needed (Tacconelli et al., 2018). Provoked by an excessive use of β-lactam antibiotics in the past decades, the incidence of MRSA strains is now worryingly high, representing on average the 20 % of all *S. aureus* clinical isolates in WHO member states, with values reaching 80 % in some countries. Even worse, the isolation frequency of *S. aureus* strains resistant to last-resort antibiotics (macrolides, carbapenem, lincosamides, type-B streptogramins, and vancomycin), is increasing (European Centre for Disease Prevention and Control, 2017). In addition, antibiotic resistant biofilms formed by *S. aureus* are the most common causes of device-related infections in hospital settings (Craft et al., 2019). A similar cause of concern is the raising diffusion of VRE strains (Miller et al., 2016a) and their concomitant co-resistance to other antibiotics. First identified in North America during the late 1980s, VRE strains currently represent ca. 15 % of all *E. faecium* strains isolated in Europe (European Centre for Disease Prevention and Control, 2017) and ca. the 30 % in the US (Center for Disease Control and Prevention (CDC), 2019). Intrinsically resistant to β-lactams, macrolides, and sulphonamides, different *E. faecium* strains, including VRE, have more recently acquired resistance to other antibiotics as aminoglycosides, daptomycin, linezolid, and tigecycline (European Centre for Disease Prevention and Control, 2017). Other widespread infections caused by MDR Gram-positive pathogens are those determined by β-lactams-, macrolide-, or lincosamide-resistant streptococci (Alves-Barroco et al., 2020), or by methicillin- and linezolid-resistant *Staphylococcus epidermidis* and *Staphylococcus haemolyticus*. These last two are the most common etiological agents of nosocomial blood infections, often originated from staphylococcal biofilm colonization of indwelling medical devices (Kranjec et al., 2021). Finally, an increasingly common Gram-positive pathogen is *Clostridioides difficile*, which causes gastrointestinal hospital-acquired infections, affecting thousands of people each year, especially those with unbalanced microbiota due to previous antibiotic treatments (Mada and Alam, 2021).

Unfortunately, the urge for novel antibiotics to treat infections caused by resistant pathogens is not mirrored by the limited number of molecules that are currently populating drug development pipeline. In the last decades, many large pharmaceutical companies have abandoned the antibiotic business due to the increasing difficulties in finding new molecules, the demanding regulatory challenges imposed by governmental agencies (i.e., the US Food and Drug Administration FDA, or the European Medicines Agency EMA), and the limited economic returns (Renwick and Mossialos, 2018). Developing a novel antibiotic requires on average ten years and huge investments, which are not always compensated by the revenue obtained after the drug introduction onto the market (Safir et al., 2020). Indeed, between 2010 and 2021, only 17 novel antibiotics were approved worldwide (Chahine et al., 2021). The majority of them were mere modifications or variations of already existing drugs. It is necessary to go back to 2004 for the last approval of a completely new chemical class of natural products active on Gram-positive pathogens, i.e., lipopeptides (daptomycin, Fig. 1). In the last decade, three novel semisynthetic members of the last resort glycopeptide antibiotic class, active towards MDR Gram-positives (the vancomycin-related molecules dalbavancin, telavancin, and oritavancin, Fig. 1), were also approved for clinical use.

To counteract the current lack of novel antibiotics and/or to better use those already available, renewed interest has been focussed on alternative antibacterial treatments, including vaccines (Troisi et al., 2020), antibacterial antibodies (Zurawski and McLendon, 2020), antimicrobial peptides (Pfalzgraff et al., 2018), faecal microbiota transplantation (Rao and Young, 2015), and combined therapies (González-Bello, 2017). Antibiotic adjuvants can be co-administered with antibiotics with different purposes, i.e., to synergistically enhance their action, as in the case of essential oils (Aljaafari et al., 2021), or to inhibit the main resistance mechanisms adopted by bacteria. In this latter case, adjuvants can, for instance, increase the antibiotic uptake through the bacterial membrane, block efflux pumps, or inhibit enzymes that would otherwise inactivate the antibiotic (Vrancianu et al., 2020). Interest has been (re)allocated also to metal-based antimicrobials, whose efficacy has been demonstrated towards both planktonic and biofilm-forming bacterial cells, including antibiotic-insensitive persister cells. Hence, Ag and Cu ions are incorporated in a number of medical devices, as wound dressing, catheter coatings, respiratory face masks, and medical garments (Turner, 2017). Other alternative approaches are species-specific bacteriophages (Domingo-Calap and Delgado-Martínez, 2018), or inducing photooxidative stress and formation of reactive oxygen species (ROS) by photodynamic therapy (Cieplik et al., 2018), or, last but not least, using inorganic or organic nanoparticles, as active therapeutic agent *per se* or as carriers for frontline antibiotics (Gupta et al., 2019; Mba and Nweze, 2021).

Due to the rapid advances of nanotechnology in medical applications, the recent literature offers a flourishing of methods to prepare nanosystems and to use them to counteract microbial infections. This review covers the last decade developments in using nanoparticles to contrast AMR arising among Gram-positive pathogens. We first briefly describe the two classes of frontline antibiotics active on MDR Gram-positive pathogens, i.e., the glycopeptide antibiotics (GPAs) and daptomycin. Then, we continue depicting the wide diversity of nanosystems available and how they are used as antimicrobial agents *per se* or as carriers for GPAs and daptomycin. We describe the different features of

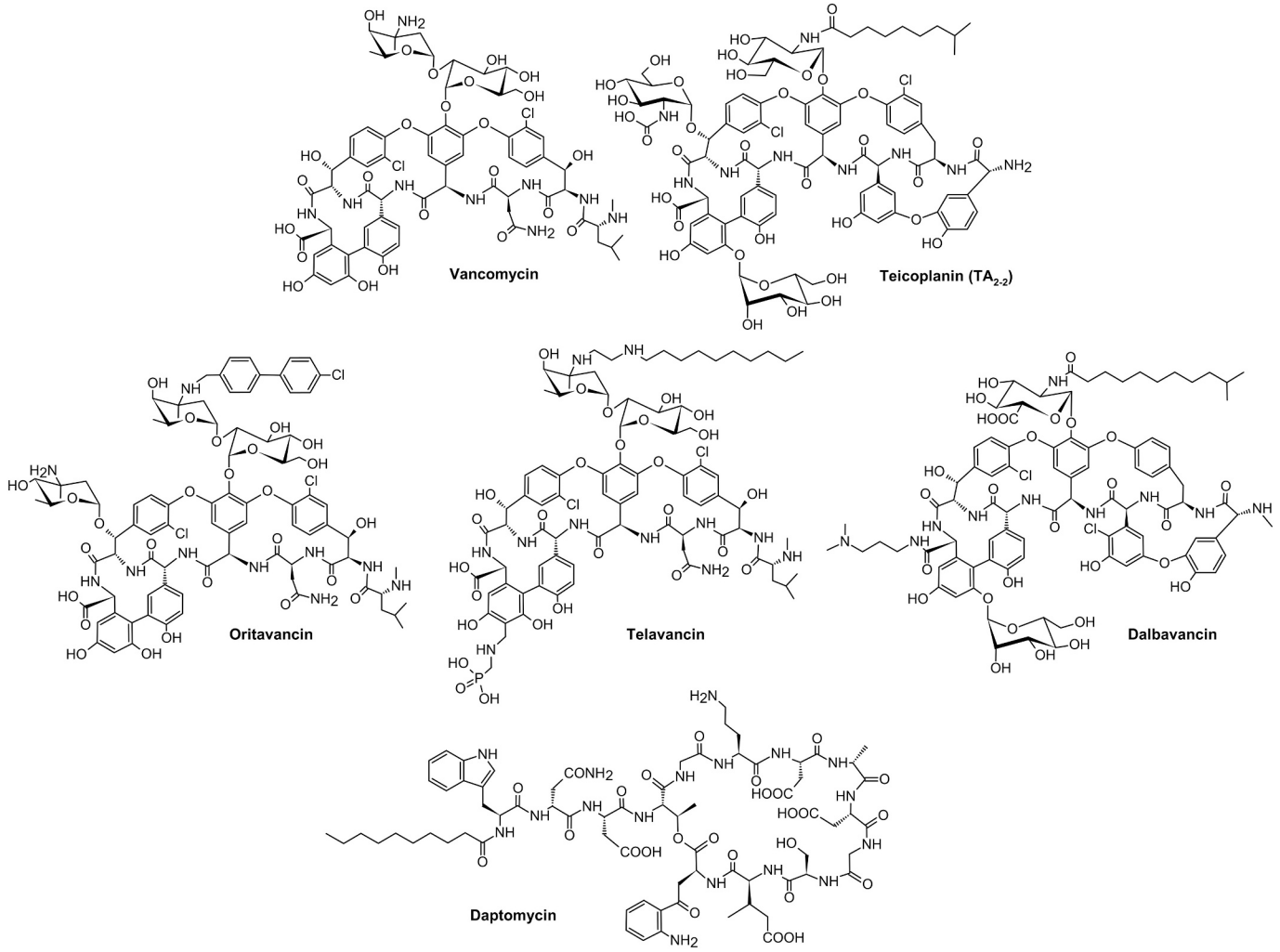

Fig. 1. Structures of first-generation (vancomycin and teicoplanin) and second-generation (oritavancin, telavancin, and dalbavancin) glycopeptide antibiotics, and of the lipopeptide antibiotic daptomycin. Clinically-used teicoplanin is a mixture of at least five GPA molecules differing in length and branching of the fatty acid tail: the figure includes the main component, named TA_{2-2}, bearing an 8-methylnonanoic (iso-C10:0) acid.

the known antibiotic-conjugated nanosystems and analyse their antimicrobial activities. Special attention is given to their use in contrasting biofilm formation. Lastly, the status of the art related to their cytotoxicity *in vivo* and *in vitro* is critically reviewed, highlighting the need for adequate animal models to understand the real potential of nanoantibiotics for clinical developments. To the best of our knowledge, all the relevant information on the last decade's use of nanosystems involving daptomycin and GPAs is reported in Tables 1, 2, and 3, which might represent useful tools for comparing different systems and their peculiar properties.

2. Glycopeptide antibiotics and daptomycin

WHO included the lipopeptide daptomycin and the GPA vancomycin and related molecules in the list of the Critically Important Antimicrobials for human medicine, i.e., among those antimicrobials that represent the sole, or one of the few, available therapies to treat serious bacterial infections and that, consequently, should be used judiciously to avoid the upsurge of AMR (World Health Organization, 2019a). Vancomycin is also part of the 'Watch' group of WHO Essential Medicine List (World Health Organization, 2019b) that includes antibiotics with a high risk of selection of bacterial resistance, thus requiring priority stewardship programs and monitoring, and whose use should be limited to few specific infectious syndromes.

Nowadays, the approved GPAs for clinical use are the first-generation vancomycin and teicoplanin (Fig. 1), and their second-generation semi-synthetic derivatives telavancin, dalbavancin, and oritavancin (Fig. 1) (Marcone et al., 2018). They are used for treating severe or MDR infections caused by staphylococci, enterococci, streptococci, and, more rarely, pneumococci, representing the frontline therapy especially for MRSA (Marcone et al., 2018). Moreover, vancomycin is increasingly used by oral administration for the treatment of *C. difficile* hospital-acquired infections. While vancomycin was introduced in clinics in 1958, and teicoplanin in 1988 and 1998 in Europe and in Japan respectively, second-generation GPAs, showing an increased antimicrobial potency and superior pharmacokinetics (Butler et al., 2014; Van Bambeke, 2015), have been approved more recently (from 2009 to 2015). From a structural point of view, GPAs are characterized by a cross-linked nonribosomal heptapeptide scaffold, formed by proteinogenic (Tyr, Leu, Asn, Ala, Glu) and nonproteinogenic amino acids (4-hydroxyphenylglycine, 3,5-dihydroxyphenylglycine, β-hydroxytyrosine), amply tailored with sugar moieties, chlorine atoms, methyl groups, and, in the case of teicoplanin and second-generation GPAs, with a hydrophobic chain (Fig. 1) (Yim et al., 2014; Yushchuk et al., 2020a). Their antimicrobial activity relies on inhibiting the last steps of cell wall synthesis in Gram-positive bacteria, by binding to the D-alanine-D-alanine (D-Ala-D-Ala) terminus of the peptidoglycan precursor lipid II, thus interfering with the action of transglycosidases and

Table 1
List of papers describing nanoformulations of vancomycin (according to the references' alphabetical order). The list was created by searching Pubmed database (accession on 11th May 2021) with the following query: (((glycopeptide) AND (antibiotic)) AND (nanoparticles)) AND (("2011/01/01"[Date - Publication] : "3000"[Date - Publication])). The results were manually checked to select only those publications actually describing the use of NPs as vancomycin carriers for antibacterial purposes. When available, data on the characterization of the nanoformulations, as well as names used by the authors for describing the nanosystems, are included. For 'Dimension': § diameter estimated by transmission electron microscopy or scanning electron microscopy; ¥ hydrodynamic diameter estimated by dynamic light scattering. For 'Targeted bacteria': ₸ bacterium inhibited by the nanosystem also in intracellular infection models. For 'Relative activity compared to free vancomycin': when nanoformulations showed higher (>), lower (<), or similar (=) antimicrobial activity in comparison to bare vancomycin, the corresponding sign is represented. For 'Antibiofilm activity': presence of absence of antibiofilm activity are indicated with the plus or minus signs, respectively.

Reference	Characteristics of the nanoantibiotic: type, dimension, shape	Antibiotic release	Antimicrobial activity				Toxicity assessment (type of assay, used cell lines)
			In vitro			*In vivo*	
			Targeted bacteria	Relative activity compared to free vancomycin (<, =, >)	Antibiofilm activity (+/-)		
Almeida Neto et al., 2019	Vancomycin loaded on nanocomposites formed by PHBV, nanodiamonds, and nanoHA. Thin film (obtained by rotary evaporator), or microspheres of 5 ± 3 μm diameter (by spray-drier)	Slight burst AR in 24 h (1.9-3.2 %), then gradual AR up to 4.8-7.1 % at day 22	MSSA	na	na	na	Non-cytotoxic and non-cytostatic (nitric oxide production, RAW 264.7 murine macrophages)
Aşik et al., 2019	Vancomycin loaded on alginate-chitosan NPs, dispersed in a vancomycin-supplemented alginate gel used for covering a polymethylmethacrylate bone cement. ~100 nm§, spherical shape	Burst AR in 24 h (43 %), then gradual AR up to 21 days	MSSA	na	na	na	>80 % cell viability (MTT assay, murine 3T3L1 hepatocyte cells)
Auñón et al., 2020	Vancomycin co-loaded with gentamicin on NTs made of fluorine- and phosphorus-doped Ti–6Al–4V alloy (bNT Ti–6Al–4V GV). Bottle-shaped	10.66 % AR in 230 min	MRSA	na	+ (MRSA)	Prevention of MRSA infection in rabbits	na
Babaei et al., 2019	Vancomycin loaded on poly (sodium 4-styrene sulfonate)-modified HA NPs, dispersed in a zein-based scaffold. <100 nm§	Burst AR in 24 h (~18-46 %, depending on HA concentration), then gradual AR up to 2 weeks	na	na	na	na	>90 % cell viability (MTT assay, MG-63 human osteosarcoma cells)
Booysen et al., 2019	Vancomycin encapsulated in PLGA NPs. 247 nm¥, spherical shape	Slight burst AR in 144 h (30 %), then gradual AR up 50 % at day 10	MSSA, MRSA	>	na	na	na
Bose et al., 2020	Vancomycin loaded on LPHNs. 150-300 nm¥ (depending on the lipid used), spherical shape	Gradual AR up to 120 h from both cationic or zwitterionic lipid layered LPHNs	MRSA	>	na	na	>70 % cell viability (CCK-8 assay, J774.1 murine macrophages). Higher viability with zwitterionic LPHNs than with cationic LPHNs >70 % cell viability (MTT assay, human retinal pigment epithelial RPE cells). No irritating effect (hen egg chlorioallantonic membrane). No toxicity *in vivo*: after injection in rat eyes, no impairments in retinal functionality, no damage on photoreceptors, neuroretina, retinal pigment epithelium and chloroid
Cardoso et al., 2021	Vancomycin loaded on DMPEI NPs coated with hyaluronic acid (VCM-DMPEI nanoparticles/HA). 154 ± 3 nm¥	Gradual AR up to 58 % at 96 h	*Staphylococcus aureus*	=	na	na	
Cerchiara et al., 2015	Vancomycin loaded on chitosan MPs and NPs. ~190-450 nm¥ (NPs), ~1100-1500 nm¥ (MPs), spherical shape	Higher AR from MPs than from NPs (~30-76 % in 6 h from MPs, ~1-35 % from NPs)	MSSA	=	na	na	na
Cerchiara et al., 2017	Vancomycin loaded on chitosan NPs, used to impregnate Spanish broom fibres.	Gradual AR up to 30 % at 360 min	MSSA	>	na	na	

(*continued on next page*)

Table 1 (*continued*)

Reference	Characteristics of the nanoantibiotic: type, dimension, shape	Antibiotic release	Antimicrobial activity				Toxicity assessment (type of assay, used cell lines)
			In vitro			*In vivo*	
			Targeted bacteria	Relative activity compared to free vancomycin (<, =, >)	Antibiofilm activity (+/-)		
	~240-450 nm[¥] (depending on chitosan concentration)						~100 % cell viability (MTT assay, HaCaT human dermal keratinocytes cells)
Chakraborty et al., 2011a	Vancomycin loaded on folic acid-tagged chitosan NPs. 260 ± 35 nm[¥], spherical shape	na	na	na	na	Reduction of VSSA and VISA infection in mice	na
Chakraborty et al., 2011b	Vancomycin loaded on folic acid-tagged chitosan NPs. 260 ± 35 nm[¥], spherical shape	na	na	na	na	Reduction of VSSA and VISA infection in mice	na
Chakraborty et al., 2012a	Vancomycin loaded on folic acid-tagged chitosan NPs. 260 ± 35 nm[¥], spherical shape	Gradual AR up to ~100 % at 480 min	VSSA, VRSA	>	+ (VSSA, VRSA)	na	na
Chakraborty et al., 2012b	Vancomycin loaded on folic acid-tagged chitosan NPs. 260 ± 35 nm[¥], spherical shape	na	na	na	na	Reduction of VSSA and VISA infection in mice	na
Chen et al., 2015	Vancomycin co-conjugated by covalent bond with UBI_{29-41} (an antibacterial peptide fragment) and the photosensitizer MPA on BSA-stabilized ZnO QD (Van@ZnO-PEP-MPA). 18 ± 8 nm[§], 104 ± 10 nm[¥], spherical shape (data relative to ZnO@BSA-PEP-MPA)	na	MSSA, *Bacillus subtilis*	>	na	Reduction of MSSA infection in murine model for skin infection	na
Chen et al., 2019	Vancomycin co-loaded with NH_2-PEG and $AgNO_3$/dopamine on ZIF-8-polyacrylic acid, containing the photosensitizer ammonium methylbenzene blue (ZIF-8-PAA-MB@AgNPs@Van-PEG). ~150 nm[§]	na	MSSA, MRSA, *Escherichia coli*	na	+ (MSSA, MRSA, *E. coli*)	Reduction of MSSA and MRSA infection in rabbit model for endophthalmitis	>95 % cell viability under dark conditions, >80 % cell viability upon NIR irradiation (CCK-8 assay, human retinal pigment epithelial RPE cells and human corneal epithelial HCECs cells) Non-irritating when injected in rabbit eyes
Chiang et al., 2015	Vancomycin co-encapsulated with polypyrrole NPs in PLGA hollow microspheres. 361 ± 19.7 μm, spherical shape	AR upon NIR irradiation up to ~70 % in 15 min	MRSA	=	na	Reduction of MRSA infection in mice with subcutaneous abscesses	na
Chowdhuri et al., 2017	Vancomycin co-loaded with folic acid on ZIF-8 (ZIF-8@FA@VAN). 75 ± 10 nm[§], 170-190 nm[¥], spherical shape	Burst AR in 10 h (~35 % at pH 7.4, ~65 % at pH 5.5), then gradual AR up to ~85 % (pH 7.4) or ~100 % (pH 5.5) at 72 h	MRSA	>	na	na	na
Cong et al., 2015	Vancomycin encapsulated in PLGA-PEG-alendronate micelles. 43 nm[§], 55.08 nm[¥], spherical shape	Burst AR in 10 h, then gradual AR up to 87-90 % (pH 5.0) or 71-73 % (pH 7.4) at 72 h	MSSA	<	na	na	>80 % cell viability (MTT assay, rat bone marrow stromal rBMSCs cells and human embryonic hepatocytes L02 cells)
Croes et al., 2018	Vancomycin (or AgNPs) loaded on Ti implants functionalized with chitosan-based coatings.	na	*Staphylococcus aureus*	na	+ (*S. aureus*)	Reduction of *S. aureus* infection in rat model for osteomyelitis	na
Efiana et al., 2019	Vancomycin incorporated in papain-palmitate-modified self-emulsifying drug delivery systems (Van-SBS-SEDDS). 200-250 nm[¥]	na	na	na	na	na	>98 % cell viability (resazurine assay, human colon cancer CaCo-2 cells)

(*continued on next page*)

Table 1 (*continued*)

Reference	Characteristics of the nanoantibiotic: type, dimension, shape	Antibiotic release	Antimicrobial activity				Toxicity assessment (type of assay, used cell lines)
			In vitro			*In vivo*	
			Targeted bacteria	Relative activity compared to free vancomycin (<, =, >)	Antibiofilm activity (+/-)		
Esmaeili and Ghobadianpour, 2016	Vancomycin conjugated to $MnFe_2O_4$ NPs, modified with chitosan crosslinked by glutaraldehyde and with PEG (Vanco-PEG-Ch-$MnFe_2O_4$ NPs). 25 nm[§], spherical shape	Burst AR in the first hours, then gradual AR up to ~36-53 % at 48 h (depending on the polymer: drug ratio)	MRSA, *Staphylococcus epidermidis, Bacillus subtilis, Escherichia coli, Pseudomonas aeruginosa*	>	na	na	na
Fulaz et al., 2020	Vancomycin loaded on MSNs with different functionalization (bare, amine, carboxyl, aromatic). ~30-37 nm[§], ~152-232 nm[¥], spherical shape	na	MSSA, MRSA	na	+ (MSSA, MRSA)	na	na
George et al., 2017	Vancomycin encapsulated in PLC NPs coated with polyelectrolyte-Vitamin C, embedded in PVA-alginate gel (D-PCL-PVc-PVA(Alg)). 35.93 ± 3 nm[§], 47.46 ± 2.5 nm[¥], spherical shape	Gradual AR up to ~50 % at 168 h	*Staphylococcus aureus*	>	na	na	>90 % cell viability (MTT assay on murine fibroblast L929 cells)
Gonzalez Gomez et al., 2019	Vancomycin encapsulated in NLs. 100-200 nm[¥]	na	MSSA	=	na	na	na
Gounani et al., 2019	Vancomycin co-loaded with polymyxin B on bare or carboxyl-modified MSNs. 72.4 ± 8.2 nm[§], ~119-128 nm[¥], spherical shape (data relative to unloaded NPs)	Burst AR in 24 h (~50 %), then gradual AR up to 72 h	MSSA, *Escherichia coli, Pseudomonas aeruginosa*	>	+ (MSSA, *P. aeruginosa*)	na	>80 % cell viability (MTT assay, human hepatoma cancer HepG2 cells, human foreskin Hff-1 fibroblasts, human embryonic kidney HEK293 cells). No haemolytic activity (human blood)
Gu et al., 2016	Vancomycin loaded on MSNs and calcium sulfate composites (Van-MSN-$CaSO_4$). 150 nm[§], spherical shape	Burst AR in 24 h (~60 %), then gradual AR up to ~83-89 % at day 10	na	na	na	na	No inhibitory effect on cell proliferation (CCK-8 assay, murine osteoblastic MC3T3-E1 cells) . No toxicity (haematological index study on New Zealand rabbits)
Guo et al., 2020	Vancomycin-conjugated oleic acid loaded on polypyrrole NPs (Van-OA@PPy). 50 nm[§], ~90 nm[¥]	na	MRSA	na	na	Reduction of MRSA infection in mice with subcutaneous abscesses	>90 % cell viability (by MTT assay, RAW 264.7 murine macrophages). No haemolytic activity (murine blood). No changes in haematological data and blood biochemicals detected in mice
Han et al., 2015	Vancomycin conjugated to oxidized sodium alginate, co-loaded with chitosan-coated BSA NPs carrying dexamethasone, on poly-dopamine layer. 262.7 ± 0.7 nm[¥], spherical shape (data relative to chitosan-coated BSA NPs)	Burst AR in 3 days (~50 %), then gradual AR up to ~95 % at day 28	*Staphylococcus epidermidis*	=	na	na	na
Han et al., 2017	Vancomycin conjugated to oxidized sodium alginate, co-loaded with chitosan-coated BSA NPs on Ti scaffolds. Structures in the micro/nano range	Gradual AR up to ~70 % at day 20	*Staphylococcus epidermidis*	>	na	na	na
Harris et al., 2017	Vancomycin co-loaded with Fe_3O_4 NPs on chitosan microbeads cross-linked with varying lengths of PEG dimethacrylate. 210 ± 40 μm[§], spherical shape	Burst AR in 2-3 days, then gradual AR up to day 8; possibility to modulate the release with different stimuli	na	na	na	na	No significant toxicity (CellTiter-Glo assay and microscope analysis, murine NIH3T3 fibroblast cells)

(*continued on next page*)

Table 1 (*continued*)

Reference	Characteristics of the nanoantibiotic: type, dimension, shape	Antibiotic release	Antimicrobial activity				Toxicity assessment (type of assay, used cell lines)
			In vitro			*In vivo*	
			Targeted bacteria	Relative activity compared to free vancomycin (<, =, >)	Antibiofilm activity (+/-)		
Hassan et al., 2017	Vancomycin conjugated by covalent bond to magnetic NPs coated by human serum albumin	na	MSSA, MRSA, VRSA, VanA- and VanB-type VRE	>	na	na	na
Hassan et al., 2020	Vancomycin loaded on chitosan-based lipid-polymer hybrid nanovesicle (VM-OLA-LPHVs1). 198 ± 14 nm[¥] at pH 7.4, 207 ± 6.69 nm[¥] at pH 6.0	Burst AR in 8 h (~73 % at pH 6.0, ~45 % at pH 7.4), then gradual AR up 97 % (pH 6.0), or 73 % (pH 7.4) at 72 h	MSSA, MRSA	>	+ (MRSA)	Reduction of MRSA infection in murine model for skin infection	>75 % cell viability (MTT assay, human hepatoma cancer HepG2 cells, human embryonic kidney HEK 293 cells, human adenocarcinoma alveolar basal epithelial A-549 cells, and human breast cancer MCF-7 cells)
Hassani Besheli et al., 2017	Vancomycin loaded on silk fibroin NPs, then entrapped in silk scaffolds. 80-90 nm[¥], spherical shape	Gradual AR with speed depending on loaded vancomycin concentration; overall slower release at pH 4.5 than 7.4	MRSA	<	na	Reduction of MRSA infection in rat model for osteomyelitis	>80 % cell viability (MTT assay, rabbit osteoblast cells)
Hernandez et al., 2014	Vancomycin loaded on mesoporous nanocapsules functionalized with an oligonucleotide probe for *S. aureus* recognition. 182.8 ± 2.3 nm[§]	Gradual AR only by specific actuation	*Staphylococcus aureus*	>	na	na	na
Hur and Park, 2016	Vancomycin conjugated to AuNPs and AgNPs. 11.01 ± 3.62 nm[§] (AuNPs), 12.08 ± 2.13 nm[§] (AgNPs), spherical shape	na	MSSA, MRSA	>	na	na	na
Kalhapure et al., 2014	Vancomycin incorporated on SLNs. 95-100 nm[§], ~100-108 nm[¥], spherical shape	Gradual AR with different speed depending on SLN composition	MSSA, MRSA	<	na	na	na
Kalhapure et al., 2017a	Vancomycin loaded on chitosan NPs, with or without anionic gemini surfactant. ~55-90 nm[§], ~202-220 nm[¥], spherical shape	Gradual AR, higher at pH 6.5 than at pH 7.4	MSSA, MRSA	<	na	Reduction of MRSA infection in murine model for skin infection	na
Kalhapure et al., 2017b	Vancomycin loaded on SLNs. 132.9 ± 9.1 nm[¥], spherical shape	Gradual AR, faster at pH 6.5 (100 % in 4 h) than at pH 7.4 (100 % in 24 h)	MSSA, MRSA	= (MSSA, pH 6.5); < (MSSA, pH 7.4; MRSA, pH 6.5 and 7.4)	na	Reduction of MRSA infection in murine model for skin infection	>75 % cell viability (MTT assay, human breast cancer MCF-7 cells, human hepatoma cancer HepG2 cells, human adenocarcinoma alveolar basal epithelial A-549 cells)
Karakeçili et al., 2019	Vancomycin loaded on ZIF-8 nanocrystals (ZIF8/VAN), then loaded onto chitosan scaffolds. 60 ± 20 nm[§], rhombic dodecahedral morphology (data relative to ZIF8/VAN)	Gradual AR from ZIF8/VAN, higher at pH 5.4 than at pH 7.4 (~70 % vs ~55 % at 24 h); gradual AR from chitosan scaffold (~45 % at pH 5.4, ~30 % at pH 7.4, at 144 h)	MSSA	na	na	na	Non-toxic effect on cell proliferation (Presto-blue assay, alkaline phosphatase activity, and Alizarin red staining; murine preosteoblast MC3T3 cells)
Kaur et al., 2019	Vancomycin conjugated to citrate-capped AgNPs (Van@AgNPs). 25 ± 5 nm[§], ~86-91 nm[¥], spherical shape	na	*Staphylococcus aureus, Escherichia coli*	>	na	na	na
Kavruk et al., 2015	Vancomycin encapsulated in aptamer-gated MSNs. 177.5 ± 2.3 nm[§]	Upon aptamer-ligand interaction, burst AR in 5 h, then gradual AR up to 24 h	*Staphylococcus aureus*	>	na	na	na
Kimna et al., 2019					na	na	

(*continued on next page*)

Table 1 (*continued*)

Reference	Characteristics of the nanoantibiotic: type, dimension, shape	Antibiotic release	Antimicrobial activity				Toxicity assessment (type of assay, used cell lines)
			In vitro			*In vivo*	
			Targeted bacteria	Relative activity compared to free vancomycin (<, =, >)	Antibiofilm activity (+/-)		
	Vancomycin loaded on chitosan/montmorillonite nanocomposites. ~210-350 nm[¥], spherical shape	Burst AR in 6 h (~38 %), then gradual AR up to ~96 % at day 30	*Staphylococcus aureus, Escherichia coli*	< (*S. aureus*); > (*E. coli*)			>95 % cell viability (murine NIH3T3 fibroblast cells and human osteosarcoma SaOS-2 cells)
Lai et al., 2015	Vancomycin conjugated to AuNPs (Van-Au NPs) 8.4 ± 1.3 nm[§], spherical shape	na	MSSA[T], MRSA[T], VRE, VSE, *Escherichia coli, Pseudomonas aeruginosa, Acinetobacter baumannii*	>	na	na	~ 80 % cell viability (MTT assay, RAW 264.7 murine macrophages)
Li et al., 2014	Vancomycin loaded on core-shell supramolecular gelatin NPs decorated with red blood cell membranes (Van⊂SGNPs@RBC). 97.3 ± 3.4 nm[§], 123.3 ± 12.7 nm[¥], spherical shape (data relative to NPs before vancomycin loading)	Upon exposure to gelatinase, burst AR in 4 h (~80 %), then gradual AR up to ~90 % at 48 h	MSSA, *Staphylococcus epidermidis*	= (MSSA); < (*S. epidermidis*)	na	na	Negligible toxicity (CCK-8 assay, human embryonic kidney 293T cells and human hepatocyte LO2 cells)
Li et al., 2018	Vancomycin conjugated to peptide-protected Au NCls. 17.77 ± 0.18 nm[§], 37.4 nm[¥], spherical shape	No release up to 48 h when incubated in fetal bovine serum or Dulbecco's modified Eagle's medium; gradual AR upon exposure to diacetyl-L-Lys-D-Ala-D-Ala, mimicking bacterial cell wall	*Staphylococcus aureus, Bacillus subtilis, Bacillus cereus*	=	na	na	>80 % cell viability (MTT assay, human breast cancer MCF-7 cells and Chinese hamster ovary CHO cells)
Lin et al., 2017	Vancomycin entrapped into porous iron-carboxylate metal−organic framework NMs. 500 nm[§], octahedral shape	Burst AR in 24 h (~95 % at pH 6.5 and 7.4, ~75 % at pH 5.5), then gradual AR up to ~100 % at 168 h.	*Staphylococcus aureus*	<	na	na	High proliferation and viability (MTT assay, murine preosteoblast MC3T3 cells)
Liu et al., 2017	Vancomycin encapsulated in PVA/PLGA NPs, deposited on Ti plates. 50-100 nm[§]	Burst AR in 2 h, then gradual AR up to day 20; higher release at acid pH	*Staphylococcus aureus*	>	na	na	High proliferation and viability (MTT assay and alkaline phosphatase activity, murine osteoblastic MC3T3-E1 cells)
Liu et al., 2020	Vancomycin encapsulated in hyaluronic acid-coated ZIF-8. 389 nm[¥]	Gradual AR, higher at pH 5.5 (~60 % after 24 h), than at pH 6.5 (~30 %) and pH 7.4 (~20 %)	MRSA[T]	>	na	Reduction of MRSA infection in murine model for pneumonia	>80 % cell viability (MTT assay, RAW 264.7 murine macrophages). No toxicity *in vivo* in a murine pneumonia model
Lotfipour et al., 2014	Vancomycin loaded on PLGA NPs. ~450-466 nm[¥]	na	*Enterococcus* spp. (40 isolates)	=/<, depending on the isolate	na	na	na
Ma et al., 2020	Vancomycin co-loaded with AgNPs, by electrostatic and hydrogen-bonding interactions, on polydopamine (PDA@Van-Ag). 290 nm[¥]	Gradual AR up to 26 h	*Staphylococcus aureus, Escherichia coli*	>	na	Reduction of *S. aureus* infection in murine model for skin infection	>90 % cell viability (MTT assay, human fibroblast MRC-5 cells). No toxicity *in vivo* in a murine skin infection model
Maji et al., 2019	Vancomycin loaded on LDHNs. 124.4 ± 2.01 nm[¥]	Gradual AR up to ~78 % (pH 6.0) and ~35 % (pH 7.4) at 48 h	MRSA	>	na	na	>78 % cell viability (MTT assay, human embryonic kidney HEK 293 cells and human breast cancer MCF-7 cells). No haemolytic activity (sheep blood)
Mas et al., 2013	Vancomycin loaded on MSNs. 80-100 nm[§], spherical shape	na	*Escherichia coli, Salmonella typhi, Erwinia caratovora*	>	na	na	na
Mhule et al., 2018	Vancomycin loaded on SLNs formed by N-(2-morpholinoethyl) oleamide	Gradual AR, 1.58 times higher at pH 6.0 than 7.4	MRSA	<	na	Reduction of MRSA infection in murine	>76 % cell viability (MTT assay, human adenocarcinoma alveolar

(*continued on next page*)

Table 1 (*continued*)

Reference	Characteristics of the nanoantibiotic: type, dimension, shape	Antibiotic release	Antimicrobial activity				Toxicity assessment (type of assay, used cell lines)
			In vitro			*In vivo*	
			Targeted bacteria	Relative activity compared to free vancomycin (<, =, >)	Antibiofilm activity (+/-)		
	(VCM_NMEO SLNs). 302.8 ± 0.12 nm[¥]					model for skin infection	basal epithelial A-549 cells, human embryonic kidney HEK 293 cells, and human hepatoma cancer HepG2 cells)
Mohapatra et al., 2018	Vancomycin loaded on chitosan microbeads embedded with Fe_3O_4 NPs. 288.4 ± 62.2 μm[§], spherical shape	Controlled AR upon exposure to an alternating magnetic field	na	na	na	na	na
Murei et al., 2020	Vancomycin conjugated to AgNPs, administered with extract from *Pyrenacantha grandiflora* tubers. 13 nm[§], nanocube shape (data relative to nude AgNPs)	na	MSSA, *Klebsiella pneumoniae*, *Escherichia coli*	>	na	na	na
Omolo et al., 2018	Vancomycin loaded on LPDHs. 52.48 ± 2.6 nm[¥], ring-shape spherical structure	Gradual AR up to 65.8 % at 48 h	MSSA, MRSA	>	+ (MRSA)	Reduction of MRSA infection in murine model for skin infection	>77 % cell viability (MTT assay, human breast cancer MCF-7 cells, human adenocarcinoma alveolar basal epithelial A-549 cells, human hepatoma cancer HepG2 cells, and human embryonic kidney HEK 293 cells)
Parent et al., 2016	Vancomycin loaded on porous HA implants, with pores of 100-200 nm[§]	Burst AR in the first hours, then gradual AR up to 100 % at day 1-5 (depending on the amount of vancomycin loaded)	MSSA	na	na	na	na
Pawar et al., 2018	Vancomycin loaded on chitosan NPs, incorporated in alginate gel containing povidone-iodine (CNPs-PI-Alg). 200-250 nm[§], 276 ± 16.48 nm[¥], spherical shape	Burst AR from the NPs alone in 4 h (~27 %), then gradual AR up to 86 % at 72 h; burst AR from the NPs embedded in the gel in the first days, then gradual AR up to 14 days	*Staphylococcus aureus*	na	+ (*S. aureus*)	na	>80 % cell viability (MTT assay, murine fibroblast L929 cells). No haemolytic activity (human blood)
Pei et al., 2017	Vancomycin encapsulated in NPs composed of PLGA, PEG, Eudragit E100, and the chitosan derivative ZWC. 837 ± 103 nm[¥]	~90 % AR at pH 5.0, ~70 % at pH 7.4	MRSA[T], *Listeria* sp. [T], *Streptococcus pneumoniae*[T], *Enterococcus faecium*[T], *Enterococcus faecalis*[T]	>	na	na	~100 % cell viability (MTS assay, J774.1 murine macrophages)
Pichavant et al., 2016	Vancomycin loaded on polynorbornene-based NPs, immobilized on Ti90A16 V4 alloy. 200-350 nm[¥]	na	MRSA	<	na	na	na
Posadowska et al., 2016	Vancomycin encapsulated in PLGA NPs, then incorporated in gellan gum. 258 ± 11 nm[¥], spherical shape	Burst AR in 24 h (~26 %), then gradual AR up to day 40	*Staphylococcus aureus*, *Staphylococcus epidermidis*	=	na	na	Good compatibility (resazurine assay, MG-63 human osteosarcoma cells)
Saidykhan et al., 2016	Vancomycin loaded on aragonite NPs (VANPs). 36 ± 6 nm[§], cubic shape	Burst AR in 15 h (~73 %), then gradual AR up to 97 % at day 5	MRSA	na	na	na	>80 % cell viability (MTT assay, human fetal osteoblast 1.19 cells)
Salih et al., 2020	Vancomycin loaded on nanovesicles of the sugar-based cationic amphiphile BCD-OLA (Beta-cyclodextrin / oleylamine). 125.1 ± 8.30 nm[¥], spherical shape	Burst AR in 4 h (~39 %), then gradual AR up to 80 % at 48 h	MSSA, MRSA[T]	>	na	na	>78 % cell viability (MTT assay, human adenocarcinoma alveolar basal epithelial A-549 cells, human embryonic kidney HEK 293 cells, and human cervix cancer HeLa cells)
Sarkar et al., 2017			na	na	na	na	

(*continued on next page*)

Table 1 (*continued*)

Reference	Characteristics of the nanoantibiotic: type, dimension, shape	Antibiotic release	Antimicrobial activity				Toxicity assessment (type of assay, used cell lines)
			In vitro			*In vivo*	
			Targeted bacteria	Relative activity compared to free vancomycin (<, =, >)	Antibiofilm activity (+/-)		
	Vancomycin loaded on carbon QD tailored calcium alginate hydrogel films. 1.5-3.7 nm, spherical shape (data relative to carbon QD)	Burst AR in 1 h, then gradual AR, higher at pH 1.5 (72 % at 120 h)					>80 % cell viability (MTT assay, human cervix cancer HeLa cells)
Seedat et al., 2016	Vancomycin loaded on LPHNs ~202-250 nm[¥], rod shape	Gradual AR up to ~36-54 % at 24 h, depending on the lipid/polymer used	MSSA, MRSA	>	na	na	na
Serri et al., 2018	Vancomycin loaded on PAMAM dendrimers	Gradual AR up to 44-63 % at 24 h	MSSA, MRSA, *Escherichia coli, Salmonella typhimurium, Klebsiella pneumoniae, Pseudomonas aeruginosa*	>	na	na	na
Sharipova et al., 2018	Vancomycin incorporated in nano-grained Fe-Ag nanocomposites	Gradual AR up to 88 % at day 7	na	na	na	na	No significant toxicity (Calcein AM assay, MG-63 human osteosarcoma cells)
Shimizu et al., 2014	Vancomycin conjugated on acryl NPs. 287 nm[¥]	na	VSE, VRE	= (VSE); > (VRE)	na	na	na
Sikwal et al., 2016	Self-assembled NPs formed by vancomycin and polyacrylic acid sodium. 229.7 ± 47.76 nm[¥], hexagonal cubic shape	Gradual AR up to ~95 % in 12 h	MSSA, MRSA	=	na	na	>76 % cell viability (MTT assay, human breast cancer MCF-7 cells, human cervix cancer HeLa cells, and human hepatoma cancer HepG2 cells)
Simon et al., 2020	Vancomycin loaded on PLGA/PVA or PLGA/DMAB polymeric NPs. <90 nm[¥] (with DMAB) or 201-210 nm[¥] (with PVA), spherical shape	na	MRSA, VISA	= (PLGA/PVA NPs); > (PLGA/DMAB NPs)	na	na	na
Sonawane et al., 2016	Vancomycin loaded on Compritol 888 ATO lipid – PAMAM dendrimer hybrid NPs. 52.21 ± 0.22 nm[¥], spherical shape	Gradual AR up to 100 % in 72 h	MSSA, MRSA	>	na	na	na
Sonawane et al., 2020	Vancomycin encapsulated in micelles of the AB2-type amphiphilic block copolymer. 131-150 nm[§], 130.33 ± 7.36 nm[¥], spherical shape	Gradual AR up to ~100 % in 48 h; faster release at pH 6.0 than at pH 7.4	MSSA, MRSA	=	na	Reduction of MRSA infection in murine model for skin infection	>76 % cell viability (MTT assay, human adenocarcinoma alveolar basal epithelial A-549 cells, human breast cancer MCF-7 cells, and human hepatoma cancer HepG2 cells)
Suchý et al., 2016	Vancomycin loaded on collagen/HA NPs composite layers. 150 nm (data relative to HA NPs)	Gradual AR up to 21 days	na	na	na	na	na
Suchý et al., 2017	Vancomycin loaded on collagen/HA NPs composite layers.	Burst AR in 24 h, then gradual AR up to 1 month	MRSA, *Staphylococcus epidermidis, Enterococcus faecalis*	= (MRSA, *S. epidermidis*); > (*E. faecalis*)	na	na	No significant toxicity (MTS assay, human osteosarcoma SaOS-2 cells)
Suchý et al., 2019	Vancomycin loaded on collagen/HA NPs electrospun layers (alone or with gentamycin)	Gradual AR up to 21 days	MRSA, *Staphylococcus epidermidis, Enterococcus faecalis*	= (MRSA, *S. epidermidis*); > (*E. faecalis*)	na	na	No significant toxicity (MTS assay, human osteosarcoma SaOS-2 cells)
Sun et al., 2017	Vancomycin conjugated to AgNPs (AgNP-VAM). 30 ± 3 nm[§], spherical shape	na	*Mycobacterium smegmatis*	>	na	na	na
Tao et al., 2020	Vancomycin NPs loaded on chitosan-based thermosensitive hydrogel (VCM-	Burst AR in 10 h (23.5 %), then gradual AR up to 65 % at day 26	*Staphylococcus aureus*	>	na	Reduction of *S. aureus* infection in rabbit	

(*continued on next page*)

Table 1 (*continued*)

Reference	Characteristics of the nanoantibiotic: type, dimension, shape	Antibiotic release	Antimicrobial activity				Toxicity assessment (type of assay, used cell lines)
			In vitro			*In vivo*	
			Targeted bacteria	Relative activity compared to free vancomycin (<, =, >)	Antibiofilm activity (+/-)		
	NPs/Gel). 140 nm[§], 182.4 ± 8.8 nm[¥], spherical shape					model for osteomyelitis	>85 % cell viability (CCK-8 assay and alkaline phosphatase activity, osteoblasts)
Uhl et al., 2017	Vancomycin encapsulated in glycerylcaldityltetraether lipid NLs. 100 nm[§], 134 ± 9.7 nm[¥], spherical shape	na	na	na	na	na	>95 % cell viability (Alamar Blue assay, human colon cancer CaCo-2 cells)
Wan et al., 2011	Vancomycin conjugated to AgNPs coated with TiO_2 (Van-Ag@TiO_2). 110 nm[§], spherical shape	na	*Desulfotomaculum* sp., *Vibrio anguillarum*	>	na	na	na
Wang et al., 2017a	Vancomycin conjugated to magnetic-based Ag microflowers (Van/Fe_3O_4@SiO_2@Ag microflowers). 700-900 nm[§], highly branched morphology	na	MRSA, *Escherichia coli*	>	na	na	na
Wang et al., 2018	Vancomycin conjugated to AuNPs (Au@Van NPs). Polygonal shape	na	VRE	>	na	na	na
Wang et al., 2019	Vancomycin conjugated to Au nanostars (AuNSs@Van). 104.4 ± 13.3 nm[§], ~120 nm[¥]	na	MSSA, MRSA	na	na	Reduction of MRSA infection in murine model for skin infection	>90 % cell viability (MTT assay, human cervix cancer HeLa cells)
Xiang et al., 2018	Vancomycin loaded on titania NTs capped by ZnO QDs conjugated with folic acid (TNTs-Van@ZnO-FA QDs)	Burst AR in the first hours, then gradual AR up to day 16; higher release at acid pHs	*Staphylococcus aureus*	na	na	na	>86 % cell viability (MTT assay, murine preosteoblast MC3T3)
Xu et al., 2020	Vancomycin co-encapsulated with WS_2 QDs in thermal-sensitive NLs (WS_2QDs-Van@lipo). <100 nm[§], 146.37 ± 0.67 nm[¥], spherical shape	na	VISA, *Escherichia coli*	>	+ (VISA)	Reduction of VISA infection in mice with subcutaneous abscesses, upon NIR irradiation	~ 100 % viability (MTT assay, human dermal keratinocytes HaCaT cells). No haemolytic activity (murine blood). No evident toxicity *in vivo* in a murine abscess model
Yan et al., 2015	Vancomycin co-loaded with fluorescein isothiocyanate and rhodamine B-based derivative on MSNs, then layered on agarose gel. ~150 nm[§]	Burst AR in 3 h (~12 % at pH 8.0, ~60 % at pH 5.0), then gradual AR up to 12 h	*Escherichia coli*	na	na	na	na
Yang et al., 2017	Vancomycin co-loaded with AgNPs on ZnO nanorod arrays	na	*Staphylococcus aureus*	na	na	na	na
Yousry et al., 2016	Vancomycin loaded on SLNs. 135-4414 nm[¥] (depending on the lipid used and the ratio lipid:antibiotic), spherical shape	na	na	na	na	na	na
Yousry et al., 2017	Vancomycin loaded on PLGA or PCL polymeric NPs, incorporated in a Carbopol®-based gel. ~170-8444 nm[¥] (depending on the formulation composition), spherical shape	Gradual AR from the NPs up to ~20-90 % (depending on the formulation) at day 3; burst AR from the gel in 15 minutes (58-73 %), then gradual AR up to 24 h	MSSA	na	na		No *in vivo* ocular irritation in albino rabbits
Yu et al., 2014	Vancomycin loaded on HA NPs, incorporated in a gel matrix formed by	Burst AR from the NPs in 24 h (61 %), then gradual AR up to 72 % at 375 h	*Staphylococcus aureus*	na	na	na	na

(*continued on next page*)

Table 1 (*continued*)

Reference	Characteristics of the nanoantibiotic: type, dimension, shape	Antibiotic release	Antimicrobial activity				Toxicity assessment (type of assay, used cell lines)
			In vitro			*In vivo*	
			Targeted bacteria	Relative activity compared to free vancomycin (<, =, >)	Antibiofilm activity (+/-)		
	oxidation of sodium alginate and gelatin. 30-40 nm[§], irregular shape						
Zakeri-Milani et al., 2013	Vancomycin loaded on PLGA NPs. 450-466 nm[¥]	Burst AR in 30 min (~10-12 %), then gradual AR up to ~100 % at 24 h	na	na	na	na	na
Zhang et al., 2017	Vancomycin loaded on N-trimethyl chitosan NPs functionalized with poly (trimethylene carbonate) (VCM/TMC NP-PTMC). 220-230 nm[§], spherical shape	Gradual AR up to ~84 % (in lipase aqueous medium) and ~19 % (in PBS) at day 36	MSSA	na	na	Reduction of MSSA infection in rabbit model for osteomyelitis	High cell proliferation (MTT assay, osteoblasts)
Zhang et al., 2018	Vancomycin loaded on gelatin nanospheres 329-387 nm[¥], spherical shape	na	na	na	na	Reduction of *S. aureus* infection in zebrafish larvae	na
Zhang et al., 2020	Vancomycin entrapped in the PVA coating of silica-coated iron oxide NPs, conjugated with a cell-penetrating hexapeptide sequence (Gly-Ala-Phe-Pro-His-Arg) (MCCC@VAN). ~32 nm[¥], spherical shape	Progressive AR, slightly slower at pH 7.2	MSSA, *Escherichia coli*	>	na	na	na
Zhao et al., 2017	Silica NPs coated with vancomycin-modified polyelectrolyte-cypate complexes (SiO_2-Cy-Van). 72.7 ± 3.2 nm[§], spherical shape	na	MRSA	na	na	Reduction of MRSA infection in mice	>90 % cell viability (MTT assay, murine NIH3T3 fibroblast cells). No toxic effect visible in collected kidney tissues from MRSA-infected mice treated with the NPs
Zhou et al., 2018	Vancomycin used to functionalize, together with Si(IV) naphthalocyanine, silica-encapsulated Ag-coated AuNPs (Au@AgNP@SiO_2@Nc-Van). 60 nm[§], 110 nm[¥] (data relative to AgNP@SiO_2)	na	*Bacillus subtilis,* VRE	< (VRE); > (*B. subtilis*)	na	Reduction of VRE infection in mice, upon NIR irradiation	>90 % cell viability under dark conditions, >75 % cell viability upon NIR irradiation (MTT assay, human dermal keratinocytes HaCaT cells)
Zou et al., 2020	CuS NPs with vancomycin as reductant and capping agent (CuS@Van). 15 ± 5 nm	na	VRE	>	na	Reduction of VRE infection in mice, upon NIR irradiation	>90 % cell viability under dark conditions, >50 % cell viability upon NIR irradiation (MTT assay, murine fibroblast 3T3 cells and rat glioma C6 cells)

In addition to abbreviations listed in the main text: AR = antibiotic release; HA = hydroxyapatite; MP = microparticle; Na = not available; NCl = nanocluster; NL = nanoliposome; NT = nanotube; PBS = phosphate buffer saline; QD = quantum dot.

transpeptidases, and ultimately leading to bacterial lysis (Fig. 2A) (Cooper and Williams, 1999). Due to the presence of their outer membrane that prevents GPAs from entering the periplasm, Gram-negatives are intrinsically resistant to these antibiotics (Cooper and Williams, 1999). A few drawbacks in the clinical use for GPAs are known: vancomycin (more than teicoplanin) presents dose-dependent nephrotoxicity and, to a lesser degree, ototoxicity; in addition, it poorly penetrates certain body tissues and bacterial biofilms (Ziglam and Finch, 2001; Jefferson et al., 2005). Another issue is the increasing AMR toward GPAs. Gram-positives become resistant to vancomycin and related molecules reprogramming cell wall biosynthesis, thus reducing the affinity of GPAs for their cellular targets. Nowadays, a worryingly high percentage of clinical enterococcal isolates harbours the genetic determinants of vancomycin resistance (Miller et al., 2016a). Horizontal gene transfer of such genes from enterococci to *S. aureus* has generated vancomycin-resistant MSSA (methicillin-sensitive *S. aureus*) and MRSA (Cong et al., 2019), whose infections are very difficult to treat. For more information on the resistance mechanisms and the different GPA-resistant phenotypes, readers are addressed to Binda et al. (2014), Yushchuk et al. (2020b), Lebreton and Cattoir (2019), Stogios and Savchenko (2020).

Daptomycin, introduced in clinical practice in 2003, is the drug used to treat Gram-positive infections for which none or at most limited therapeutic alternatives are available, as those caused by VRSA, VISA (vancomycin intermediate *S. aureus*), VRE, and penicillin-resistant streptococci (Heidary et al., 2018). It finds also application as a last resort for the treatment of complicated skin infections, bacteraemia, and right-sided endocarditis caused by Gram-positives, including MSSA and MRSA, streptococci, and enterococci. Daptomycin is one of the few membrane-targeting antibiotics that are applied systemically, although under medical control due to the possible serious side effects that can arise even at low-dose administration (Osorio et al., 2021). It is formed by 13 amino acids: 10 are arranged in a macrocyclic polypeptide core closed by an ester bond that includes four proteinogenic amino acids (L-Asp, L-Gly, L-Thr, L-Trp) and six nonproteinogenic and D-amino acids (kynurenine, ornithine, 3-methylglutamic acid, D-Ala, D-Ser, D-Asn). The remaining three amino acids (L-Asn, L-Asp, and L-Trp) form an N-terminal tripeptide, to whom a *n*-decanoyl fatty acid tail is attached at position 1 (Fig. 1) (Heidary et al., 2018). Daptomycin exerts its bactericidal activity by binding in a calcium-dependent manner to phosphatidylglycerol (PG)-containing membranes in actively dividing regions of bacterial cells (Fig. 2A) (Miller et al., 2016b). The resulting insertion of the antibiotic lipophilic tail into the bacterial cell membrane induces a rapid cell membrane reorganization that in turn causes pore-like structures formation, leakage of solutes as Na^+, K^+, and alkaline metal ions, and depolarization (Miller et al., 2016b). Adverse effects caused by daptomycin include myopathy and rhabdomyolysis, in addition to eosinophilic pneumonia and anaphylactic hypersensitivity (Echevarria et al., 2005). Although still limited in number, reports of daptomycin resistance in *S. aureus, E. faecium,* and *Enterococcus faecalis* were published (Sader et al., 2013). Resistance is determined by a decrease of daptomycin-binding PG residues in the membrane, an augment of the membrane cardiolipin content at the expense of PG, or an increase of positive charges on bacterial cell surface causing electrostatic repulsion of the calcium-daptomycin complex (Miller et al., 2016b).

3. Nanoparticles to counteract AMR in Gram-positive bacteria

3.1. Introduction to nanoparticles

Despite a certain disparity in definitions (Boholm and Arvidsson, 2016), the word 'nanomaterial' (NM) defines materials where more than 50 % of the constituent particles have at least one dimension in the nanorange (1-100 nm) (https://ec.europa.eu/environment/chemicals/nanotech/faq/definition_ en.htm). Accordingly, NMs that have all dimensions in the 1-to-100 nm range are appointed as nanoparticles (NPs). Other NMs are characterized by one dimension (nanotubes, nanorods, nanowires) or two dimensions (graphene, nanofilms, nanolayers, nanocoatings) outside the nanoscale, respectively (Pokropivny and Skorokhod, 2007). Nanosystems can be classified also depending on their composition in inorganic, organic, or carbon-based material (Fig. 3). Inorganic nanosystems include mainly transition metal (Ag, Au, Pt, Zn, Ti, Fe, etc) and metal oxide (ZnO, TiO_2, Fe_3O_4, CuO, SiO_2, etc) NPs (Arias et al., 2018; Ermini and Voliani, 2021; Piacenza et al., 2018a), mesoporous silica NPs (Bernardos et al., 2019), and quantum dots (Martínez-Carmona et al., 2018). Organic ones comprise -without being limited to- liposomes and other lipid-based NPs (Arana et al., 2021; Gonzalez Gomez and Hosseinidoust, 2020), dendrimers (Alfei and Schito, 2020), synthetic and natural polymeric NPs. These latter include, for example, those formed by polylactic acid-co-glycolic acid (PLGA) (Booysen et al., 2019), polycaprolactone (PCL) (Yousry et al., 2017), chitosan (Naskar et al., 2019), or gelatin (Li et al., 2014). Finally, carbon-based nanostructures include graphene and its derivatives, fullerenes, carbon nanotubes, carbon nanocapsules, carbon nanofibers, carbon nanodiamonds, carbon nanodots, carbon onions, carbon black, carbon rings, etc (Khalid et al., 2020).

NPs have today a large variety of applications in our everyday life, including agriculture (Ashraf et al., 2021), food processing and conservation (Ashraf et al., 2021), electronics (Tawade et al., 2021), transportation (Shafique and Luo, 2019), energy (Banin et al., 2021), wastewater treatment (El-Gendy and Nassar, 2021), and cosmetics (Fytianos et al., 2020), among others. In pharmaceutical and biomedical fields, they are prevalently used for tissue regeneration, for preparing medical implants, for bioseparation purposes, for carrying DNA and RNA in gene therapy, and for antitumor drug delivery (Anselmo and Mitragotri, 2019; Mba and Nweze, 2021). NPs are used as antibacterial coatings for implantable devices or as medical preparations to prevent infections and to promote wound healing (Bernardos et al., 2019; Piacenza et al., 2017; Pormohammad et al., 2021), they are used in vaccine formulations and as nanocarriers for antibiotic delivery (Gupta et al., 2019; Mba and Nweze, 2021).

Particularly versatile for biomedical purposes are superparamagnetic metal and metal oxide NPs, first of all iron oxide NPs (Fe_3O_4NPs) (Anderson et al., 2019; Arias et al., 2018). Due to their magnetic nature, Fe_3O_4NPs can be visualized by magnetic resonance imaging and used for diagnostic and theragnostic applications. Since they generate heat after exposure to an alternating magnetic field, they find application in magnetic hyperthermia treatment of cancer patients. Furthermore, they can be directed by an external magnetic field, thus becoming ideal cargos for delivering drugs at tumour sites (Dadfar et al., 2019).

NPs are traditionally synthesized by chemical or physical methods, generally divided into bottom-up and top-down approaches. In the first case, synthesis is achieved starting from atomic and/or molecular precursors, assembled by diverse protocols of chemical vapor deposition, sol-gel processes, co-precipitation, microwave-assisted methods, or laser pyrolysis, among others. Instead, in top-down methods the size of the starting bulk material is reduced by laser ablation, mechanical milling or grinding, sputtering, or electro-explosion, until nanostructured entities are obtained (Arias et al., 2018; Piacenza et al., 2018a). NP synthesis by bottom-up approaches is usually the preferred choice at laboratory scale, while top-down methods are more commonly adopted in industrial settings, since they are more scalable. Developing cost-effective large-scale production of NPs is a not-yet completely solved issue in nanotechnology. The production of high-quality nanostructures often requires sophisticated and costly instrumentation, it is a time and energy consuming process, which is conducted in harsh and dangerous operational conditions, using toxic reductants and stabilizing agents. More recently, environmental-friendlier approaches, such as green synthesis of metallic NPs, using ionic and supercritical liquids (Seitkalieva et al., 2021) or biological systems (Drummer et al., 2021; Piacenza et al., 2018b), have been developed. Green synthesis exploits the capacity of plants, bacteria, fungi, and algae, to adapt to environments rich in harsh

Table 2
List of papers describing nanoformulations of teicoplanin (according to the references' alphabetical order). The list was created by searching Pubmed database (accession on 11th May 2021) with the following query: (((glycopeptide) AND (antibiotic)) AND (nanoparticles)) AND (("2011/01/01"[Date - Publication] : "3000"[Date - Publication])). The results were manually checked to select only those publications actually describing the use of NPs as teicoplanin carriers for antibacterial purposes. When available, data on the characterization of the nanoformulations, as well as names used by the authors for describing the nanosystems, are included. For 'Dimension': § diameter estimated by transmission electron microscopy or scanning electron microscopy; ¥ hydrodynamic diameter estimated by dynamic light scattering. For 'Relative activity compared to free teicoplanin': when nanoformulations showed higher (>), lower (<), or similar (=) antimicrobial activity in comparison to bare teicoplanin, the corresponding sign is represented. For 'Antibiofilm activity': presence of absence of antibiofilm activity are indicated with the plus or minus signs, respectively.

Reference	Characteristics of the nanoantibiotic (type, dimension, shape)	Antibiotic release	Antimicrobial activity				Toxicity assessment (type of assay, used cell lines)
			In vitro			*In vivo*	
			Targeted bacteria	Relative activity compared to free teicoplanin (<, =, >)	Antibiofilm activity (+/-)		
Armenia et al., 2018	Teicoplanin conjugated by covalent bond to magnetic iron oxide NPs (NP-teico). 13.6 nm§, 568.2 ± 0.6 nm¥, spherical shape	na	MSSA, MRSA, *Enterococcus faecalis, Bacillus subtilis*	<	+ (MSSA)	na	>80 % cell viability (RealTime Glo™ MT Cell viability assay, human ovarian adenocarcinoma SKOV-3 cells and human adipose-derived hASC stem cells)
Gonzalez Gomez et al., 2019	Teicoplanin encapsulated in NLs. 100-200 nm ¥	na	MSSA	<	na	na	na
Ucak et al., 2020	Teicoplanin encapsulated in PLGA NPs, functionalized with *S. aureus* aptamers. 226 ± 5.57 nm¥, spherical shape	Burst AR in 2 h (58 %), then gradual AR up to 75 % at 245 h	MSSA, MRSA, *Staphylococcus epidermidis*	>	na	na	na

In addition to abbreviations listed in the main text: AR = antibiotic release; Na = not available; NL = nanoliposome.

metal ions, bioconverting them into their less toxic elemental forms, then accumulated as intracellular nanostructures or deposits. The method is cost-effective, requires relatively low energy, and is more sustainable and safer than traditional physico-chemical synthesis methods, being in line with green chemistry principles. An additional advantage is that biogenic NMs are usually further stabilized through interactions with macromolecules and secondary metabolites produced by the host system itself. Although these strategies are still in a developmental stage, they are attracting wide interest due to economic prospects and scale-up feasibility. Using plant extracts, in particular, is currently appreciated as the easiest strategy for mass production of metallic NPs (Piacenza et al., 2018b).

3.2. Nanoparticles as active antibacterial agents per se

By now, evidence exists on the antibacterial properties of different nanosystems, which can be effective in eradicating bacterial infections, caused either by Gram-positive or Gram-negative bacteria, including resilient MDR-bacteria. Antibacterial properties of NPs are extensively reviewed in different papers (Bernardos et al., 2019; Gupta et al., 2019; Mba and Nweze, 2021; Naskar and Kim, 2019; Sánchez-López et al., 2020; Wang et al., 2017b). In this section, the latest advances are briefly discussed, looking at the possible pros and cons. Fig. 2B illustrates NPs' main mechanisms of action on bacterial cells. Metallic NPs are known for their intrinsic large-spectrum antibacterial properties (Gómez-Núñez et al., 2020). Silver NPs (AgNPs) are the most effective and commonly used antibacterial agents (Amaro et al., 2021; Durán et al., 2016). Silver has been recognized since ancient times for its antimicrobial effect and it is currently incorporated on the surface of medical devices used for dentistry and orthopaedic applications, to confer them long-lasting antibacterial activity (Xiang et al., 2017; Xie et al., 2018). AgNPs are employed as components of medical textiles as surgical masks (Valdez-Salas et al., 2021), food packages (Ediyilyam et al., 2021), and membrane filters used for water treatment (Beisl et al., 2019). AgNPs are described in literature as active against both Gram-positive and Gram-negative bacteria, in addition to fungi, some parasites as *Leishmania tropica* and *Plasmodium* spp., and viruses including HIV strains and SARS-CoV-2 (Merkl et al., 2021). A detailed description of the antibacterial mode of action of AgNPs is out of the scope of the present review, and readers can refer to several recent and exhaustive papers (Amaro et al., 2021; Bruna et al., 2021; Dakal et al., 2016; Durán et al., 2016; Kędziora et al., 2018; Salleh et al., 2020). Briefly, the popularity of AgNPs as antimicrobial agents is due to the multiple effects they exert. Thanks to their reduced size and high specific surface area, AgNPs interact with proteins of the bacterial cell wall and infiltrate within the cell membrane, thus causing its depolarization and permeabilization, with the consequent leakage of cellular contents. They inhibit cell division and ion transport processes by interacting with nucleic acids, membrane transport, and respiratory chain proteins. AgNPs can disturb transcription, translation, and protein synthesis, while causing also protein dysfunction and denaturation, and altering metabolism. By releasing Ag^{+}, they trigger the generation of ROS as superoxide anions, hydrogen peroxide, and hydroxyl radicals, which in turn cause DNA destabilization, protein denaturation, and lipid peroxidation, thus contributing to membrane damage and ultimately leading to bacterial death (Amaro et al., 2021; Durán et al., 2016; Ferdous and Nemmar, 2020) (Fig. 2B).

Besides silver, other metal and metal oxide NPs with proven antibacterial activities are gold NPs (AuNPs) (Okkeh et al., 2021), zinc oxide NPs (ZnONPs) (Gharpure and Ankamwar, 2020), copper (CuNPs) and copper oxide NPs (CuONPs) (Ermini and Voliani, 2021), iron oxide NPs (Fe_3O_4NPs) (Gabrielyan et al., 2019), and titanium oxide NPs (TiO_2NPs) (Liao et al., 2020). AuNPs with diameter <20 nm, for instance, were reported to penetrate within bacterial membranes of both Gram-positive (e.g., *S. aureus* (Zheng et al., 2017) and *Streptococcus pneumoniae* (Ortiz-Benítez et al., 2019)) and Gram-negative (e.g., *Escherichia coli* (Zheng et al., 2017) and *P. aeruginosa* (Zhao et al., 2010)) bacteria, forming irreversible pores. Bigger AuNPs (80-100 nm) were unable to freely translocate across the bacterial cell membrane, but their absorption onto the bacterial surface generated a membrane tension that ultimately

Table 3
List of papers describing nanoformulations of daptomycin (according to the references' alphabetical order). The list was created by searching Pubmed database (accession on 11th May 2021) with the following query: ((((daptomycin) AND (antibiotic)) AND (nanoparticles)) AND (("2011/01/01"[Date - Publication] : "3000"[Date - Publication])). The results were manually checked to select only those publications actually describing the use of NPs as daptomycin carriers for antibacterial purposes. When available, data on the characterization of the nanoformulations, as well as names used by the authors for describing the nanosystems, are included. For 'Dimension': § diameter estimated by transmission electron microscopy or scanning electron microscopy; ¥ hydrodynamic diameter estimated by dynamic light scattering. For 'Relative activity compared to free daptomycin': when nanoformulations showed higher (>), lower (<), or similar (=) antimicrobial activity in comparison to bare daptomycin, the corresponding sign is represented. For 'Antibiofilm activity': presence of absence of antibiofilm activity are indicated with the plus or minus signs, respectively.

Reference	Characteristics of the nanoparticle (type, dimension, shape)	Antibiotic release	Antimicrobial activity				Toxicity assessment (type of assay, used cell lines)
			In vitro			*In vivo*	
			Targeted bacteria	Relative activity compared to free daptomycin (<, =, >)	Antibiofilm activity (+/-)		
Costa et al., 2015	Daptomycin encapsulated in chitosan-coated alginate NPs (CS-ALG-NPs). ~383-421 nm¥	na	MSSA, MRSA, *Staphylococcus epidermidis, Staphylococcus capitis, Staphylococcus hominis, Staphylococcus haemolyticus, Staphylococcus warneri*	=	na	na	na
Li et al., 2013	Daptomycin encapsulated in flexible NLs (DAP-FL). 55.4 nm¥, round shape	na	MSSA	na	+ MSSA)	Reduction of MSSA biofilm in mice	na
Meeker et al., 2016	Daptomycin loaded by non-covalent interactions on polydopamine-coated Au NCas, conjugated with an antibody targeting *S. aureus*' protein A (AuNC@Dap/PDA−aSpa). ~200 nm§ (AuNC@Dap)	Controlled AR upon NIR irradiation with diode laser at 808 nm (release proportional to the duration or irradiation)	MSSA, MRSA	na	+ (MRSA)	na	na
Meeker et al., 2018	Daptomycin loaded by non-covalent interactions on polydopamine-coated Au NCas, conjugated with antibodies targeting *S. aureus*' protein A (AuNC@Dap/PDA-aSpa), or the lipoprotein SACOL0486 (AuNC@Dap/PDA-aLpp), or the manganese transporter SACOL0688 (AuNC@Dap/PDA-aMntC). ~78 nm§ (AuNC@Dap)	Low AR in dark conditions; controlled AR upon NIR irradiation with diode laser at 808 nm (release proportional to the duration or irradiation)	MRSA	na	+ (MRSA)	na	na
Silva et al., 2015	Daptomycin encapsulated in chitosan NPs (CS-ALG NPs) ~140-205 nm¥, spherical shape	Total AR in 4 h	MSSA, MRSA, *Staphylococcus epidermidis, Staphylococcus lugdunensis, Staphylococcus haemolyticus, Staphylococcus hominis, Staphylococcus warneri, Enterococcus faecalis*	<	na	na	na
Tong et al., 2019	Daptomycin co-conjugated with Ag NPs, by covalent bond, to reduced GO nanocomposites (rGO@Ag@Dap). 70 nm§, spherical shape	>90 % AR in 12 h	*Staphylococcus aureus, Bacillus subtilis*	>	na	Reduction of *S. aureus* infection in murine model for skin infection	>80 % cell viability (MTT assay, murine NIH3T3 fibroblast cells). No haemolytic activity (human blood). No toxic effect detected *in vivo* in a murine model
Wang et al., 2020a	Daptomycin-Au NFs (Dap-Au_nNFs). 30 nm§ (Dap-Au_3NFs), or 80 nm§ (Dap-Au_6NFs), monodispersed flower-like shape; 4 nm§, spherical shape (Dap-Au_1NFs)	na	*Staphylococcus aureus, Escherichia coli*	>	na	na	>90 % cell viability under dark conditions, ca. 13 % cell viability upon NIR irradiation (MTT assay, human cervix cancer HeLa cells)

(*continued on next page*)

Table 3 (*continued*)

Reference	Characteristics of the nanoparticle (type, dimension, shape)	Antibiotic release	Antimicrobial activity				Toxicity assessment (type of assay, used cell lines)
			In vitro			*In vivo*	
			Targeted bacteria	Relative activity compared to free daptomycin (<, =, >)	Antibiofilm activity (+/-)		
Zheng et al., 2016	Daptomycin conjugated by covalent bond to Ag NCl (D-AgNCs). Network of ~100 nm[§], ~200 nm[¥]	na	MSSA	>	na	na	na
Zheng et al., 2019	Daptomycin conjugated by covalent bond to Au NCl (Dap-AuDAMP). 190 nm[¥], agminated network shape	na	MRSA	>	na	na	na

In addition to abbreviations listed in the main text: AR = antibiotic release; GO = graphene oxide; Na = not available; NCa = nanocage; NCl = nanocluster; NF = nanoflower; NL = nanoliposome.

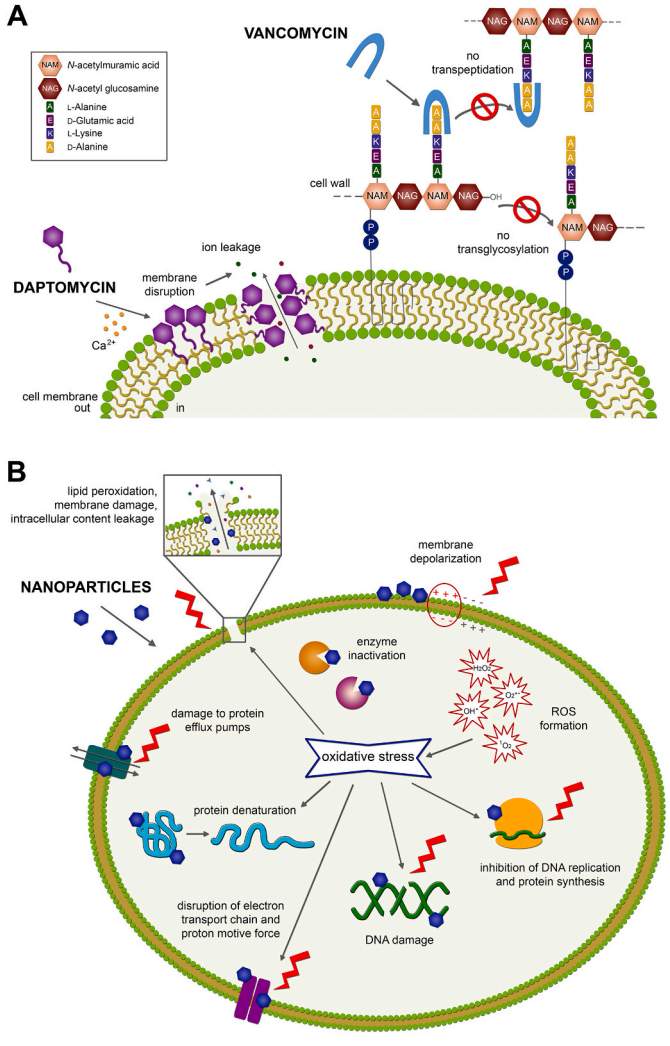

Fig. 2. Schematic diagram showing (A) the antimicrobial mechanisms of daptomycin and vancomycin (this latter as representative of glycopeptide antibiotics), and (B) the different mechanisms of action that nanoparticles exert on bacterial cells.

resulted in its deformations and ruptures. AuNPs can interfere with DNA replication and transcription, alter membrane potential, decrease ATP synthase activity and, consequently, reduce metabolic activities, and provoke ROS formation (Okkeh et al., 2021). As reviewed by Gharpure and Ankamwar (2020) and Lallo da Silva et al. (2019), antibacterial activity of ZnONPs mainly relies on their physical interaction with bacterial membranes, causing loss of cellular integrity and leakage of intracellular contents. Additionally, released Zn^{2+} ions interfere with intracellular components, including enzymes involved in metabolic functions, while ROS generation determines damages to DNA, proteins, and lipids, as above described for AgNPs. ROS formation, lipid peroxidation, DNA damage, protein oxidation, and membrane alteration are at the base of the antimicrobial activity of CuNPs and CuONPs (Ermini and Voliani, 2021), and of TiO_2NPs (Liao et al., 2020), too. By direct binding to bacterial cell wall, Fe_3O_4NPs can damage cell integrity. Fe_3O_4NPs interfere with the function of F0/F1-ATPase and reduce the flux of H^+ through the membrane, while inhibiting DNA replication through topoisomerase inactivation. They can inhibit essential enzymes by binding to mercapto, amino, and carboxyl groups of proteins, and, last but not least, they induce ROS formation (Gabrielyan et al., 2019).

CuONPs, ZnONPs, and, although to a lesser extent, Fe_3O_4NPs, and TiO_2NPs, also eradicate biofilms of a wide range of bacterial species, as recently reviewed by Shkodenko et al. (2020). When metallic NPs penetrated deep within the biofilms, they could exert mechanical destruction of the matrix structure, causing a destabilization of biofilm architecture (Li et al., 2019), although these effects occurred at relatively high concentrations, i.e., in the range of several mg/ml (Li et al., 2019; Shkodenko et al., 2020). Metallic NPs (AgNPs, AuNPs, SeNPs, and ZnONPs) were proven effective in reducing *P. aeruginosa* virulence by targeting its quorum sensing mechanism, attenuating pyocyanin, elastase, and protease production, and reducing biofilm formation (Elshaer and Shaaban, 2021; García-Lara et al., 2015; Shah et al., 2019). The exact mechanism behind this quorum quenching activity of metallic NPs has not been fully elucidated yet: it is believed that it can be mediated by the two-component response regulator CzcR, whose interaction with NPs leads to a downregulation of crucial genes for quorum sensing cascade (Lee et al., 2014).

Although metal NPs are by far the most studied nanosystems endowed with antibacterial activity, carbon-based NPs have been also reported to affect bacterial survival. For instance, the edges of graphene oxide, a two-dimensional nanostructure formed by oxidized graphene sheets, mechanically damaged cell membranes and killed bacteria (Yu et al., 2020). Moreover, graphene oxide either interacted with and extracted phospholipids from cell membranes, causing cell disintegration (Yu et al., 2014), or triggered oxidative stress (Liu et al., 2011). A

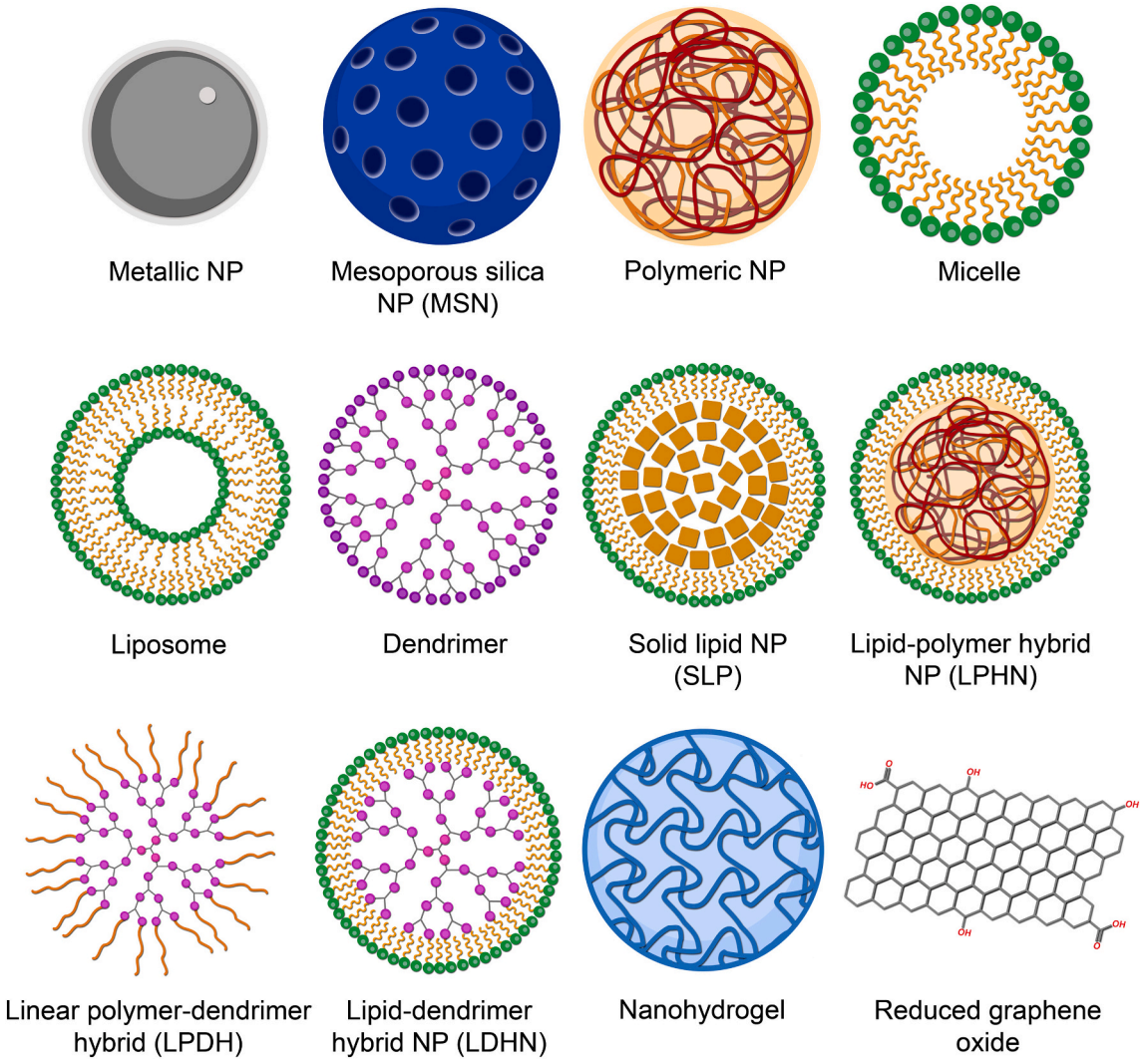

Fig. 3. Schematic illustration of different nanomaterials used as carriers for glycopeptide antibiotics and/or daptomycin.

combination of membrane damage and oxidative stress were also reported to explain the action of carbon nanotubes (Kang et al., 2008) and, in association with an induced fragmentation of genomic DNA, of carbon quantum dots (Li et al., 2016).

Finally, an intrinsic antibacterial activity is typical of different polymers employed in organic NPs preparations. Above all, chitosan, a non-toxic, polycationic deacetylated derivative of the natural polysaccharide chitin, establishes electrostatic interactions with the negatively-charged bacterial cell wall, causing the leakage of intracellular proteins or electrolytes. Moreover, it chelates metal ions and nutrients, which are indeed essential for bacterial survival. Chitosan degradation products may also interact with bacterial DNA, thus interfering with protein synthesis (Matica et al., 2019).

3.2.1. *Factors affecting NPs' antibacterial activity*

A general consideration is that the antibacterial activity of NPs is overall influenced not only by their chemical composition, but also by their shape, size, and surface functionalization (Gupta et al., 2019). NPs are similar in size to biomolecules, as membrane receptors, antibodies, and proteins, thus enabling additional multivalent interactions and exerting a stronger antimicrobial effect when compared to larger counterparts of the same chemical composition (Arias et al., 2018). In particular, the antibacterial activity often inversely correlates with the particle size, probably due to the possibility for smaller NPs to cross more easily the cell membrane. Additionally, in the case of metal NPs, the release of metal ions from smaller NPs is faster, thanks to their higher surface area-to-volume ratio. Hence, ZnONPs with diameter lower than 10 nm were found to exert bactericidal activity on *S. aureus*, differently from bigger NPs that showed only a bacteriostatic effect (Lallo da Silva et al., 2019). Similarly, 7-nm AgNPs were associated with minimum inhibitory concentration (MIC) values against *S. aureus* of ca. 2.2- and 4.5-fold lower than AgNPs with 29-nm and 89-nm diameter, respectively (Martínez-Castañón et al., 2008). Also the antibacterial activity of carbon nanotubes (Kang et al., 2008) and graphene oxide (Perreault et al., 2015) was reported to be enhanced by reducing their sizes and diameters.

Positively-charged NPs were generally proved to be more effective, thanks to their electrostatic interactions with the negatively-charged bacterial membranes and biofilms (Javanbakht et al., 2016). The hydrophobicity of nanosystems was also shown to be beneficial for such interactions: hence, the interaction of bacteria with the hydrophilic graphene oxide was slower and reversible, if compared to the interaction with correlated -but hydrophobic- graphene and reduced graphene oxide (Romero-Vargas Castrillón et al., 2015).

Coating agents, mainly used to prevent metal NPs agglomeration/coagulation during synthesis, can also increase or even impart antimicrobial activity to NPs, on the other hand improving their cytocompatibility and bioavailability (Gupta et al., 2019; Javed et al., 2020).

Biocompatible polymers like poly(ethylene glycol) (PEG), chitosan, polyvinylpyrrolidone (PVP), poly (vinyl alcohol) (PVA), as well as surfactants, proteins (as bovine serum albumin, BSA), and oligonucleotides, are the most frequently employed capping agents (Javed et al., 2020). For example, capping AgNPs with the surfactants sodium dodecyl sulphate or Tween-80, or with the polymer PVP-360, increased both the stability of the nanocomposite and its antibacterial activity over a panel of Gram-positive and Gram-negative bacteria, compared to unmodified AgNPs (Kvítek et al., 2008). By using chitosan as reducing and stabilizing agent for AuNPs synthesis, Regiel-Futyra and co-workers prepared chitosan-Au nanocomposites endowed with bactericidal activity against both Gram-positive (*S. aureus*) and Gram-negative (*P. aeruginosa*) biofilm-forming bacteria. This antibacterial effect was determined by chitosan interaction with the bacterial surface, causing membrane disruption and facilitating Au internalization. Notably, AuNPs internalization in eukaryotic cells was instead hindered by the biocompatible layer formed by chitosan, thus making the NM less cytotoxic to mammalian cell lines (Regiel-Futyra et al., 2015).

3.2.2. Possible limitations in using NPs as antibacterial agents

Differently from classical antibiotics that mostly interfere with a specific target, NPs act on multiple microbial pathways. For this reason, it was initially believed that bacteria may unlikely develop resistance to such materials, as multiple simultaneous mutations would have been required. However, evidence that bacteria can develop resistance upon continuous exposure to metallic NPs has emerged over the last decade (Mitchell et al., 2019; Mann et al., 2021). Bacteria resistant to AgNPs and CuNPs were isolated from clinical and non-clinical environments (Finley et al., 2015; Vasileiadis et al., 2015). As thoroughly reviewed by Niño-Martínez et al. (2019) and Amaro et al. (2021), the mechanisms of resistance towards NPs are numerous, including reduction of NPs uptake or adsorption (for instance through down-regulation of cation-selective porins in Gram-negative bacteria (Finley et al., 2015)), enhanced production of efflux pumps, or alteration of the electrical charge of bacterial surface, thus creating electrostatic repulsion towards NPs (Abbaszadegan et al., 2015). To cope with high intracellular concentrations of metal ions and ROS formation, bacteria can resort to metal ion-sequestering proteins and pigments (Randall et al., 2015) or upregulate their antioxidant mechanisms, e.g., by overproducing ROS scavenging systems (Gou et al., 2010). In addition to individual responses, bacteria can activate collective defence mechanisms, forming microbial aggregates and biofilms, where cells are surrounded by an extracellular polymeric matrix that traps NPs. Additionally, if biofilms are exposed to sub-lethal NPs concentrations, a so-called hormesis process can be elicited, resulting in the reinforcement of the biofilm itself through increased lipopolysaccharide and extracellular polymeric substances formation (Niño-Martínez et al., 2019).

Another side of the coin is that the lack of specificity of NPs in their antimicrobial mode of action do not allow to discriminate between pathogens and beneficial microorganisms, with a possible negative effect on the host microbiota. More importantly, at the concentrations needed to exert a significant bactericidal action, NPs might be cytotoxic to mammalian cells, as these last share, at least in part, the metabolic pathways targeted in bacteria. Hence, NMs have been proven to induce ROS formation *in vitro* in various mammalian cells lines, leading to oxidative stress-induced damages in subcellular organelles as mitochondria, and to tissue phospholipid and protein oxidation. Moreover, NPs were shown to inhibit cell proliferation by downregulating cell cycle genes, to induce the release of cytokines, and to imbalance macromolecules function (lipids, nucleotides, proteins) by directly interacting with them. Furthermore, they can trigger apoptosis (Ferdous and Nemmar, 2020; Lopez-Chaves et al., 2018). Some NPs features, such as reduced size or charged surface, that positively correlate with antimicrobial activity, were reported to be associated with increased toxicity towards mammalian cells (Gómez-Núñez et al., 2020).

Although the literature available on the antimicrobial and potential cytotoxic activity of NPs *in vitro* is vast, much less is known on their effects *in vivo*. Their action, biodistribution, accumulation, and potential deleterious effects have been poorly investigated in animal models and within the human body. Few, and sometimes contradictory, results obtained from *in vivo* studies suggest that both metallic and carbon-based NPs can cross biological barriers and accumulate in organs as the liver, intestine, spleen, and lungs (Amrollahi-Sharifabadi et al., 2018; Lopez-Chaves et al., 2018). As recently reviewed by Ferdous and Nemmar, the effect on the animal body of AgNPs bioaccumulation is still unclear. In some studies, none adverse effect was reported following various routes of AgNPs administration, whereas in others, apoptosis, inflammatory responses, and oxidative stress in different body districts were observed, with severity ranging from mild to acute. These differences can be attributed to the intrinsic characteristics of the used NPs preparations (e.g., size, shape, and coating), as well as to the diverse administration protocols, which varied for route and duration of exposure, doses, or end point measurement time. What is still unknown is whether the inflammatory response observed is due to the AgNPs *per se*, or to the Ag ions released, or to both (Ferdous and Nemmar, 2020).

3.3. Nanoparticles as carriers for last resort drugs against Gram-positive pathogens

An emerging application of NPs is their use as carriers for antibiotics, which can be loaded either at the exterior or at the interior of the nanosystem via chemical conjugation, adsorption, or encapsulation. Nano-based drug delivery systems were introduced in clinics in the early 1990s and used hereafter mainly in oncology and cancer immunotherapy. They might represent a promising tool also in antiinfective therapies (Anselmo and Mitragotri, 2019; Arana et al., 2021; Mamun et al., 2021). When used as antibiotic carriers, NPs might enhance the antibacterial efficacy of the loaded drugs by a combination of mechanisms that include (i) protecting them from enzymatic inactivation and oxidation, (ii) enhancing solubility, prolonging systemic circulation time and improving their pharmacokinetic profile, (iii) improving antibiotic conveyance to the desired tissue, facilitating physiological barrier crossing and increasing local drug concentration at infection sites, while minimizing nonspecific distribution in healthy organs and tissues, (iv) promoting the interaction with pathogen cells and/or enhancing the internalization of the drugs within cells or into bacterial biofilms (Gao et al., 2021; Naskar and Kim, 2019; Van Giau et al., 2019). Due to their penetration capability, antibiotics carried on nanosystems might be used also for treating pathogenic bacteria colonizing the inside of mammalian cells, whose intracellular compartments are barely reached by free antibiotics (Wang et al., 2020b). Examples are infections within macrophages, that typically require long-term antibiotic intake and that can act as 'Trojan horse' to cause a relapse of infection at secondary sites (Bose et al., 2020) (see also section 3.3.5). By delivering the carried antibiotic specifically at the infection site and increasing its local cellular uptake, NPs can contribute to reducing drug administration frequency and dosage, and this aspect could be particularly relevant in the case of last resort drugs (for instance daptomycin) known for its toxic side effects. Dose reduction can be achieved also if the NPs themselves exhibit some antimicrobial activity (see section 3.2), thus exerting a synergic and/or additive effect with the loaded drug. Finally, reduced antibiotic administrations might alleviate the negative effect on the commensal microbiota, thus limiting the transfer of resistant determinants between bacteria (Naskar and Kim, 2019; Van Giau et al., 2019).

In the following sections, we report an overview of the papers published in the last decade covering the preparation and characterization of NPs as carriers for the frontline antibiotics daptomycin and GPAs used to treat severe infections by MDR Gram-positive bacteria.

3.3.1. Types of nanocarriers developed for GPAs and daptomycin

According to the literature search conducted following the criteria

described in detail in the captions of Tables 1-3, more than 100 papers were published in the last decade reporting the use of NPs as GPAs or daptomycin carriers for antibacterial purposes. The great majority of them (96 papers) deals with nanoformulations of vancomycin, which is one of the molecules more investigated in absolute in the field of nanoantibiotics (Table 1). Surprisingly, only 3 publications report the preparation of NPs with teicoplanin (Table 2), whereas there are no examples of second-generation GPAs (i.e., dalbavancin, oritavancin, and telavancin) nanosystems. Regarding daptomycin, only 9 are the papers describing its use in nanoformulations (Table 3).

In Tables 1-3, readers could find the information retrieved from this literature search in terms of the type of NPs used to carry vancomycin (Table 1), teicoplanin (Table 2), or daptomycin (Table 3). When available, indications on shapes and sizes of the nanosystems, usually determined by dynamic light scattering or electron microscopy, are also reported.

3.3.1.1. Organic NPs used for vancomycin delivery. The wide diversity of nanosystems used for vancomycin is based on organic and inorganic NPs, or nanocomposites containing both organic and inorganic elements (Fig. 3). Primarily employed are polymeric organic NPs (Fig. 3), including biocompatible natural or synthetic polymers with sizes ranging from a few dozens to hundreds of nanometres, as gelatin (Li et al., 2014; Zhang et al., 2018), silk fibroin (Hassani Besheli et al., 2017), and N,N-dodecyl,methyl-polyethylenimine (DMPEI) (Cardoso et al., 2021). DMPEI is a hydrophobic cationic polymer capable of killing bacteria upon contact and preventing biofilm formation. For instance, vancomycin-loaded DMPEI NPs, coated with hyaluronic acid for further improving their biocompatibility, proved their efficiency against *S. aureus* in treating ophthalmic infections (Cardoso et al., 2021). Another widely used polymeric material is PLGA, an FDA-approved biocompatible and biodegradable synthetic polymer, whose molecular weight and lactide:glycolide ratio might be modulated to control the antibiotic release (Zakeri-Milani et al., 2013). In 2015, Chiang and co-workers created injectable hollow microspheres for the treatment of subcutaneous bacterial infections, formed by a PLGA shell surrounding an aqueous core containing vancomycin and the photothermal agent polypyrrole: their exposure to an external near-infrared (NIR) laser provoked a localized heat, with the double effect of heat-stimulated bacterial damage and heat-related reorganization of the PLGA shell, thus resulting in a controlled vancomycin release at a high local concentration (Chiang et al., 2015). Alternatively, a polymer also widely used for vancomycin nanosystems is chitosan (see, for instance, Cerchiara et al. (2015), Costa et al. (2015), and Kalhapure et al. (2017a)). Characterized by good compatibility, biodegradability, low toxicity and intrinsic antibacterial activity (see section 3.2), thanks to its positive charges, chitosan-based NPs easily interact with the negatively-charged cell walls, thus facilitating antibiotic penetration within the cells (Naskar et al., 2019). In other works, organic polymers were used as stabilizers of interactions between molecules of vancomycin, forming nanoplexes; in the work of Sikwal et al. (2016) the cationic group of vancomycin interacted with the anionic polyacrylic acid sodium, self-assembling in hexagonal cubic-shaped NPs with potent antibacterial activity against MSSA and MRSA strains. The Authors aimed to develop an inhalation delivery system for treating patients affected by cystic fibrosis, suffering from lung infections (Sikwal et al., 2016).

Although liposomes and micelles (Fig. 3), produced by lipid self-assembling, are widely used for drug delivery (Marchianò et al., 2020), relatively few are the examples of nanoliposomes or micelles carrying vancomycin (Cong et al., 2015; Gonzalez Gomez et al., 2019; Sonawane et al., 2020; Uhl et al., 2017; Xu et al., 2020). In 2017, Uhl and co-workers encapsulated vancomycin in liposomes formed by tetraether lipids, commonly found as components of archaea membranes, where they act as stabilizers thanks to their reduced susceptibility to hydrolysis and oxidation. The so-prepared vancomycin liposomal formulation was stable in gastric fluids and showed an improved oral availability, thus suggesting its possible use as an oral delivery system (Uhl et al., 2017). In another work (Xu et al., 2020), vancomycin was co-incapsulated with tungsten sulphite quantum dots in thermal-sensitive liposomes: temperature increase, by laser excitation of the quantum dots, stimulated liposome rupture and vancomycin release. The resulting nanosystem showed promising antibacterial efficacy *in vitro* and *in vivo* against VISA, penetrating and disrupting staphylococcal biofilms (Xu et al., 2020).

A recent alternative to liposomes are the solid lipid NPs (SLNs) (Fig. 3). This term refers to NPs with a hydrophobic internal core composed of natural or synthetic lipids that are solid at room or body temperature, covered by an external stabilizing layer formed by amphiphilic surfactants and co-surfactants (Arana et al., 2021). Characterized by low toxicity, high stability, biodegradability, narrow distribution, and easy production at large scale, SLNs were investigated in a few cases for vancomycin delivery (Kalhapure et al., 2014, 2017b; Mhule et al., 2018; Yousry et al., 2016). In one of them, Kalhapure and colleagues created a dual antibacterial system effective in inhibiting MSSA and MRSA, by loading vancomycin on SLNs formed by linoleic acid that has an intrinsic antibacterial activity (Kalhapure et al., 2014).

Other types of organic NPs for vancomycin delivery are dendrimers (Fig. 3). These are highly symmetrical, globular macromolecules, formed by a central core composed of an atom or group of atoms, surrounded by layers of hyperbranched macromolecules with active terminal surface groups. Antibiotics can be either encapsulated in the interior cavities formed within the branched outer layer, or covalently attached to the terminal surface groups (Alfei and Schito, 2020). As reported below in section 3.3.3.1, when conjugated to PAMAM (4-poly amidoamine) dendrimers, vancomycin conserved the same antimicrobial activity of the free GPA towards Gram-positive bacteria but it became active also against Gram-negative pathogens, probably thanks to an increased permeation through their outer cell membrane (Serri et al., 2018). In addition to classical dendrimers, the lipid-dendrimer hybrid NPs (LDHNs, Fig. 3) combine the positive attributes of both dendrimer and lipid systems. Hence, vancomycin was successfully loaded on hybrids formed by globular PAMAM dendrimer as polymeric core and Compritol 888 ATO (Sonawane et al., 2016) or oleylamine (Maji et al., 2019) as lipid shell. Based on a similar principle, the end groups of poly ester amine dendrimers were modified with the linear block polymer methoxypoly(ethylene glycol)-b-poly (ε-caprolactone), thus creating a linear polymer-dendrimer hybrid (LPDH, Fig. 3) nanosystem, formed by a dendrimer core and a block copolymer shell: this hybrid was capable of self-assembling into nanovesicles, in which vancomycin was efficiently encapsulated (Omolo et al., 2018). Finally, vancomycin was encapsulated into lipid-polymer hybrid NPs (LPHN, Fig. 3), i.e., core-shell nanostructures where a polymeric core is enveloped by a lipid layer and that combine the structural integrity and stability of polymeric material with the biocompatibility of liposomes (Bose et al., 2020; Hassan et al., 2020; Seedat et al., 2016).

3.3.1.2. Inorganic NPs used for vancomycin delivery. Among inorganic nanosystems, the mostly employed for carrying vancomycin are metal and metal oxide NPs (Fig. 3). This popularity derives from various factors, first of all that, as reported in section 3.2, these NPs are known for their intrinsic antibacterial properties, thus exerting a possible synergic and/or additive effect with the loaded antibiotic. In addition, their reduced size facilitates penetration through biological barriers, addressing the carried glycopeptide at specific infection sites and allowing tissue and biofilm localized delivery (Berini et al., 2021; Sánchez-López et al., 2020; Shkodenko et al., 2020). Finally, their synthesis may be relatively easy at laboratory scale; they can be prepared in different shapes, and various protocols are available for their surface functionalization (Berini et al., 2021; Armenia et al., 2018; Hassan et al., 2017). Ag and Au are the preferred metals used for preparing these nanoantibiotics. Vancomycin was conjugated on the surface of spherical

AuNPs (see, for instance, Hur and Park (2016); Lai et al. (2015); Li et al. (2018)) or AgNPs (Hur and Park, 2016; Kaur et al., 2019; Sun et al., 2017; Wan et al., 2011); it was linked to nanocube-shaped AgNPs (Murei et al., 2020), polygonal AuNPs (Wang et al., 2018), Au nanostars (Wang et al., 2019), and Ag microflowers (Wang et al., 2017a). These last were characterized by a highly branched structure that, compared to the smooth surface of conventional spherical NPs, provided a larger surface-to-volume ratio for facilitating the antibiotic contact with bacterial cells and, with a synergistic antibacterial effect, favourited the release of Ag^{+} ions (Wang et al., 2017a) (see section 3.2). In a few papers (Esmaeili and Ghobadianpour, 2016; Hassan et al., 2017; Zhang et al., 2020), vancomycin was conjugated to Fe_3O_4NPs, which offer the advantage to be remotely moved to infection sites by applying an external magnetic field (Dulińska-Litewka et al., 2019), as anticipated above (see section 3.1). In other works, inorganic NPs were covered by biocompatible and non-immunogenic materials to improve their stability and half-life in biological fluids, reducing the risk of agglomeration and opsonization. This was the case of Hassan et al. (2017) and Esmaeili and Ghobadianpour (2016), who covered their magnetic NPs with a monolayer of human serum albumin or with chitosan crosslinked by glutaraldehyde and PEG, respectively.

Another widely used inorganic carriers for vancomycin are mesoporous silica NPs (MSNs, Fig. 3). MSNs are biocompatible, biodegradable, inert, and stable amorphous solids, easily prepared even at large-scale and characterized by high surface area and tuneable particle size and morphology (Bernardos et al., 2019; Gounani et al., 2019; Gu et al., 2016; Hernandez et al., 2014; Kavruk et al., 2015; Mas et al., 2013). MSNs present inner pores and void volumes, in which antibiotics can be efficiently trapped. Notably, the inner cavities of MSNs are characterized by electron-deficient and electron-rich areas. Hence, oppositely charged antibiotics can be easily and simultaneously trapped in different cavities, creating a multi-antibiotic delivery system for fighting polymicrobial infections. Gounani and co-workers co-loaded vancomycin and polymyxin B on MSNs, and these nanosystems were effective against both the Gram-positive *S. aureus* and the Gram-negative *E. coli* and *P. aeruginosa* (Gounani et al., 2019). Surface functionalization of vancomycin-loaded MSNs can be crucial for their antibacterial efficacy. Fulaz and colleagues demonstrated that positively-charged MSNs penetrated more efficiently than bare or negatively-charged NPs into MSSA and MRSA biofilms due to their electrostatic interactions with the negatively charged bacterial peptidoglycan (Fulaz et al., 2020). Surface functionalization with a complementary substrate or an antibody that targets specific structures of the pathogen or virulence factors, might facilitate active targeting of vancomycin towards the pathogens (Van Giau et al., 2019). An example, reported in Table 1, is the vancomycin-loaded MSNs functionalized with an aptamer for the recognition of *S. aureus* surface antigens prepared by Kavruk and co-workers. With their nanosystem, the Authors exploited also another feature of MSNs, i.e., the possibility to control antibiotic release by blocking inner pores with 'molecular gates'. These include organic or inorganic compounds (organic polymers, inorganic NMs, or biomacromolecules) that can respond to specific stimuli (such as pH, temperature, light, or interaction with small molecules) releasing entrapped drug on demand (Bernardos et al., 2019). Hence, upon interaction between the aptamer and *S. aureus* surface antigens, vancomycin was released to inhibit the pathogen. Instead, the antibiotic was not released when the nanoantibiotic was exposed to *S. epidermidis*, confirming the high specificity of the 'molecular gate' system (Kavruk et al., 2015).

3.3.1.3. Nanocomposites and nanohydrogels used for vancomycin delivery. Numerous are the papers listed in Table 1 on the use of nanocomposites, comprising organic and inorganic materials, incorporating vancomycin, mainly formulated for bone regeneration in orthopaedic applications. These NMs have a porous supporting structure, with thermal, morphological and mechanical properties similar to those of the bones, in which cells can penetrate and form a three-dimensional tissue. Organic materials commonly found in these nanocomposites are biodegradable natural polymers as PHVB (poly(3-hydroxybutyrate-co-3-6%hydroxyvalerate)) (Almeida Neto et al., 2019), alginate (Aşik et al., 2019; Yu et al., 2014), zein (Babaei et al., 2019), chitosan (Kimna et al., 2019), and collagen (Suchý et al., 2017), which enhance the biocompatibility of the implants. Inorganic nanofillers as hydroxyapatite (Almeida Neto et al., 2019; Babaei et al., 2019; Suchý et al., 2017; Yu et al., 2014), PMMA (polymethyl methacrylate) (Aşik et al., 2019), calcium sulphate composites (Gu et al., 2016), or montmorillonite (Kimna et al., 2019) are added either to increase the mechanical robustness of implants or to promote osteogenesis and implant osteointegration. This is the case for instance of hydroxyapatite, which is the principal component of mammals' bone and teeth, and it is inserted as external layer of the coating to promote osteointegration of the implant (generally made out of titanium or similar material). The incorporation of vancomycin prevents bacterial biofilm formation on the implant surface, which is one of the most critical challenges in the treatment of bone injuries. To prevent microbial biofilm formation, vancomycin is also directly used for coating medical devices. As an example, Han and co-workers conjugated vancomycin to oxidized sodium alginate and then co-loaded it with chitosan-coated BSA NPs on adhesive poly-dopamine films to be deposited on implantable devices (Han et al., 2015) or directly on titanium scaffolds (Han et al., 2017). Other vancomycin-loaded materials commonly used for orthopaedic or cardiovascular implants are metal-organic zeolitic imidazole framework-8 (ZIF-8) supported by a chitosan scaffold (Karakeçili et al., 2019), PVA/PLGA NPs deposited on titanium plates (Liu et al., 2017), polynorbornene-based NPs immobilized on Ti90A16 V4 alloy (Pichavant et al., 2016), Fe-Ag nanocomposites (Sharipova et al., 2018), or nanotubes made of Ti-6Al-4V alloy (Auñón et al., 2020).

Finally, nanostructured hydrogels (Fig. 3) loaded with vancomycin were recently used for their topical delivery in skin or ocular diseases or as wound dressing material (Pawar et al., 2018; Tao et al., 2020; Yousry et al., 2017). These gels are viscoelastic liquid-like or solid-like materials, made up of a liquid phase immobilized in a solid three-dimensional matrix, with favourable characteristics like biocompatibility, biodegradability, high adsorption capacity, and no toxicity (Kumar et al., 2019). As an example, George and co-workers embedded vancomycin-loaded, vitamin C-coated PCL NPs in injectable PVA-alginate gel, thus creating a nanoparticulate system that, in addition to the antibiotic release at the infectious site, created a moist and acidic environment for promoting faster wound healing (George et al., 2017). A similar principle was followed for impregnating vegetable fibres with vancomycin-loaded chitosan NPs, creating a nanocomposite proposed for replacing cotton in wound care (Cerchiara et al., 2017).

A common trait of these vancomycin-loaded bone fillings, implant coatings and hydrogels, is that the materials employed should allow a sustained and controlled antibiotic delivery, possibly following a two-step release model: a burst release profile in the first hours to overcome local infections in the post-implantation period, has to be followed by a sustained release period of several days or weeks, during which the antibiotic is delivered at a slower rate but in a sufficient amount to protect against bacterial recolonization and biofilm formation (Kimna et al., 2019). As reported in Table 1, examples of vancomycin-loaded nanocomposite materials or hydrogels with this two-step release profile are illustrated in Almeida Neto et al. (2019), Aşik et al. (2019), Babaei et al. (2019), Gu et al. (2016), Han et al. (2015), Kimna et al. (2019), Liu et al. (2017), Parent et al. (2016), Pawar et al. (2018), Posadowska et al. (2016), Suchý et al. (2017), Tao et al. (2020), Xiang et al. (2018), Yu et al. (2014).

3.3.1.4. Nanosystems used for teicoplanin delivery. Teicoplanin clinical efficacy is comparable to -if not better than- vancomycin, being conveniently administered once-a-day instead of twice-a-day, and having less

adverse effects than vancomycin (see section 2). Nevertheless, as reported in Table 2, only three research groups investigated its potential in nanoformulations. Target delivery of teicoplanin was realized by using PLGA NPs functionalized with an aptamer for the specific binding to *S. aureus* cell surface antigens (Ucak et al., 2020). Compared to the free antibiotic, teicoplanin encapsulated in aptamer-PLGA NPs showed a 32-fold and a 64-fold MIC decrease for MSSA and MRSA, respectively. In a different paper, teicoplanin was covalently conjugated to magnetic Fe_3O_4NPs, conserving its antimicrobial activity *in vitro* and being active against *S. aureus* biofilms, to which it could be directed using an external magnet (Armenia et al., 2018). Finally, Gonzalez Gomez and co-workers extended to teicoplanin the use of nanoliposomes. However, differently from what they observed for vancomycin, which fully retained its antimicrobial activity after encapsulation, the potency of nanocaptured teicoplanin against *S. aureus* declined as a result of the sonication required for nanoliposome generation (Gonzalez Gomez et al., 2019).

3.3.1.5. Nanosystems used for daptomycin delivery. In the nine papers dealing with the nanosystems carrying daptomycin, a common goal was improving the antibiotic efficacy, consequently reducing the administered doses and mitigating the risk of AMR insurgence. Daptomycin-loaded chitosan NPs (Silva et al., 2015) and chitosan-coated alginate NPs (Costa et al., 2015) were investigated as non-invasive alternatives for the treatment of endophthalmitis. Applied directly to eyes, these nanoformulations reduced the toxicity associated with daptomycin systemic administration, while extending the drug contact time on the cornea due to the adhesive properties of chitosan (Costa et al., 2015; Silva et al., 2015). Flexible liposomes formed by lecithin and sodium cholate encapsulating daptomycin were used to treat topical infections by *S. aureus* (Li et al., 2013).

Among the inorganic nanosystems, ultra-small Ag and Au nanoclusters, packed with the antibiotic covalently bound onto them, were generated and used to create networks of hybrid antibacterial agents: the localization of daptomycin on the network surface facilitated its lipid tail insertion into bacterial membranes, synergistically potentiating the intrinsic antimicrobial activity of Au and Ag (see section 3.2) (Zheng et al., 2017, 2019). Thanks to daptomycin amphiphilic nature, self-assembled micelles containing the antibiotic were used to build Au nanoflowers, with both antibacterial and antitumor properties (Wang et al., 2020a). In 2016, Meeker and co-workers prepared polydopamine-coated Au nanocages loaded with daptomycin and conjugated with an antibody allowing the release of the entrapped antibiotic only after recognition of *S. aureus* species-specific surface protein A (Spa) (Meeker et al., 2016). The specificity of this system was demonstrated by the lack of interaction with mammalian cells and with the Spa-deficient *S. epidermidis*. Two years later, the same group expanded this approach creating daptomycin-loaded Au nanocages conjugated with alternative antibodies targeting *S. aureus'* lipoprotein Lpp or the manganese transporter SACOL0688, both expressed at higher levels by biofilm-embedded *S. aureus* cells (Meeker et al., 2018). Notably, in both cases the antibacterial efficacy of the systems against MSSA and MRSA was enhanced upon NIR irradiation, which caused not only a laser-induced photothermal effect attributable to the stimulated Au nanocage and resulting in a physical destruction of bacterial cells, but also a destabilization of the polydopamine coating leading to antibiotic release. Finally, Tong and co-workers co-conjugated daptomycin and AgNPs on reduced graphene oxide (Fig. 3), thus generating a nanocomposite with marked and cooperative antibacterial activity against Gram-positive bacteria (Tong et al., 2019). While graphene oxide has been widely used in the last decade for anticancer drugs delivery (Dash et al., 2021), its employment as antibiotic carrier has been so far less exploited; it would likely merit further investigations considering its intrinsic antibacterial properties (see section 3.2).

3.3.2. Antibiotic release by GPAs and daptomycin nanocarriers

As anticipated in the previous sections, the possibility to control antibiotic release represents one of the substantial advantages of nanosystems. For this reason, the information, whenever available, on the conditions regulating the antibiotic release in the different nanosystems hereby described, has been included in Tables 1-3.

As reported in section 3.3.1.3, vancomycin is commonly included in nanocomposite materials used for bone fillings, implant coatings, and hydrogels. For these applications, we anticipated that vancomycin should be released following a two-step model (Canaparo et al., 2019), which implies that antibiotic release has to be controlled over time. After a first burst, a long-term release controlling the local antibiotic concentration is essential to prevent bacterial infection without causing systemic toxicity (Kimna et al., 2019; Parent et al., 2016). Vancomycin absorbed on surface of the NM and/or interacting with it by electrostatic attractions is fast released in the first hours after implantation, whereas antibiotic molecules hidden in the internal cavities and/or interacting with the NM with covalent bonds slowly diffuse at a latter period, usually with a slow zero or first order release kinetics. The composition and porosity of the NM can be modulated to support antibiotic long-term delivery and each drug delivery system performs differently from the other (Table 1). Consequently, different mathematical models can be applied to describe antibiotic release kinetics and have to be determined on an empirical base (Pourtalebi Jahromi et al., 2020).

A different concept is at the base of the antibiotic release that can be achieved by using stimuli-responsive NPs, i.e., materials that undergo structural or chemical changes in response to specific external stimuli, thus allowing localized drug delivery. These stimuli can be remotely-applied, as a magnetic field (Harris et al., 2017; Mohapatra et al., 2018) or a temperature shift caused by laser treatment (Chiang et al., 2015; Xu et al., 2020), or they can be determined by the microenvironment conditions created by infection and inflammation, as the acid pH or the presence of excreted enzymes as esterases or gelatinases at infections sites (Li et al., 2014). Thus, stimuli-responsive NPs offer the advantage that the antibiotic is suddenly released in the targeted biological compartment, minimizing the risk of systemic side effects and antibiotic accumulation in healthy tissues, and reducing the exposure of commensal microbiota (Canaparo et al., 2019). For instance, magnetically-responsive nanostructures were generated by co-loading vancomycin and superparamagnetic Fe_3O_4NPs on chitosan microbeads (Harris et al., 2017; Mohapatra et al., 2018). Their exposure to a high-frequency, alternating magnetic field caused vancomycin release rate up to 200 % compared to samples not stimulated by magnetic excitation, from which the antibiotic was slowly and only partially released by diffusion (Mohapatra et al., 2018). On-demand release of vancomycin was achieved also by loading it on core-shell supramolecular gelatin NPs, covered with red blood cell membranes to improve their biocompatibility: drug release upon incubation with gelatinase-positive bacteria as *S. aureus* or *P. aeruginosa* was up to 92 %, compared to a 20 % cumulative release achieved with gelatinase-negative bacteria (Li et al., 2014). Following a similar approach, daptomycin was released from Au nanocages after the recognition between their conjugated surface antibodies and the *S. aureus* surface proteins (Meeker et al., 2016, 2018, see section 3.3.1.5). Even more frequently, nanoantibiotics delivery systems are pH-sensitive, i.e., they are designed to permit the antibiotic release only at the acidic pH that is typical of bacterial infection sites. Change in the pH causes electrostatic repulsive forces that result in swelling, deswelling, or breakdown of the carrier, with the consequent release of the encapsulated antibiotic (Canaparo et al., 2019). PLGA-PEG-alendronate micelles (Cong et al., 2015), chitosan NPs (Kalhapure et al., 2017b), chitosan-based lipid-polymer hybrid nanovesicles (Hassan et al., 2020), hyaluronic acid-coated ZIF-8 (Liu et al., 2020), oleylamine-PAMAM dendrimer hybrid NPs (Maji et al., 2019), and N-(2-morpholinoethyl) oleamide SLNs (Mhule et al., 2018), are among the pH-responsive nanosystems reported for vancomycin delivery (Table 1). In addition to these, vancomycin was encapsulated in micelles of the

AB2-type amphiphilic block copolymer, containing a hydrazone linkage rapidly hydrolysing at acid pH (Sonawane et al., 2020). Vancomycin was also bound to nanocomposites composed of a blend of PLGA, PEG, Eudragit E100, and ZWC, this last being a chitosan derivative that is positively charged only at acid pH, thus enhancing drug release through electrostatic repulsion of E100-bound vancomycin (Pei et al., 2017). And, finally, vancomycin was encapsulated into SLNs formed by the acid cleavable lipid SA-3M (Kalhapure et al., 2017b).

3.3.3. *Microbiological activity of nanoconjugated GPAs and daptomycin*

Considering the variety of nanosystems used to carry vancomycin, and, although to a much less extent, teicoplanin and daptomycin, it is intuitive that a comparative evaluation of their antimicrobial activity is not an easy task. Different formulations confer peculiar chemical and physical properties to the diverse nanosystems, making almost impossible a direct comparison of their efficacy. As described in many papers reported in Tables 1-3, even comparing the activity of the nanoconjugated antibiotic versus its nonconjugated control is not straightforward, since the intrinsic antimicrobial activity of the NPs used, as well as their changed water solubility, pH stability, external charge, and lipophilicity alter the antimicrobial profile of the carried molecule *per se*. To give a practical example, when the antimicrobial activity is measured as the diameter of pathogen inhibition halo around the antibiotic spot, the nanoconjugated antibiotic might diffuse into the agar medium differently from the free antibiotic (Armenia et al., 2018), making the results difficult to be interpreted. This scenario is further complicated by the different methods that various Authors used to test the antimicrobial activity. In a very few papers MICs were reported (see, for instance, Lai et al. (2015) or Booysen et al. (2019)). In others, microdilution assays following the Clinical and Laboratory Standard Institute (CLSI) guidelines (Simon et al., 2020), or the National Committee for Clinical Laboratory Standards indications (Hassan et al., 2017), among others, Kirby-Bauer tests (Chiang et al., 2015; Posadowska et al., 2016), or time killing (Chakraborty et al., 2012a) assays were instead used. With the aim to provide the readers with an overview of the antimicrobial potential of the different nanosystems discussed in this review, in Tables 1-3 the list of bacteria against whom the nanoantibiotics proved to be effective *in vitro* is reported, together with indications on whether the nanoconjugation conferred an improved, diminished, or comparable antibacterial potency in comparison to the free antibiotic. Another column of Tables 1-3 includes data on the studies conducted to investigate the *in vivo* antibacterial activity of the antibiotic nanosystems. Only a couple dozen among the papers on vancomycin-based nanosystems reported *in vivo* studies, they were two for daptomycin, and none for teicoplanin, indicating that further investigations in this sense are probably needed to better understand the clinical potential of nanoconjugated antibiotics. Animal models for skin infections (e.g., Tong et al., 2019), subcutaneous abscesses (e.g., Guo et al., 2020), osteomyelitis (e.g., Zhang et al., 2017), or pneumonia (Liu et al., 2020) were employed. Generally, mice models were the most used (e.g., Chen et al., 2015; Hassan et al., 2020; Omolo et al., 2018; Xu et al., 2020; Zou et al., 2020), but also rabbits (Auñón et al., 2020; Chen et al., 2019; Tao et al., 2020; Zhang et al., 2017), rats (Croes et al., 2018; Hassani Besheli et al., 2017), and zebrafish larvae (Zhang et al., 2018) were utilized.

3.3.3.1. *Antibacterial activity of vancomycin loaded on organic NPs.*

Vancomycin loaded on NPs formed by biocompatible polymers generally maintains an antibacterial activity comparable to nonconjugated vancomycin, although some exceptions are reported (Cardoso et al., 2021; Posadowska et al., 2016). Vancomycin loaded on core-shell supramolecular gelatin NPs, covered with red blood cell membranes, presented a MIC comparable to the one of the control antibiotic (3 versus 1.5 μg/ml, respectively, towards a gelatinase-producing *S. aureus*) (Li et al., 2014). NIR-irradiated PLGA NPs containing vancomycin and polypyrrole (HM-Van-PPyNPs) showed *in vitro* the same inhibition halos than the control free antibiotic. However, when injected in a murine model with a subcutaneous abscess caused by a MRSA strain, NIR-irradiated HM-Van-PPyNPs exerted a stronger bactericidal effect than the free antibiotic (80 % reduction of viable bacterial cells *vs* 50 % for the bare GPA) (Chiang et al., 2015). In Simon et al. (2020), PVA or DMBA (didodecyldimethylammonium bromide) surfactants were added to the NPs preparation: DMBA-added NPs were more active and the Authors hypothesized that their positive charge, combined with the small size, favoured the interaction with bacteria and, consequently, the antibiotic up-take (Simon et al., 2020). Booysen and co-workers found that the MIC of vancomycin encapsulated in PLGA NPs was about 5-fold lower than the control antibiotic against MRSA and MSSA (Booysen et al., 2019). On a contrary, in the study of Lotfipour and colleagues, PLGA NPs-carried vancomycin was found generally less active versus a large number of *S. aureus* clinical strains (40 isolates) than the free vancomycin. In this case, Authors hypothesized that the hydrophobic and negatively charged PLGA NPs associated strongly with the cationic vancomycin, slowing down its release (Lotfipour et al., 2014).

Chitosan-carried vancomycin performed as free vancomycin in batch systems measuring the decay in the growth curves of *S. aureus* exposed to high antibiotic concentration (Cerchiara et al., 2015). Differently, a synergic effect between vancomycin and chitosan (see section 3.1), and therefore a potentiated antibacterial activity, were highlighted in other papers, as for example in Zhang et al. (2017) or Chakraborty et al. (2012a). In the latter, an exhaustive microbiological study was used to characterize folic acid-tagged chitosan NPs. Nanocarried vancomycin showed MICs significantly lower than the free GPA on VSSA (vancomycin sensitive *S. aureus*) and VRSA, with a more rapid bactericidal activity. In morphological studies, a reduction of cell wall thickness was observed after bacterial interaction with chitosan NPs, likely leading to cytoplasmic membrane leakage (Chakraborty et al., 2012a). Enhanced bioactivity against MRSA upon laser irradiation was observed also by Guo and co-Authors for their multi-component NPs, formed by the photothermal polymer polypyrrole and methacrylate, and loaded with both vancomycin and oleic acid (Van-OA@PPy). Combining the antibacterial activity of both vancomycin and oleic acid, with the photothermal activity upon NIR irradiation of polypyrrole, allowed MRSA eradication at a dose of 250 μg/ml, 2- and 4-fold lower than that required to obtain an equivalent result with polypyrrol or vancomycin/oleic acid alone, respectively. Consistently, in mice model, irradiated Van-OA@PPy were more effective than any other condition tested for reducing subcutaneous abscesses (Guo et al., 2020).

No difference in the MIC values (1.7 μg/ml) was observed between auto-assembled vancomycin in nanoplexes and the control antibiotic against both MSSA and MRSA (Sikwal et al., 2016). Differently, the MIC of the vancomycin delivered by the auto-assembled micelles of PLGA-PEG-alendronate at physiological pH was higher than for the free antibiotic, 16 and 2 μg/ml, respectively (Cong et al., 2015). Liposome-carried vancomycin generally showed the same activity of the free antibiotic if the delivery system responded adequately to an external stimulus, completely releasing the encapsulated antibiotic, for example after the liposome boost induced by Triton-X (Gonzalez Gomez et al., 2019). Vancomycin encapsulated in micelles of the amphiphilic block polymer [OA-C=N-NH-$(PEG)_2$] showed the same MIC of the free antibiotic (0.97 μg/ml) against MRSA and MSSA, but its antimicrobial activity was definitely lasting more at the infection site particularly at acid pHs (Sonawane et al., 2020). The antimicrobial activity of vancomycin carried by SLNs resulted generally higher than the free antibiotic (Kalhapure et al., 2014, 2017b). The Authors hypothesized that the increased lipophilicity of SLNs could facilitate bacterial membranes crossing (Kalhapure et al., 2014). Mhule and colleagues prepared pH-responsive SLNs, able to release their cargo in the acid environment at the infection sites (see section 3.3.2). In this case, free vancomycin was more sensitive to acid pH than the nanoconjugated version, probably due to decreased GPA solubility. In mice models for skin infection, this nanosystem determined a 4.14-fold higher reduction in MRSA load than

the bare vancomycin, confirming that GPA encapsulation in SLNs favoured its antimicrobial action (Mhule et al., 2018). Salih and co-Authors developed a novel sugar-based cationic amphiphile derivative (BCD-OLA) from a β-cyclodextrin head and long C18 carbon chain with a terminal amine oleylamine for antibiotic delivery. The microdilution test showed MIC values of BCD-OLA/vancomycin 2- and 4-fold lower than that of the free vancomycin, versus both MSSA and MRSA, respectively (Salih et al., 2020).

As already cited in section 3.3.1.1, vancomycin encapsulated in dendrimers maintained its MICs towards Gram-positive MSSA and MRSA, but it gained some activity against Gram-negative bacteria (Serri et al., 2018). Indeed, compared to the free antibiotic, vancomycin-PAMAM dendrimers allowed a significant decrease in MIC values against *E. coli, Klebsiella pneumoniae, Salmonella typhimurium,* and *P. aeruginosa*, probably due to the cationic nature of the dendrimers adhering to the anionic outer membrane of Gram-negative bacteria, favouring vancomycin penetration (Serri et al., 2018). A clear advantage observed after GPA loading on LDHNs (Sonawane et al., 2016) or on LPDHs (Omolo et al., 2018) was a prolonged antibacterial action on MSSA and MRSA, as a result of the antibiotic controlled release. For example, Omolo and co-workers proved that after 24-h treatment, the MIC for vancomycin carried on the LPDH 3-mPEA was 7- and 16-fold lower than that of free vancomycin against MSSA and MRSA, respectively. Such potentiated activity was also highlighted *in vivo*, as a 20-fold reduction in MRSA population in a skin infection mice model, compared to free vancomycin administration, was observed (Omolo et al., 2018). A potentiated and prolonged antibacterial activity was highlighted also when vancomycin was loaded on pH-sensitive LDHNs formed by PAMAM dendrimers and oleylamine (Maji et al., 2019). After 72-h treatment, LDHNs-loaded vancomycin showed MIC values 4- and 8-fold times lower than the free antibiotic at pH 7.4 and 6.0, respectively. In the same study, through a co-culture assay conducted on HEK 293 cells infected with MRSA, Authors proved the ability of the nano-antibiotic to kill intracellular bacteria upon cellular uptake. After 22-h incubation with a 5x MIC concentration, bacteria viable count after eukaryotic cell lysis was significantly lower in cells treated with vancomycin-loaded LDHNs than in untreated HEK 293 cells or in cells exposed to bare vancomycin (Maji et al., 2019).

Other hybrid nanosystems that proved effective in enhancing the antibacterial activity of vancomycin are reported in Table 1 and include the chitosan-, oleic acid-, and sodium alginate-based LPHNs prepared by Seedat et al. (2016), or the similar pH-responsive, chitosan- and oleylamine-based LPHNs synthesized by Hassan et al. (2020). In the first case, the fractional inhibiting concentration (FIC) index showed a synergistic effect between vancomycin, oleic acid, and chitosan as a plausible explanation for the increased susceptibility of MRSA to the nanosystem (Seedat et al., 2016). Instead, in the second paper the same methodological approach revealed an additive, rather than a synergic, effect between the different components of the nanostructure: the outcome was approximately 53-fold and 13-fold improvement of the antibacterial activity against MRSA, at pH 6.0 and 7.4, respectively. The nanosystems proved effective in killing MRSA also in a murine model of infection, with a 95-fold improvement in its efficacy compared to free vancomycin (Hassan et al., 2020).

3.3.3.2. Antibacterial activity of vancomycin carried by inorganic NPs. As stated in section 3.3.1.2, different papers reported in Table 1 describe vancomycin conjugation to NPs formed by the metals Ag and Au. In some cases, the nanoantibiotic maintained an antimicrobial potency similar to the one of the free vancomycin, as in the vancomycin-loaded peptide-protected Au nanocluster generated by Li and colleagues: exposure to Gram-positive bacteria triggered an 'on demand' vancomycin release, resulting in a comparable antimicrobial activity to free vancomycin against *S. aureus, Bacillus subtilis,* and *Bacillus cereus* (Li et al., 2018). In other papers, instead, the antibiotic conjugation conferred an increased efficacy to vancomycin. As example, Lai and co-Authors inhibited *S. aureus* growth by means of vancomycin immobilized on spherical AuNPs, recording MIC values 4- and 8-fold lower than the free GPA towards MSSA and MRSA, respectively (Lai et al., 2015). Similarly, when antibiotic-loaded AgNPs were tested by Sun et al., they prevented *Mycobacterium smegmatis* growth in suspended cultures more efficiently than the free antibiotic, being better internalized into the bacterial cells, as highlighted by transmission electron microscope observations and UV-vis analysis (Sun et al., 2017).

An additional common outcome of vancomycin conjugation to AuNPs or AgNPs was the extension of the GPA antimicrobial activity spectrum to Gram-negative bacteria (Kaur et al., 2019; Ma et al., 2020; Wang et al., 2017a). Vancomycin-modified magnetic-based Ag microflowers were effective in killing both MRSA and *E. coli*, being the Gram-negative more sensitive than *S. aureus* (Wang et al., 2017a). Authors hypothesized a possible alteration of *E. coli* membrane permeability caused by the nanosystem, favouring both Ag^+ ion penetration and the display of D-Ala-D-Ala groups to whom vancomycin could bind (Wang et al., 2017a). A synergic effect between AgNPs and the GPA was also observed against both *S. aureus* and *E. coli* by vancomycin loaded on citrate-capped AgNPs (Kaur et al., 2019). Au and AgNPs proved effective also as part of combined therapies summing synergistically vancomycin antimicrobial effect and the photothermal activity of the metallic nanocarrier (Ma et al., 2020; Wan et al., 2011; Wang et al., 2018). When administered to suspended cultures of two clinical isolates of VREs in dark conditions, vancomycin-modified polygonal-shaped Au nanostars (AuNSs@Van) caused a dose-dependent killing rate, higher than the one determined by an equivalent concentration of free vancomycin. Upon NIR irradiation, the amount of AuNSs@Van required for inhibiting VREs was 16-fold lower than that of free vancomycin (Wang et al., 2018). Wan and colleagues combined the antibacterial activity of vancomycin and that of Ag^+ ions with the photocatalytic response of TiO_2: when irradiated under UV light for 1 h in the presence of VanAg@TiO_2, a 7-log unit decrease in the viability of a Gram-positive sulphate-reducing bacterium was observed. Such killing rate was higher than that elicited by the same nanosystem under dark incubation (2-log unit decrease), and than that of unfunctionalized Ag@TiO_2 (1-log unit reduction) (Wan et al., 2011).

Conjugation of vancomycin to inorganic magnetic NPs, generally conferred an improved antimicrobial activity to the GPA. In a microdilution liquid test, vancomycin-loaded $MnFe_2O_4$ NPs, with chitosan crosslinked by glutaraldehyde as shell and PEG modification, showed decreased MIC values compared to free vancomycin against MSSA, MRSA, *S. epidermidis,* and *B. subtilis* (Esmaeili and Ghobadianpour, 2016). With a similar approach, Hassan et al. demonstrated that vancomycin covalently bound to magnetic NPs, coated by human serum albumin, showed 18-fold and 6-fold reduction in MICs towards VanB-type *E. faecalis* and VRSA, respectively, if compared to free vancomycin (Hassan et al., 2017). A clearer expansion of vancomycin antimicrobial spectrum towards Gram-negative bacteria was achieved by Zhang and co-workers by conjugating vancomycin-entrapped PVA-coated Fe_3O_4NPs with a cell-penetrating hexapeptide sequence: while the free GPA was active almost exclusively on *S. aureus*, nanoconjugated vancomycin was effective both on *S. aureus* and on *E. coli*, even at low concentrations, thanks to the NPs internalization, as showed by confocal microscope analysis (Zhang et al., 2020).

Loading vancomycin onto MSNs, as investigated in some of the papers reported in Table 1, was another efficient strategy to simultaneously treat a wide spectrum of pathogens. This goal could be achieved by conjugating different antimicrobials on the same MSNs, as done by Mas et al. (2013) with vancomycin and ε-poly-L-lysine, or by Gounani et al. (2019) uploading vancomycin and polymyxin B. By acting on the outer membrane of Gram-negative bacteria, polymyxin B facilitated vancomycin access to its site of action. Consequently, in time-kill curves, the nanosystem showed additive and synergic effect on *E. coli* and *P. aeruginosa*, respectively (Gounani et al., 2019; see also section 3.3.1.2). Specific vancomycin release in the presence of the target

pathogen was pursued by creating so-called 'molecular gate' systems, by co-loading the antibiotic on mesoporous-silica nanocapsules with a probe for *S. aureus* recognition (Hernandez et al., 2014; Kavruk et al., 2015). This probe could be an oligonucleotide degraded by micrococcal nucleases secreted by *S. aureus* (Hernandez et al., 2014), or an aptamer recognizing *S. aureus* receptors (Kavruk et al., 2015). In both cases, the probe functioned blocking the nanopore and allowing vancomycin release only when the nanosystem entered in contact with the pathogen (see section 3.3.1.2): MIC values showed a slightly better performance of the nanoconjugated GPA on *S. aureus* compared to free vancomycin (Hernandez et al., 2014; Kavruk et al., 2015).

3.3.3.3. Antibacterial activity of vancomycin included in nanocomposites and nanohydrogels. Generally, vancomycin included in the multiple nanocomposites described in Table 1, for bone fillings in orthopaedic applications, implant coatings, or nanostructured hydrogels, fully maintained its antimicrobial activity. Vancomycin controlled release (see also sections 3.3.1.3 and 3.3.2) from orthopaedic free-standing polydopamine films based on alginate/chitosan/BSA NPs (Han et al., 2015), porous hydroxyapatite implants (Parent et al., 2016), or collagen/hydroxyapatite layers (Suchý et al., 2017), proved effective in inhibiting the growth of multiple pathogens, including MRSA, *S. epidermidis*, *E. faecalis*, with a higher efficacy than the corresponding un-loaded nanocomposite (Suchý et al., 2017). ZIF-8 scaffolds, commonly used for orthopaedic applications, functionalized with hyaluronic acid (Liu et al., 2020), folic acid (Chowdhuri et al., 2017), or polyacrylic acid (Chen et al., 2019), and then loaded with vancomycin, were able to reduce the bacterial adhesion, although at different extent. The best formulation was a multifunctional metal-organic material based on ZIF-8, encapsulating vancomycin and functionalized with folic acid, which showed a significantly lower MIC value, in comparison to other combinations, against MDR *S. aureus*. Authors indicated that this potentiated activity could be ascribed to folic acid, which likely improved vancomycin cell penetration through endocytosis, enhancing its antibacterial activity (Chowdhuri et al., 2017). In another paper, entrapment of vancomycin in porous iron-carboxylate metal-organic framework (MOF-53(Fe)@Van) resulted in a dose-dependent killing activity over *S. aureus* that was slightly lower (92 %) than that achieved with free vancomycin (ca. 99 %) or with MOF-53 mixed with free vancomycin (96 %), probably due in this case to the gradual release of the antibiotic from MOF-53(Fe)@Van (Lin et al., 2017). Numerous are the examples reported in Table 1 of nanocomposites based on titanium scaffolds, in the form of titanium plates with deposited vancomycin-carrying PVA/PLGA NPs (Liu et al., 2017), titanium alloy grafted with polynorbomene-based NPs (Pichavant et al., 2016), titanium nanotubes capped by folic acid onto the surface of ZnO quantum dots (Xiang et al., 2018), or titanium scaffolds with alginate/chitosan/BSA NPs (Han et al., 2017). In all of them, vancomycin release conferred to these nanocomposites a relevant antibacterial activity against staphylococci, with a killing effect generally higher at acid pH, as a result of the increased antibiotic release in acid environment (Liu et al., 2017; Xiang et al., 2018) (see section 3.3.2).

Co-loading of multiple antibiotics on nanocomposites offers the advantage to prevent multi pathogen infections. This was the case of the vancomycin- and gentamicin-loaded nanoclay composite, formed by chitosan/montmorillonite, produced by Kimna et al.: bacteria colonization was prevented at low antibiotic concentration (0.25 μg/ml of vancomycin and gentamycin for *E. coli*, 0.75 μg/ml vancomycin and 2 μg/ml gentamycin for *S. aureus*) and the antimicrobial activity lasted for at least 25 days (Kimna et al., 2019). With a similar principle, Chen and colleagues co-loaded vancomycin, AgNPs, and the broad-spectrum photosensitizer methylbenzene blue on pH-responsive ZIF-8-polyacrlic acid scaffolds, creating a multifactorial system with activity against both Gram-positive (MSSA and MRSA) and Gram-negative (*E. coli*) bacteria. The killing rate, especially on MRSA, was potentiated by irradiation at 630 nm for 5 minutes (Chen et al., 2019).

Vancomycin included in the different nanostructured hydrogels listed in Table 1 generally showed a higher and more prolonged antimicrobial activity than the free antibiotic (George et al., 2017; Pawar et al., 2018; Tao et al., 2020). As an example, the thermosensitive hydrogel recently engineered by Tao and co-workers, containing vancomycin-loaded chitosan NPs (VCM-NPs/gel), was proven to be more effective against *S. aureus* than the equivalent gel supplemented with free vancomycin (VCM/Gel). VCM-NPs/Gel maintained the antimicrobial activity for more than 20 days, while the supplemented VCM/Gel lost it in less than 10 days. When tested in a rabbit model for osteomyelitis, VCM-NPs/gel controlled effectively the infection and accelerated bone regeneration (Tao et al., 2020). Finally, the wound dressing prepared by Cerchiara et al. with Spanish broom fibres impregnated with vancomycin-loaded chitosan NPs, demonstrated an increased inhibitory activity on *S. aureus* than that exerted by vancomycin alone, or by Spanish broom fibres combined with free vancomycin (Cerchiara et al., 2017).

3.3.3.4. Antibacterial activity of nanosystems carrying teicoplanin. As previously anticipated, in the three papers reporting about teicoplanin nanosystems (Table 2), the antibiotic was included in PLGA NPs functionalized with a *S. aureus* aptamer (Ucak et al., 2020), or covalently conjugated to magnetic Fe_3O_4NPs (Armenia et al., 2018), or finally encapsulated in nanoliposomes (Gonzalez Gomez et al., 2019). The different outcomes of these nanoformulations in terms of antibiotic activity are described in section 3.3.1.4. Hereby, we would like to highlight that the most comprehensive microbiological study used to describe the influence of nanoconjugation on the antibiotic activity is the one of Armenia et al. (2018), where different microbiological methods were used including disc diffusion agar test, broth dilution method, killing kinetic experiments, and transmission electronic microscopy analyses. The integration of these approaches demonstrated that the nanoantibiotic was effective in inhibiting the growth of a panel of Gram-positive bacteria, including pathogens of clinical relevance as MRSA and VanB-type *E. faecalis*, with an efficacy that was only slightly reduced when compared to the free GPA. By fluorescence and transmission electron microscopy, Authors proved that naked Fe_3O_4NPs interacted with Gram-positive and Gram-negative bacteria, partially altering cell morphology and favouring the formation of cellular clusters, but their interaction was only transient and bacteriostatic, significantly different from the bactericidal action of the carried antibiotic (Armenia et al., 2018).

3.3.3.5. Antibacterial activity of daptomycin-loaded nanosystems. As reported in section 3.3.1.5, nine papers describe daptomycin-carrying nanosystems (Table 3). The antibiotic was loaded on chitosan-coated alginate NPs (Costa et al., 2015) or on chitosan NPs (Silva et al., 2015). Slightly different was the result in terms of antibacterial activity. In the first case, microdilution tests did not highlight any significant difference ($p > 0.05$) among the MICs of free or entrapped daptomycin over a panel of staphylococci (Costa et al., 2015). In the paper by Silva and co-Authors, the same technique revealed a decrease in antimicrobial susceptibility of 2-to-4 fold when daptomycin was encapsulated in the nanosystems; this reduction was imputed to chitosan, which may bind to the negatively charged bacterial surface and block daptomycin access to its binding sites (Silva et al., 2015). In a third paper, Li et al. demonstrated that loading daptomycin on flexible nanoliposomes could enhance its skin permeation capacity, maintaining the antibiotic bacteriostatic activity against *S. aureus,* indicating the potential of this nanosystem to be used for topical skin therapy (Li et al., 2013).

When daptomycin was loaded onto inorganic nanocarriers, its antimicrobial activity was generally potentiated by the interaction of the metallic nanoclusters with the cell membrane, favouring the antibiotic mode of action (see section 3.2) (Zheng et al., 2016, 2019). Upon

treatment of *S. aureus* cultures, nanoformulations of daptomycin-conjugated Ag nanoclusters (Zheng et al., 2016) and of daptomycin-loaded Au nanoclusters (Zheng et al., 2019) showed an improved inhibitory effect compared to the bare antibiotic and to the mere mixture of daptomycin with the NPs. Combining daptomycin antibacterial activity with the photothermal stress induced by laser irradiation of the metallic nanocarrier was another approach giving promising results (Table 1). When daptomycin-Au nanoflowers were irradiated at 808 nm, an increased antimicrobial activity was observed not only against *S. aureus*, but also on *E. coli*, widening the antibiotic antimicrobial spectrum (Wang et al., 2020a). Irradiation of polydopamine (PDA)-coated Au nanocages loaded with daptomycin determined an additive eradication activity against different *S. aureus* strains. As already described in section 3.3.1.5, the efficacy and the specificity of the nanostructure was further improved by co-conjugating antibodies specific for *S. aureus* surface proteins, whose recognition enhanced the nanoantibiotic localization at the bacterial cell surface and triggered daptomycin controlled release at infection sites (Meeker et al., 2016, 2018).

Finally, as anticipated in section 3.3.1.5, Tong and colleagues prepared nanocomposites in which reduced graphene oxide was used for simultaneously anchoring AgNPs and daptomycin (rGO@Ag@Dap). *In vitro* microdilution test, agar diffusion assay, confocal microscopy study, and kinetic-killing experiments, together with *in vivo* tests in mice model for skin infection, clearly demonstrated that rGO@Ag@Dap exhibited an enhanced antibacterial activity on *S. aureus* compared to AgNPs and free daptomycin (Tong et al., 2019). Authors hypothesized a slow release of Ag^{+} ions and daptomycin, with consequent membrane damage -as shown by confocal microscopy analysis-, stress induction and, ultimately, cell death (Tong et al., 2019).

3.3.4. Nanoconjugated GPAs and daptomycin activity against biofilms

If the comparison of the antimicrobial potency among the variety of NPs used to carry GPAs and daptomycin is challenging (as reported in section 3.3.3), the task becomes even more complicated for the anti-biofilm potential of these nanosystems due to the lack of standardized methods. Relatively few are the papers in the last decade dealing with the use of nanoantibiotics against biofilm formation, but their number has progressively increased during the last years, as highlighted in Tables 1-3. This is not surprising due to the alarming incidence of difficult-to-threat infections caused by biofilm formation especially among hospitalized and/or elder populations (see Introduction) (Bowler et al., 2020).

3.3.4.1. Antibiofilm activity of vancomycin-carrying nanosystems. Among organic polymeric NPs used to carry vancomycin (Table 1), in the study of Chakraborty et al. -already cited in section 3.3.3.1-, free vancomycin and vancomycin-loaded folic acid-tagged chitosan NPs were compared in inhibiting the formation of VSSA and VRSA biofilms in borosilicate glass tubes. Crystal-violet staining proved that nanoconjugated vancomycin significantly decreased ($p < 0.05$) biofilm formation of both VSSA and VRSA strains, by 53.11 % and 42.86 %, respectively. Free vancomycin was effective only on VSSA, with an inhibition rate of 25.19 % (Chakraborty et al., 2012a). In another work, when a 4-day old MRSA biofilm grown on coverslip was treated for 12 h with vancomycin loaded on chitosan- and oleylamine-based LPHNs, a substantial biofilm eradication was detectable (Hassan et al., 2020). Anti-biofilm activity was observable also for nanoliposomes co-encapsulating vancomycin and photothermal WS_2 quantum dots under NIR irradiation (Xu et al., 2020), and for vancomycin loaded on LPDHs (Omolo et al., 2018). In the study of Fulaz and co-workers, biofilm penetration and anti-biofilm activity of MSNs with different surface functionalization (bare, amine, carboxyl, or aromatic) were compared. Positively charged MSNs (amine- or aromatic-functionalized) primarily localized around bacterial cells in MSSA and MRSA biofilms, while negatively charged MSNs (bare or carboxyl-functionalized) interacted more with the extracellular polymeric matrix. The results indicated that nanoconjugated vancomycin showed a more pronounced activity than the equivalent concentration of free GPA and, among the different MSNs, positively charged MSNs performed better than negatively charged ones (Fulaz et al., 2020). On a contrary, co-conjugation of vancomycin and polymyxin B on MSNs by Gounani and co-workers resulted in higher MBIC (minimum biofilm inhibitory concentration) and MBEC (minimum biofilm eradication concentration) than free antibiotics towards *S. aureus* and *P. aeruginosa* biofilms (Gounani et al., 2019). Authors indicated as a possible explanation of this poor performance, the size (> 50 nm) of the nanosystem and its negative charge in electrostatic repulsion with the negatively charged biofilm matrix.

Prosthetic joint infection, often exacerbated by biofilm formation, is one of the most devastating complications in orthopaedic surgery. Hence, in a handful of the studies already cited in sections 3.3.1.3 and 3.3.3.3, efficacy of including vancomycin in nanocomposites in preventing or eradicating bacterial biofilms was evaluated (Auñón et al., 2020; Chen et al., 2019; Croes et al., 2018; Pawar et al., 2018). For example, a *S. aureus* strain isolated from a 62-year-old patient with acute infection of hip prosthesis was used by Auñón et al. for colonizing bottle-shaped nanotubes made of Ti-6Al-4V alloy. The nanostructure, as-it-is or conjugated with gentamycin and vancomycin, was then implanted in the femur of a rabbit model, removed four weeks later and sonicated for releasing, if formed, the adherent biofilm. The results of the microbiological studies showed that, differently from the bare nanotubes, the nanocomposite releasing antibiotics was effective in preventing biofilm formation (Auñón et al., 2020). Similarly, chitosan-based coatings, engineered for treating implant-associated infections and incorporating AgNPs or vancomycin, were incubated for 1-to-6 days with bacterial suspensions of *S. aureus*. GPA-loaded coating was proved more effective than the Ag-carrying one in inhibiting biofilm: neither sessile, nor floating viable cells were recovered following the nanoconjugated vancomycin treatment. Higher antibacterial efficacy of antibiotic-loaded coating with respect to the AgNPs-loaded one was confirmed also in an *in vivo* tibia implant model (Croes et al., 2018).

3.3.4.2. Antibiofilm activity of teicoplanin-carrying nanosystems. In the case of teicoplanin (Table 2), only the paper of Armenia and co-Authors indicated a possible application of the nanoconjugated antibiotic to control biofilm formation by MSSA. Nonconjugated and nanoconjugated teicoplanin inhibited the biofilm formation at a concentration of 2.5 μg/ml and 5 μg/ml, respectively, while no inhibitory effect was observed after adding an equivalent amount of naked Fe_3O_4NPs. At the highest tested concentration (10 μg/ml), the effect of nanoconjugated GPA was significantly higher than the one of the nonconjugated antibiotic (Armenia et al., 2018). The antibiofilm activity of teicoplanin carried by Fe_3O_4NPs was recently confirmed by Berini et al.: the effect was potentiated, compared to free teicoplanin, by the possibility to attract, and therefore concentrate, the nanoantibiotic at the biofilm site using an external magnet (Berini et al., 2021).

3.3.4.3. Antibiofilm activity of daptomycin-carrying nanosystems. For daptomycin, three out of the nine papers describing the antibiotic-carrying nanosystems reported on biofilm inhibition. Li et al. observed a clear effect on a 7-day-old *S. aureus* biofilm treated with daptomycin-loaded flexible nanoliposomes (see section 3.3.3.5) in comparison to untreated biofilms. This result was confirmed *in vivo*, in mice implanted with silicon membrane contaminated by *S. aureus*: 4 days after the administration of antibiotic loaded nanoliposomes, only scattered cells could be observed on the silicon membranes, differently from those from untreated mice that appeared thickly covered by viable bacterial cells (Li et al., 2013). In the two studies by Meeker and colleagues already discussed above (see sections 3.3.1.5 and 3.3.3.5), the PDA-coated daptomycin-loaded Au nanocages carrying different anti-*S. aureus*

antibodies were tested on MRSA biofilm, using a model of catheter-associated biofilm formation. Briefly, a coated catheter sample was inoculated with MRSA and incubated for 24 h at 37°C. Upon treatment with the nanoformulations for 2 h, each catheter was NIR irradiated to elicit photo-thermal stress. After sonication, a significant reduction in cell viability, proportional to the irradiation time, was detected and the anti-biofilm activity was lasting for 24 h after irradiation (Meeker et al., 2016, 2018).

3.3.5. Nanoantibiotics and phagocytosis

After oral intake or intravenous injection, nanoantibiotics, once in the bloodstream, can be rapidly taken up by the cells of the mononuclear phagocytic system that recognize them as foreign, and be then cleared by the reticuloendothelial system (Patra et al., 2018). Uptake by phagocytic cells, considered in many cases an obstacle, can provide great benefits in the treatment of infection diseases, such as those caused by MRSA. As anticipated in section 3.3, staphylococci are able to invade and survive inside phagocytic cells allowing them to act as 'Trojan horses': the result is the dissemination of bacteria from the initial infection site, causing multiple simultaneous infections throughout the body and, as a consequence, complicating the antibacterial therapy (Bose et al., 2020). Hence, conjugating antibiotics active against Gram-positive pathogens with NPs that could be uptaken by the mononuclear phagocytic system is a strategy that has been increasingly investigated in the past years for the treatment of intracellular bacterial infections.

Unfortunately, one of the most recurrent modifications of nanoantibiotics, i.e., functionalization with PEG molecules, designed to increase their stability and half-life in blood circulation, and to provide stealth capabilities to escape the host immune system (see, for instance, Chen et al. (2019), Cong et al. (2015), Esmaeili and Ghobadianpour (2016)), frequently hampers intracellular anti-MRSA activity. Hence, efforts were devoted to defining alternative formulations. A few are the papers listed in Table 1 where Authors evaluated the capability of vancomycin-carrying nanostructures for fighting intracellular infections. No information is, instead, available for nanosystems with teicoplanin or daptomycin.

In the study of Salih et al., already cited in section 3.3.3.1, nanovesicles formed by β-cyclodextrin and oleylamine (BCD-OLA), thanks to their lipophilic nature, reached the cytoplasmic environment of both human embryonic kidney cells (HEK 293) and THP-1 macrophages. In co-culture experiments with eukaryotic cells and MRSA, the vancomycin-loaded BCD-OLA system at a concentration equal to the antibacterial MIC showed a 459-fold reduction of intracellular bacteria in infected HEK 293 cells and an 8-fold reduction in THP-1 infected macrophages, compared to bare vancomycin. At 5x MIC, vancomycin/BCD-OLA completely eradicated intracellular MRSA colonization (Salih et al., 2020). Equally promising as an intracellular carrier of vancomycin was the nanocomposite synthesized by Pei and co-workers, formed by a mixture of the PLGA, PEG, Eudragit E100, and ZWC (PpZEV-NPs) polymers (see section 3.3.2). Observed in time-lapse microscopy, this NM, conveniently modified to carry a fluorescent derivative of vancomycin with a BODIPY moiety, appeared to be rapidly and efficiently uptaken by J774A.1 macrophages: after 3 h, fluorescence signals were detected in cells incubated with the nanocarried fluorescent GPA, whereas no fluorescence was visualized in macrophages exposed to free BODIPY-derivatized vancomycin. When used to treat macrophages infected by MRSA, *Listeria* sp., *S. pneumoniae, E. faecium,* or *E. faecalis*, vancomycin-loaded PpZEV-NPs showed a superior antibacterial activity (up to 100-fold) than bare vancomycin (Pei et al., 2017). In another study, modulating the surface charge of LPHNs loaded with vancomycin (see section 3.3.3.1), and in particular moving from LPHNs incorporating zwitterionic lipids to cationic-LPHNs, increased macrophage uptake (93 % for cationic-LPHNs *vs* 49 % with zwitterionic-LPHNs) and improved the nanosystem efficacy in fighting intracellular MRSA infections (Bose et al., 2020).

Organic NPs are not the only type of nanosystems that could be uptaken by macrophages. Indeed, in the study by Lai et al., vancomycin-loaded AuNPs were rapidly engulfed by macrophages through endocytosis and proved effective in killing intracellular infection by MSSA and MRSA (Lai et al., 2015). Finally, Liu and co-Authors showed that hyaluronic acid-modified organic metal framework material ZIF-8 (see section 3.3.1.3), carrying vancomycin, could eradicate MRSA in macrophages with high efficiency. The presence of hyaluronic acid acted in reducing agglomeration of the nanosystem, thus improving its water dispersibility. Moreover, Authors suggested that hyaluronic acid could specifically bind to CD44 receptors, highly expressed on macrophages, thus facilitating the intracellular uptake of the nanoantibiotic by endocytosis and enhancing its antibacterial potency (Liu et al., 2020).

3.3.6. Evaluation of the safety of nanoconjugated GPAs and daptomycin

Another aspect that is important to consider is that the interactions that NPs have with biological systems may elicit undesired effects (Fadeel and Alexiou, 2020). Indeed, it may occur that the efforts devoted to enhancing the therapeutic characteristics of NPs may result in the unintentional exacerbation of their toxicity (Shvedova et al., 2016). For instance, some NPs are known to cross biological barriers, such as blood-brain (Nguyen et al., 2021), blood-testis (Castellini et al., 2014), and placental barriers (Aengenheister et al., 2021), and, for this reason, they are considered promising candidates to act pharmacologically on relevant targets situated in difficult-to-reach body districts. For the very same reason, however, they can be quite dangerous since they penetrate in such specifically protected organs. These considerations are valid also for nanosystems conjugated to antibiotics. Consequently, several Authors investigated the safety of their newly synthetized nanosystems by means of toxicity tests. Almost half of the papers on GPAs and daptomycin-carrying nanosystems analyzed in this review reported on their cytotoxicity evaluation (see Tables 1-3). Most of the nanotoxicity tests were performed on cell cultures because several are the advantages of using *in vitro* systems, not last the compliance with the 3Rs concept, calling for replacement, reduction, and refinement of animal experimentation (Kirk, 2018). Looking at the information included in Tables 1-3, it becomes evident that the great majority of these *in vitro* studies evaluated the nanosystem cytotoxicity by measuring cell metabolic activity by means of the MTT assay (as done, for instance, by Lai et al. (2015), Ma et al. (2020), or Zhang et al. (2017)) as an indication of cell viability and proliferation. Other methods for quantification of viable cells that were used, although less frequently, are CCK-8 (e.g., Bose et al., 2020; Gu et al., 2016; Li et al., 2014), MTS (Pei et al., 2017; Suchý et al., 2017, 2019), Alamar Blue (Uhl et al., 2017), Resazurin (Efiana et al., 2019; Posadowska et al., 2016), or CellTiter-Glo (Armenia et al., 2018; Harris et al., 2017) assays. Unfortunately, NPs are known to interfere with the readouts of the classically used cytotoxicity assays, MTT included (Almutary and Sanderson, 2016; Costa et al., 2016; Pem et al., 2018). Therefore, a careful evaluation of possible assay interferences due to the chemo-physical nature of the NM in use appears an essential step to adopt a trustable assay, although often underestimated by several Authors. To give a practical example, it is recommended to introduce additional washing steps when MTT assay is used in presence of AgNPs and magnetic NPs (Pem et al., 2018) or, for fluorescence or photoluminescence assays, it is suggested to characterize the excitation-emission spectra of each nanoformulation (MacCormack et al., 2021).

Much more variable is the choice of the cell lines that are employed for the tests. Some of the most recurrently used were murine RAW 264.7 (e.g., Almeida Neto et al., 2019; Guo et al., 2020) and J774.1 (Bose et al., 2020; Pei et al., 2017) macrophages, human hepatoma cancer cells (HepG2) (e.g., Mhule et al., 2018; Sikwal et al., 2016), human embryonic kidney cells (HEK 293) (e.g., Gounani et al., 2019; Maji et al., 2019; Salih et al., 2020), human adenocarcinoma alveolar basal epithelial cells (A-549) (e.g., Kalhapure et al., 2017b; Sonawane et al., 2020), human breast cancer cells (MCF-7) (e.g., Hassan et al., 2020; Li et al., 2018; Omolo et al., 2018), and human cervix cancer cells (HeLa) (e.g., Sarkar

et al., 2017; Wang et al., 2019, 2020a). However, much longer is the complete list of cell lines identified during this literature survey, including, without being limited to, murine NIH3T3 and L929 fibroblast cells (Kimna et al., 2019; Pawar et al., 2018), human embryonic hepatocytes L02 (Cong et al., 2015), human colon cancer CaCo-2 cells (Uhl et al., 2017), human dermal keratinocytes HaCaT (Xu et al., 2020), or human osteosarcoma SaOS-2 cells (Suchý et al., 2017). In a few papers, the haemolytic activity of the nanoantibiotics was evaluated on red blood cells extracted from human, murine, or sheep blood samples (Gounani et al., 2019; Guo et al., 2020; Maji et al., 2019; Pawar et al., 2018; Tong et al., 2019; Xu et al., 2020). As a general rule, cell lines should be chosen considering the most probable entry route in the body of the NM that has to be tested: lung cells are recommended for assessing air borne NPs, skin cells for NPs that are present in cosmetics or medicinal creams and ointments, and blood cells for nanodrugs. Peripheral blood leukocytes, Jurkat T-cells, lymphoid cells, acute myeloid leukaemia HL-60 cells, monocytes, macrophages, and dendritic cells might be used for immunotoxicity evaluation of NPs (Petrarca et al., 2014, 2015; Tirumala et al., 2021), while stem cells (embryonic, mesenchymal, neural, and other stem cell lines) have become a common tool for assessing developmental toxicity (Hu et al., 2022), and Balb/3T3 cells can be used to evaluate the morphological transformation potential induced by NPs exposure (Sabbioni et al., 2014). It cannot be denied, however, that, in most of the experiments hereby reported for testing NPs, the choice of cell lines does not follow the above guidelines and appears to be dictated more by a mere laboratory convenience than by a coherent experimental design. Equally varied are the protocols followed by the Authors for the toxicity assessment, as well as the concentrations of the nanoantibiotics investigated, or the controls introduced in their studies, thus making results comparison quite challenging, as previously indicated also for the antimicrobial and antibiofilm assays (sections 3.3.3 and 3.3.4).

Organic and inorganic NPs developed as vancomycin carriers passed the toxicity tests they were subjected to. Indeed, in all studies included in Table 1, reported cell viabilities were always above the 70 % threshold set by the guidelines for determination of *in vitro* cytotoxicity of medical devices (DIN EN ISO 10993-5) (Cerchiara et al., 2017). As an example, in the recent study of Guo and co-workers, MTT assay applied to RAW 264.7 murine macrophages treated with vancomycin-conjugated oleic acid-loaded polypyrrole NPs (Van-OA@PPy), highlighted only a minimal reduction of cell viability up to 1 mg/ml concentration. Negligible was also the haemolytic activity *in vitro* on mouse red blood cells, as well as the alterations in haematological data and blood biochemicals of Balb/c mice after injection with Van-OA@PPy (Guo et al., 2020). When vancomycin was co-loaded with polymyxin B on MSNs, NP functionalization influenced both antibacterial activity and cytotoxicity. Indeed, carboxyl-modified MSNs were contemporarily the most effective against bacteria (see section 3.3.1.2) and the less cytotoxic on three cell lines (HepG2, HEK 293, and human foreskin Hff-1 fibroblasts), while showing also no haemolytic effect on human blood (Gounani et al., 2019).

Numerous and well-detailed are the toxicity studies conducted on the nanocomposites (Almeida Neto et al., 2019; Babaei et al., 2019; Cerchiara et al., 2017; Hassani Besheli et al., 2017; Karakeçili et al., 2019; Kimna et al., 2019; Lin et al., 2017; Suchý et al., 2017, 2019; Xiang et al., 2018) and nanohydrogels (Aşik et al., 2019; George et al., 2017; Pawar et al., 2018; Posadowska et al., 2016; Sarkar et al., 2017; Tao et al., 2020) carrying vancomycin and developed for orthopaedic applications or as wound healing materials, as reported in Table 1. For example, Liu and colleagues demonstrated the biocompatibility of titanium plates where vancomycin-loaded PVA/PLGA NPs were deposited on them: osteoblasts were more vital, osteogenic differentiation was promoted, and cell adhesion was enhanced in comparison to nude titanium scaffolds (Liu et al., 2017).

In the case of nanoconjugated teicoplanin (Table 2), only the paper by Armenia co-workers includes data on its potential cytotoxicity. Tests, conducted on the immortalized tumor cell line SKOV-3 and on primary mesenchymal stem cells extracted from human adipose tissue (hASC), highlighted that both cell lines responded to the exposure to the nanoantibiotic in a concentration-dependent manner. However, even when cells were treated with an amount of nanoantibiotic 3-fold higher than the antibacterial MIC, reduction in viability after 96 h was low. This toxic effect was significantly less pronounced than that exerted by unconjugated Fe_3O_4NPs, thus demonstrating that antibiotic conjugation could improve the biocompatibility of metallic nanocarriers (Armenia et al., 2018).

Regarding daptomycin, two out of the nine papers listed in Table 3 dealt with the topic of nanotoxicity. When investigated through MTT assay, murine NIH3T3 fibroblasts exposed to 20 μg/ml of the nanocomposite (rGO@Ag@Dap) synthesized by Tong et al. (see sections 3.3.1.5 and 3.3.3.5) maintained ca. 80 % of their viability, while showing also a haemolytic rate lower than 2 % (Tong et al., 2019). In the study of Wang and colleagues, more than 90 % viability was observed in HeLa cells exposed to daptomycin-gold nanoflowers (Dap-Au_6NFs), as well as to the free antibiotic, up to 200 μM. An equivalent concentration of nude nanoflowers, instead, reduced cell viability, thus further substantiating the concept that covering the surface of metallic NPs with biocompatible molecules mitigate their intrinsic cytotoxicity (Wang et al., 2020a). When cytotoxicity tests were conducted following 10-min irradiation with 808-nm laser, the viability of cells exposed to Dap-Au_6NFs dropped to 13 %: Authors considered this result an indication of the nanosystem potential for cancer therapy (Wang et al., 2020a).

Very few toxicological studies of NPs carrying antibiotics have been performed *in vivo*. Only half a dozen papers (out of 96) reported on the safety of vancomycin-carrying NPs in mammalian models (Gu et al., 2016; Guo et al., 2020; Ma et al., 2020; Liu et al., 2020; Yousry et al., 2017; Zhao et al., 2017) (Table 1); only one was found for nanoconjugated daptomycin (Tong et al., 2019) (Table 3). An example is the study of Cardoso and co-workers, where *in vitro* studies on human retinal pigment epithelial cells and on hen egg chlorioallantonic membrane were followed by biocompatibility assessment *in vivo*. Intravitreal injection of vancomycin-loaded DMPEI NPs in rat eyes caused neither impairment in retinal functionality nor damages in ocular tissues, confirming the potential of the nanosystem for endophthalmitis treatment (Cardoso et al., 2021). Vancomycin-loaded polymeric NPs were tested *in vivo* in rabbits by Yousry et al.: the nanosystem was proved non-irritating and safe for ophthalmic administration through Draize test (Yousry et al., 2017). Murine models for skin infection and pneumonia were, instead, used to prove the lack of toxicity of vancomycin encapsulated in hyaluronic acid-coated ZIF-8 (Liu et al., 2020) and of polydopamine NPs carrying vancomycin and AgNPs (Ma et al., 2020), respectively. As regards daptomycin, Tong and co-Authors included in their study an initial *in vivo* nanotoxicity assessment. When injected in Balb/c mice, reduced graphene oxide nanocomposites carrying daptomycin and AgNPs (rGO@Ag@Dap) did not cause any change in body weight, thus suggesting the biosafety of this NM (Tong et al., 2019).

4. Conclusions

The last decade's progresses in manufacturing and testing a large variety of novel nanosystems clearly point out to their undeniable potential for contrasting the alarming diffusion of AMR. Many different inorganic, organic, and composite NMs have been intensively investigated both for their intrinsic antibacterial activity and as carriers of last-resort antibiotics. In this review, we have focused our attention on the medical need to prolong the clinical longevity of the frontline antibiotics that are currently in use to treat infections caused by MDR Gram-positive pathogens, i.e., the vancomycin-type GPAs and the lipopeptide daptomycin. Our analysis illustrates that most of the nanotechnology efforts have been applied to vancomycin, which, although still extensively used in clinical practice, is the oldest -and somehow the less performant- among the currently available GPAs. Teicoplanin

nanoconjugation appears a promising alternative, although very poorly investigated yet. Teicoplanin has several advantages over vancomycin in the treatment of serious infections, as longer half-life and lower nephrotoxicity and ototoxicity (Ziglam and Finch, 2001). Recent results indicate that teicoplanin is more active than vancomycin towards MSSA and MRSA biofilms, and that this antibiofilm activity is preserved by teicoplanin conjugated on magnetic Fe_3O_4NPs. Magnetic NPs offer the advantage to remotely address the antibiotic towards biofilms/infection sites by applying an external magnetic field, increasing its localized concentration and reducing side effects (Armenia et al., 2018; Berini et al., 2021). To the best of our knowledge, none Author has invested till now in nanoformulations of second-generation GPAs, i.e., oritavancin, telavancin, and dalbavancin. Since these recently approved GPAs are endowed with a better antimicrobial potency and a wider antimicrobial spectrum in comparison to vancomycin (Butler et al., 2014; Van Bambeke, 2015), it would be interesting to transfer them the knowledge acquired on vancomycin- and teicoplanin-based nanosystems. This would be particularly relevant, for instance, considering the improved pharmacokinetics / pharmacodynamics of dalbavancin that, for its extended half-like of over 300 h in the human body, can be administered once a week (Butler et al., 2014). On the other side, it cannot be neglected that vancomycin use is well consolidated in many clinical applications, first of all in orthopaedics, and that this GPA is gaining an increasingly important role in curing *C. difficile* infections, too (Mada and Alam, 2021). Considering that the cost of second-generation GPAs largely exceeds that of vancomycin, it is reasonable to argue that restoring the clinical potential of vancomycin, without the need to develop alternative drugs, remains an important goal and nanotechnology offers promising tools to reach it. Similarly, it emerges that an attractive perspective might be widening the nature of daptomycin-based nanosystems. Further work on nanoconjugation of daptomycin needs to be planned not only to improve topical application of this antibiotic, but also to mitigate the adverse side effects that currently limit its systemic application. Daptomycin represents the very last resort antibiotic towards severe MDR Gram-positive infections, including those that have acquired resistance towards GPAs (Heidary et al., 2018), but it has to be used under medical control due to its possible systemic toxicity.

Undoubtedly, recent advances in the synthesis and in the chemical/biological characterization of variegated classes of novel NMs nowadays guarantee optimal tailored solutions for improving existing drugs and their target-oriented delivery, potentially reducing their dosage and the associated risk of increasing AMR. We have herein reported several examples of antibiotic-loaded NPs or nanocomposites that exhibit a potentiated and prolonged antimicrobial activity at the site of infection, or that have acquired extended antimicrobial spectrum, covering both Gram-positive and Gram-negative bacteria, or that are used to protect medical devices and implants. Promising are the reports about the monocyte phagocytosis that allows nonantibiotics to treat intracellular bacterial infections, and those on their anti-biofilm activity, although further investigations are needed for a better comprehension of the interactions between different NMs and cellular components.

Thus, we would like to conclude by pinpointing a few critical issues and make room for further developments. One critical persisting issue is the economical sustainability of producing at large scale the diverse types of NMs listed in this review, as well as of functionalizing them with last resort antibiotics such as GPAs and daptomycin. The current perception is that the cost of most of these NMs is still elevated and calls for most effective production methods to assure product profitability without creating economic barriers to antibiotic use in patients. Additionally, the transition of NMs production processes towards a 'green synthesis' approach is still in its infancy. Indeed, increasing attention has been dedicated in the past few years to design safer, more sustainable, less toxic, and energy-efficient synthesis procedures. However, larger investments for better defying biogenic approaches and/or developing ideal solvents systems, as well as for translating them from a laboratory-scale to an industrial-setting, are urgently required (Drummer et al., 2021). Lastly, the contradictory results obtained thus far on the safety profile of NMs, as well as on their stability in complex physiological environments, can limit or delay their translation into clinics. A complete assessment of nanosystem toxicity requires considering their administration routes, distribution and stability inside the different body districts, factors that can be investigated only through *in vivo* studies. Since the whole is greater (and different) that the sum of its parts, it is not possible to completely infer the response of an organism to nanoconjugated antibiotics, only on the bases of *in vitro* evidence. Unfortunately, experiments on mammalians, although predictive of what occurs in humans, are costly, they require specific facilities and skills, and have to be managed considering ethical concerns and regulatory constraints. Consequently, it is generally recognized that adequate alternative infection animal models are needed for testing NMs' topic, oral, or systemic use in preclinical phases. Since genes and biological processes are highly conserved among vertebrates, other species with lower neural complexity, such as zebrafish (Vranic et al., 2019) and *Xenopus* (Bonfanti et al., 2020), may be preferred as alternative models to study the interactions between living systems and NPs at the organismic level. Due to their great advantages (i.e., safe handling, low rearing costs, low antibiotic amount needed, no restrictions imposed by ethical and regulatory issues), invertebrate infection models could also help in rapidly solving the still-pending issues about *in vivo* efficacy and toxicity of nanoconjugated antibiotics, accelerating their transition from the preclinical studies to the clinical applications (Montali et al., 2020).

Funding sources

This work was supported by the University of Insubria grant "Fondo di Ateneo per la Ricerca" 2020 to FM, VO, and FB; by the University of Insubria "Starting Grant" 2020 and 2021 to FB; and by the HOTZYMES project (EU's Horizon 2020 Programme, FET OPEN, grant agreement n° 829162) to RG and GB.

CRediT authorship contribution statement

Francesca Berini: Conceptualization, Data curation, Investigation, Methodology, Writing – original draft, Writing – review & editing. **Viviana Orlandi:** Data curation, Investigation, Writing – original draft. **Rosalba Gornati:** Data curation, Investigation, Writing – original draft. **Giovanni Bernardini:** Data curation, Funding acquisition, Investigation, Writing – original draft. **Flavia Marinelli:** Conceptualization, Funding acquisition, Writing – review & editing.

Declaration of Competing Interest

The authors declare that they have no conflict of interest.

Acknowledgements

We are grateful to Consorzio Interuniversitario per le Biotecnologie for supporting FB.

References

Abbaszadegan, A., Ghahramani, Y., Gholami, A., Hemmateenejad, B., Dorostkar, S., Nabavizadeh, M., Sharghi, H., 2015. The effect of charge at the surface of silver nanoparticles on antimicrobial activity against gram-positive and gram-negative bacteria: a preliminary study. J. Nanomater. 16, 53. https://doi.org/10.3390/pharmaceutics12090821.

Aengenheister, L., Favaro, R.R., Morales-Prieto, D.M., Furer, L.A., Gruber, M., Wadsack, C., Markert, U.R., Buerki-Thurnherr, T., 2021. Research on nanoparticles in human perfused placenta: State of the art and perspectives. Placenta. 104, 199–207. https://doi.org/10.1016/j.placenta.2020.12.014.

Alfei, S., Schito, A.M., 2020. From nanobiotechnology, positively charged biomimetic dendrimers as novel antibacterial agents: a review. Nanomaterials (Basel). 10 (10), 2022. https://doi.org/10.3390/nano10102022.

Aljaafari, M.N., AlAli, A.O., Baqais, L., Alqubaisy, M., AlAli, M., Molouki, A., Ong-Abdullah, J., Abushelaibi, A., Lai, K.S., Lim, S.E., 2021. An overview of the potential therapeutic applications of essential oils. Molecules. 26 (3), 628. https://doi.org/10.3390/molecules26030628.

Almeida Neto, G.R., Barcelos, M.V., Ribeiro, M.E.A., Folly, M.M., Rodríguez, R.J.S., 2019. Formulation and characterization of a novel PHBV nanocomposite for bone defect filling and infection treatment. Mater. Sci. Eng. C Mater. Biol. Appl. 104, 110004 https://doi.org/10.1016/j.msec.2019.110004.

Almutary, A., Sanderson, B.J., 2016. The MTT and crystal violet assays: potential confounders in nanoparticle toxicity testing. Int. J. Toxicl. 35 (4), 454–462. https://doi.org/10.1177/1091581816648906.

Alves-Barroco, C., Rivas-García, L., Fernandes, A.R., Baptista, P.V., 2020. Tackling multidrug resistance in streptococci - from novel biotherapeutic strategies to nanomedicines. Front. Microbiol. 11, 579916 https://doi.org/10.3389/fmicb.2020.579916.

Amaro, F., Morón, Á., Díaz, S., Martín-González, A., Gutiérrez, J.C., 2021. Metallic nanoparticles-friends or foes in the battle against antibiotic-resistant bacteria? Microorganisms. 9 (2), 364. https://doi.org/10.3390/microorganisms9020364.

Amrollahi-Sharifabadi, M., Koohi, M.K., Zayerzadeh, E., Hablolvarid, M.H., Hassan, J., Seifalian, A.M., 2018. In vivo toxicological evaluation of graphene oxide nanoplatelets for clinical application. Int. J. Nanomedicine 13, 4757–4769. https://doi.org/10.2147/ijn.s168731.

Anderson, S.D., Gwenin, V.V., Gwenin, C.D., 2019. Magnetic functionalized nanoparticles for biomedical, drug delivery and imaging applications. Nanoscale Res. Lett. 14 (1), 188. https://doi.org/10.1186/s11671-019-3019-6.

Anselmo, A.C., Mitragotri, S., 2019. Nanoparticles in the clinic: an update. Bioeng. Transl. Med. 4 (3), e10143 https://doi.org/10.1002/btm2.10143.

Antimicrobial Resistance Collaborators, 2022. Global burden of bacterial antimicrobial resistance in 2019: a systematic analysis. Lancet S0140-6736 (21). https://doi.org/10.1016/S0140-6736(21)02724-0, 02724-0.

Arana, L., Gallego, L., Alkorta, I., 2021. Incorporation of antibiotics into solid lipid nanoparticles: a promising approach to reduce antibiotic resistance emergence. Nanomaterials (Basel). 11 (5), 1251. https://doi.org/10.3390/nano11051251.

Arias, L.S., Pessan, J.P., Vieira, A.P.M., Lima, T.M.T., Delbem, A.C.B., Monteiro, D.R., 2018. Iron oxide nanoparticles for biomedical applications: a perspective on synthesis, drugs, antimicrobial activity, and toxicity. Antibiotics (Basel). 7 (2), 46. https://doi.org/10.3390/antibiotics7020046.

Armenia, I., Marcone, G.L., Berini, F., Orlandi, V.T., Pirrone, C., Martegani, E., Gornati, R., Bernardini, G., Marinelli, F., 2018. Magnetic nanoconjugated teicoplanin: a novel tool for bacterial infection site targeting. Front. Microbiol. 9, 2270. https://doi.org/10.3389/fmicb.2018.02270.

Ashraf, S.A., Siddiqui, A.J., Elkhalifa, A.E.O., Khan, M.I., Patel, M., Alreshidi, M., Moin, A., Singh, R., Snoussi, M., Adnan, M., 2021. Innovations in nanoscience for the sustainable development of food and agriculture with implications on health and environment. Sci. Total Environ. 768, 144990 https://doi.org/10.1016/j.scitotenv.2021.144990.

Aşik, M.D., Kaplan, M., Yalınay, M., Güven, E.Ö., Bozkurt, M., 2019. Development of a sequential antibiotic releasing system for two-stage total joint replacement surgery. J. Biomed. Nanotechnol. 15 (11), 2193–2201. https://doi.org/10.1166/jbn.2019.2850.

Auñón, Á., Esteban, J., Doadrio, A.L., Boiza-Sánchez, M., Mediero, A., Eguibar-Blázquez, D., Cordero-Ampuero, J., Conde, A., Arenas, M.Á., de-Damborenea, J.J., Aguilera-Correa, J.J., 2020. *Staphylococcus aureus* prosthetic joint infection is prevented by a fluorine- and phosphorus-doped nanostructured Ti-6Al-4V alloy loaded with gentamicin and vancomycin. J. Orthop. Res. 38 (3), 588–597. https://doi.org/10.1002/jor.24496.

Babaei, M., Ghaee, A., Nourmohammadi, J., 2019. Poly (sodium 4-styrene sulfonate)-modified hydroxyapatite nanoparticles in zein-based scaffold as a drug carrier for vancomycin. Mater. Sci. Eng. C Mater. Biol. Appl. 100, 874–885. https://doi.org/10.1016/j.msec.2019.03.055.

Banin, U., Waiskopf, N., Hammarström, L., Boschloo, G., Freitag, M., Johansson, E.M.J., Sá, J., Tian, H., Johnston, M.B., Herz, L.M., Milot, R.L., Kanatzidis, M.G., Ke, W., Spanopoulos, I., Kohlstedt, K.L., Schatz, G.C., Lewis, N., Meyer, T., Nozik, A.J., Beard, M.C., Armstrong, F., Megarity, C.F., Schmuttenmaer, C.A., Batista, V.S., Brudvig, G.W., 2021. Nanotechnology for catalysis and solar energy conversion. Nanotechnology. 32 (4), 042003 https://doi.org/10.1088/1361-6528/abbce8.

Beisl, S., Monteiro, S., Santos, R., Figueiredo, A.S., Sanchez-Loredo, M.G., Lemos, M.A., Lemos, F., Minhalma, M., de Pinho, M.N., 2019. Synthesis and bactericide activity of nanofiltration composite membranes - cellulose acetate/silver nanoparticles and cellulose acetate/silver ion exchanged zeolites. Water Res. 149, 225–231. https://doi.org/10.1016/j.watres.2018.10.096.

Berini, F., Orlandi, V.T., Gamberoni, F., Martegani, E., Armenia, I., Gornati, R., Bernardini, G., Marinelli, F., 2021. Antimicrobial activity of nanoconjugated glycopeptide antibiotics and their effect on *Staphylococcus aureus* biofilm. Front. Microbiol. 12, 657431 https://doi.org/10.3389/fmicb.2021.657431.

Bernardos, A., Piacenza, E., Sancenón, F., Hamidi, M., Maleki, A., Turner, R.J., Martínez-Máñez, R., 2019. Mesoporous silica-based materials with bactericidal properties. Small 15 (24), 1900669. https://doi.org/10.1002/smll.201900669.

Binda, E., Marinelli, F., Marcone, G.L., 2014. Old and new glycopeptide antibiotics: action and resistance. Antibiotics (Basel). 3 (4), 572–594. https://doi.org/10.3390/antibiotics3040572.

Boholm, M., Arvidsson, R.A., 2016. Definition framework for the terms nanomaterial and nanoparticle. NanoEthics. 10, 25–40. https://doi.org/10.1007/s11569-015-0249-7.

Bonfanti, P., Colombo, A., Saibene, M., Fiandra, L., Armenia, I., Gamberoni, F., Gornati, R., Bernardini, G., Mantecca, P., 2020. Iron nanoparticle bio-interactions evaluated in *Xenopus laevis* embryos, a model for studying the safety of ingested nanoparticles. Nanotoxicology. 14 (2), 196–213. https://doi.org/10.1080/17435390.2019.1685695.

Booysen, E., Bezuidenhout, M., van Staden, A.D.P., Dimitrov, D., Deane, S.M., Dicks, L.M.T., 2019. Antibacterial activity of vancomycin encapsulated in poly(DL-lactide-co-glycolide) nanoparticles using electrospraying. Probiotics Antimicrob. Proteins. 11 (1), 310–316. https://doi.org/10.1007/s12602-018-9437-4.

Bose, R.J.C., Tharmalingam, N., Choi, Y., Madheswaran, T., Paulmurugan, R., McCarthy, J.R., Lee, S.H., Park, H., 2020. Combating intracellular pathogens with nanohybrid-facilitated antibiotic delivery. Int. J. Nanomedicine 15, 8437–8449. https://doi.org/10.2147/IJN.S271850.

Bowler, P., Murphy, C., Wolcott, R., 2020. Biofilm exacerbates antibiotic resistance: is this a current oversight in antimicrobial stewardship? Antimicrob. Resist. Infect. Control 9, 162. https://doi.org/10.1186/s13756-020-00830-6.

Breijyeh, Z., Jubeh, B., Karaman, R., 2020. Resistance of Gram-negative bacteria to current antibacterial agents and approaches to resolve it. Molecules 25 (6), 1340. https://doi.org/10.3390/molecules25061340.

Bruna, T., Maldonado-Bravo, F., Jara, P., Caro, N., 2021. Silver nanoparticles and their antibacterial applications. Int. J. Mol. Sci. 22 (13), 7202. https://doi.org/10.3390/ijms22137202.

Butler, M.S., Hansford, K.A., Blaskovich, M.A., Halai, R., Cooper, M.A., 2014. Glycopeptide antibiotics: back to the future. J. Antibiot. (Tokyo). 67 (9), 631–644. https://doi.org/10.1038/ja.2014.111.

Canaparo, R., Foglietta, F., Giuntini, F., Della Pepa, C., Dosio, F., Serpe, L., 2019. Recent developments in antibacterial therapy: focus on stimuli-responsive drug-delivery systems and therapeutic nanoparticles. Molecules. 24 (10), 1991. https://doi.org/10.3390/molecules24101991.

Cardoso, J.F., Perasoli, F.B., Almeida, T.C., Marques, M.B.F., Toledo, C.R., Gil, P.O., Tavares, H.D.S., Da Paz, M.C., Mussel, W.D.N., Magalhães, J.T., Silva, G.N.D., Da Silva-Cunha, A., Granjeiro, P.A., Klibanov, A.M., Da Silva, G.R., 2021. Vancomycin-loaded N,N-dodecyl,methyl-polyethylenimine nanoparticles coated with hyaluronic acid to treat bacterial endophthalmitis: development, characterization, and ocular biocompatibility. Int. J. Biol. Macromol. 19, 330–341. https://doi.org/10.1016/j.ijbiomac.2020.12.057.

Cassini, A., Högberg, L.D., Plachouras, D., Quattrocchi, A., Hoxha, A., Simonsen, G.S., Colomb-Cotinat, M., Kretzschmar, M.E., Devleesschauwer, B., Cecchini, M., Ouakrim, D.A., Cravo Oliveira, T., Struelens, M.J., Suetens, C., Monnet, D.L., the Burden of AMR Collaborative Group, 2019. Attributable deaths and disability-adjusted life-years caused by infections with antibiotic-resistant bacteria in the EU and the European Economic Area in 2015: a population-level modelling analysis. Lancet Infect. Dis. 19 (1), 56–66. https://doi.org/10.1016/S1473-3099(18)30605-4.

Castellini, C., Ruggeri, S., Mattioli, S., Bernardini, G., Macchioni, L., Moretti, E., Collodel, G., 2014. Long-term effects of silver nanoparticles on reproductive activity of rabbit buck. Syst Biol Reprod Med 60 (3), 143–150. https://doi.org/10.3109/19396368.2014.891163.

Center for Disease Control and Prevention (CDC), 2019. Antibiotic resistance threats in the United States, 2019. https://www.cdc.gov/drugresistance/pdf/threats-report/2019-ar-threats-report-508.pdf (last accessed on 24th June 2021).

Cerchiara, T., Abruzzo, A., di Cagno, M., Bigucci, F., Bauer-Brandl, A., Parolin, C., Vitali, B., Gallucci, M.C., Luppi, B., 2015. Chitosan based micro- and nanoparticles for colon-targeted delivery of vancomycin prepared by alternative processing methods. Eur. J. Pharm. Biopharm. 92, 112–119. https://doi.org/10.1016/j.ejpb.2015.03.004.

Cerchiara, T., Abruzzo, A., Ñahui Palomino, R.A., Vitali, B., De Rose, R., Chidichimo, G., Ceseracciu, L., Athanassiou, A., Saladini, B., Dalena, F., Bigucci, F., Luppi, B., 2017. Spanish Broom (*Spartium junceum* L.) fibers impregnated with vancomycin-loaded chitosan nanoparticles as new antibacterial wound dressing: preparation, characterization and antibacterial activity. Eur. J. Pharm. Sci. 99, 105–112. https://doi.org/10.1016/j.ejps.2016.11.028.

Chahine, E.B., Dougherty, J.A., Thornby, K.A., Guirguis, E.H., 2021. Antibiotic approvals in the last decade: Are we keeping up with resistance? Ann. Pharmacother. 10600280211031390 https://doi.org/10.1177/10600280211031390.

Chakraborty, S.P., Mahapatra, S.K., Sahu, S.K., Das, S., Tripathy, S., Dash, S., Pramanik, P., Roy, S., 2011a. Internalization of *Staphylococcus aureus* in lymphocytes induces oxidative stress and DNA fragmentation: possible ameliorative role of nanoconjugated vancomycin. Oxidative Med. Cell. Longev. 9422123. https://doi.org/10.1155/2011/942123, 2011.

Chakraborty, S.P., Mahapatra, S.K., Sahu, S.K., Chattopadhyay, S., Pramanik, P., Roy, S., 2011b. Nitric oxide mediated *Staphylococcus aureus* pathogenesis and protective role of nanoconjugated vancomycin. Asian Pac. J. Trop. Biomed. 1 (2), 102–109. https://doi.org/10.1016/S2221-1691(11)60005-1.

Chakraborty, S.P., Sahu, S.K., Pramanik, P., Roy, S., 2012a. In vitro antimicrobial activity of nanoconjugated vancomycin against drug resistant *Staphylococcus aureus*. Int. J. Pharm. 436 (1-2), 659–676. https://doi.org/10.1016/j.ijpharm.2012.07.033.

Chakraborty, S.P., Das, S., Chattopadhyay, S., Tripathy, S., Dash, S.K., Pramanik, P., Roy, S., 2012b. *Staphylococcus aureus* infection induced redox signaling and DNA fragmentation in T-lymphocytes: possible ameliorative role of nanoconjugated vancomycin. Toxicol. Mech. Methods 22 (3), 193–204. https://doi.org/10.3109/15376516.2011.629236.

Chen, H., Zhang, M., Li, B., Chen, D., Dong, X., Wang, Y., Gu, Y., 2015. Versatile antimicrobial peptide-based ZnO quantum dots for in vivo bacteria diagnosis and treatment with high specificity. Biomaterials. 53, 532–544. https://doi.org/10.1016/j.biomaterials.2015.02.105.

Chen, H., Yang, J., Sun, L., Zhang, H., Guo, Y., Qu, J., Jiang, W., Chen, W., Ji, J., Yang, Y. W., Wang, B., 2019. Synergistic chemotherapy and photodynamic therapy of endophthalmitis mediated by zeolitic imidazolate framework-based drug delivery systems. Small. 15 (47), e1903880 https://doi.org/10.1002/smll.201903880.

Chiang, W.L., Lin, T.T., Sureshbabu, R., Chia, W.T., Hsiao, H.C., Liu, H.Y., Yang, C.M., Sung, H.W., 2015. A rapid drug release system with a NIR light-activated molecular switch for dual-modality photothermal/antibiotic treatments of subcutaneous abscesses. J. Control. Release 199, 53–62. https://doi.org/10.1016/j.jconrel.2014.12.011.

Chowdhuri, A.R., Das, B., Kumar, A., Tripathy, S., Roy, S., Sahu, S.K., 2017. One-pot synthesis of multifunctional nanoscale metal-organic frameworks as an effective antibacterial agent against multidrug-resistant *Staphylococcus aureus*. Nanotechnology. 28 (9), 095102 https://doi.org/10.1088/1361-6528/aa57af.

Cieplik, F., Deng, D., Crielaard, W., Buchalla, W., Hellwig, E., Al-Ahmad, A., Maisch, T., 2018. Antimicrobial photodynamic therapy - what we know and what we don't. Crit. Rev. Microbiol. 44 (5), 571–589. https://doi.org/10.1080/1040841X.2018.1467876.

Cong, Y., Quan, C., Liu, M., Liu, J., Huang, G., Tong, G., Yin, Y., Zhang, C., Jiang, Q., 2015. Alendronate-decorated biodegradable polymeric micelles for potential bone-targeted delivery of vancomycin. J. Biomater. Sci. Polym. Ed. 26 (11), 629–643. https://doi.org/10.1080/09205063.2015.1053170.

Cong, Y., Yang, S., Rao, X., 2019. Vancomycin resistant *Staphylococcus aureus* infections: a review of case updating and clinical features. J. Adv. Res. 21, 169–176. https://doi.org/10.1016/j.jare.2019.10.005.

Cooper, M.A., Williams, D.H., 1999. Binding of glycopeptide antibiotics to a model of a vancomycin-resistant bacterium. Chem. Biol. 6 (12), 891–899. https://doi.org/10.1016/s1074-5521(00)80008-3.

Costa, J.R., Silva, N.C., Sarmento, B., Pintado, M., 2015. Potential chitosan-coated alginate nanoparticles for ocular delivery of daptomycin. Eur. J. Clin. Microbiol. Infect. Dis. 34 (6), 1255–1262. https://doi.org/10.3109/10717544.2013.858195.

Costa, C., Brandão, F., Bessa, M.J., Costa, S., Valdiglesias, V., Kiliç, G., Fernández-Bertólez, N., Quaresma, P., Pereira, E., Pásaro, E., Laffon, B., Teixeira, J.P., 2016. In vitro cytotoxicity of superparamagnetic iron oxide nanoparticles on neuronal and glial cells. Evaluation of nanoparticle interference with viability tests. J. Appl. Toxicol. 36 (3), 361–372. https://doi.org/10.1002/jat.3213.

Craft, K.M., Nguyen, J.M., Berg, L.J., Townsend, S.D., 2019. Methicillin-resistant *Staphylococcus aureus* (MRSA): antibiotic-resistance and the biofilm phenotype. Medchemcomm. 10 (8), 1231–1241. https://doi.org/10.1039/c9md00044e.

Croes, M., Bakhshandeh, S., van Hengel, I.A.J., Lietaert, K., van Kessel, K.P.M., Pouran, B., van der Wal, B.C.H., Vogely, H.C., Van Hecke, W., Fluit, A.C., Boel, C.H. E., Alblas, J., Zadpoor, A.A., Weinans, H., Amin Yavari, S., 2018. Antibacterial and immunogenic behavior of silver coatings on additively manufactured porous titanium. Acta Biomater. 81, 315–327. https://doi.org/10.1016/j.actbio.2018.09.051.

Dadfar, S.M., Roemhild, K., Drude, N.I., von Stillfried, S., Knüchel, R., Kiessling, F., Lammers, T., 2019. Diagnostic, therapeutic and theranostic applications. Adv. Drug Deliv. Rev. 138, 302–325. https://doi.org/10.1016/j.addr.2019.01.005.

Dakal, T.C., Kumar, A., Majumdar, R.S., Yadav, V., 2016. Mechanistic basis of antimicrobial actions of silver nanoparticles. Front. Microbiol. 7, 1831. https://doi.org/10.3389/fmicb.2016.01831.

Dash, B.S., Jose, G., Lu, Y.J., Chen, J.P., 2021. Functionalized reduced graphene oxide as a versatile tool for cancer therapy. Int. J. Mol. Sci. 22 (6), 2989. https://doi.org/10.3390/ijms22062989.

Domingo-Calap, P., Delgado-Martínez, J., 2018. Bacteriophages: protagonists of a post-antibiotic era. Antibiotics. 7, 66. https://doi.org/10.3390/antibiotics7030066.

Drummer, S., Madzimbamuto, T., Chowdhury, M., 2021. Green synthesis of transition-metal nanoparticles and their oxides: a review. Materials (Basel). 14 (11), 2700. https://doi.org/10.3390/ma14112700.

Dulińska-Litewka, J., Łazarczyk, A., Hałubiec, P., Szafrański, O., Karnas, K., Karewicz, A., 2019. Superparamagnetic iron oxide nanoparticles-current and prospective medical applications. Materials (Basel). 12 (4), 617. https://doi.org/10.3390/ma12040617.

Durán, N., Durán, M., de Jesus, M.B., Seabra, A.B., Fávaro, W.J., Nakazato, G., 2016. Silver nanoparticles: a new view on mechanistic aspects on antimicrobial activity. Nanomedicine. 12, 789–799. https://doi.org/10.1016/j.nano.2015.11.01.

Echevarria, K., Datta, P., Cadena, J., Lewis, J.S., 2005. Severe myopathy and possible hepatotoxicity related to daptomycin. J. Antimicrob. Chemother. 55 (4), 599–600. https://doi.org/10.1093/jac/dki058.

Ediyilyam, S., George, B., Shankar, S.S., Dennis, T.T., Wacławek, S., Černík, M., Padil, V. V.T., 2021. Chitosan/gelatin/silver nanoparticles composites films for biodegradable food packaging applications. Polymers (Basel). 13 (11), 1680. https://doi.org/10.3390/polym13111680.

Efiana, N.A., Dizdarević, A., Huck, C.W., Bernkop-Schnürch, A., 2019. Improved intestinal mucus permeation of vancomycin via incorporation into nanocarrier containing papain-palmitate. J. Pharm. Sci. 108 (10), 3329–3339. https://doi.org/10.1016/j.xphs.2019.05.020.

El-Gendy, N.S., Nassar, H.N., 2021. Biosynthesized magnetite nanoparticles as an environmental opulence and sustainable wastewater treatment. Sci. Total Environ. 774, 145610 https://doi.org/10.1016/j.scitotenv.2021.145610.

Elshaer, S.L., Shaaban, M.I., 2021. Inhibition of quorum sensing and virulence factors of *Pseudomonas aeruginosa* by biologically synthesized gold and selenium nanoparticles. Antibiotics 10, 1461. https://doi.org/10.3390/antibiotics10121461.

Ermini, M.L., Voliani, V., 2021. Antimicrobial nano-agents: the copper age. ACS Nano 15 (4), 6008–6029. https://doi.org/10.1021/acsnano.0c10756.

Esmaeili, A., Ghobadianpour, S., 2016. Vancomycin loaded superparamagnetic $MnFe_2O_4$ nanoparticles coated with PEGylated chitosan to enhance antibacterial activity. Int. J. Pharm. 501 (1-2), 326–330. https://doi.org/10.1016/j.ijpharm.2016.02.013.

European Centre for Disease Prevention and Control, 2017. Antimicrobial resistance surveillance in Europe 2016. https://www.ecdc.europa.eu/sites/default/files/documents/AMR%202017_Cover%2BInner-web_v3.pdf (last accessed on 24th June 2021).

Fadeel, B., Alexiou, C., 2020. Brave new world revisited: focus on nanomedicine. Biochem. Biophys. Res. Commun. 533 (1), 36–49. https://doi.org/10.1016/j.bbrc.2020.08.046.

Ferdous, Z., Nemmar, A., 2020. Health impact of silver nanoparticles: a review of the biodistribution and toxicity following various routes of exposure. Int. J. Mol. Sci. 21 (7), 2375. https://doi.org/10.3390/ijms21072375.

Finley, P.J., Norton, R., Austin, C., Mitchell, A., Zank, S., Durham, P., 2015. Unprecedented silver resistance in clinically isolated Enterobacteriaceae: major implications for burn and wound management. Antimicrob. Agents Chemother. 59, 4734–4741. https://doi.org/10.1128/AAC.00026-15.

Flemming, H.C., Wingender, J., Szewzwyk, U., Steinberg, P., Rice, S.A., Kjelleberg, S., 2016. Biofilms: an emergent form of bacterial life. Nat. Rev. Microbiol. 14 (9), 563–575. https://doi.org/10.1038/nrmicro.2016.94.

Fulaz, S., Devlin, H., Vitale, S., Quinn, L., O'Gara, J.P., Casey, E., 2020. Tailoring nanoparticle-biofilm interactions to increase the efficacy of antimicrobial agents against *Staphylococcus aureus*. Int. J. Nanomedicine 15, 4779–4791. https://doi.org/10.2147/IJN.S256227.

Fytianos, G., Rahdar, A., Kyzas, G.Z., 2020. Nanomaterials in cosmetics: recent updates. Nanomaterials (Basel). 10 (5), 979. https://doi.org/10.3390/nano10050979.

Gabrielyan, L., Hovhannisyan, A., Gevorgyan, V., Ananyan, M., Trchounian, A., 2019. Antibacterial effects of iron oxide (Fe_3O_4) nanoparticles: distinguishing concentration-dependent effects with different bacterial cells growth and membrane-associated mechanisms. Appl. Microbiol. Biotechnol. 103 (6), 2773–2782. https://doi.org/10.1007/s00253-019-09653-x.

Gao, Y., Chen, Y., Cao, Y., Mo, A., Peng, Q., 2021. Potentials of nanotechnology in treatment of methicillin-resistant *Staphylococcus aureus*. Eur. J. Med. Chem. 213, 113056 https://doi.org/10.1016/j.ejmech.2020.113056.

García-Lara, B., Saucedo-Mora, M.Á., Roldán-Sánchez, J.A., Pérez-Eretza, B., Ramasamy, M., Lee, J., Coria-Jimenez, R., Tapia, M., Varela-Guerrero, V., García-Contreras, R., 2015. Inhibition of quorum-sensing-dependent virulence factors and biofilm formation of clinical and environmental *Pseudomonas aeruginosa* strains by ZnO nanoparticles. Lett. Appl. Microbiol. 61 (3), 299–305. https://doi.org/10.1111/lam.12456.

George, L., Bavya, M.C., Rohan, K.V., Srivastava, R., 2017. A therapeutic polyelectrolyte-vitamin C nanoparticulate system in polyvinyl alcohol-alginate hydrogel: an approach to treat skin and soft tissue infections caused by *Staphylococcus aureus*. Colloids Surf. B: Biointerfaces 160, 315–324. https://doi.org/10.1016/j.colsurfb.2017.09.030.

Gharpure, S., Ankamwar, B., 2020. Synthesis and antimicrobial properties of zinc oxide nanoparticles. J. Nanosci. Nanotechnol. 20 (10), 5977–5996. https://doi.org/10.1166/jnn.2020.18707.

Gómez-Núñez, M.F., Castillo-López, M., Sevilla-Castillo, F., Roque-Reyes, O.J., Romero-Lechuga, F., Medina-Santos, D.I., Martínez-Daniel, R., Peón, A.N., 2020. Nanoparticle-based devices in the control of antibiotic resistant bacteria. Front. Microbiol. 11, 563821 https://doi.org/10.3389/fmicb.2020.563821.

Gonzalez Gomez, A., Hosseinidoust, Z., 2020. Liposomes for antibiotic encapsulation and delivery. ACS Infect. Dis. 6 (5), 896–908. https://doi.org/10.1021/acsinfecdis.9b00357.

Gonzalez Gomez, A., Xu, C., Hosseinidoust, Z., 2019. Preserving the efficacy of glycopeptide antibiotics during nanoencapsulation in liposomes. ACS Infect. Dis. 5 (10), 1794–1801. https://doi.org/10.1021/acsinfecdis.9b00232.

González-Bello, C., 2017. Antibiotic adjuvants – a strategy to unlock bacterial resistance to antibiotics. Bioorg. Med. Chem. Lett. 27, 4221–4228. https://doi.org/10.1016/j.bmcl.2017.08.027.

Gou, N., Onnis-Hayden, A., Gu, A.Z., 2010. Mechanistic toxicity assessment of nanomaterials by whole-cell-array stress genes expression analysis. Environ. Sci. Technol. 44, 5964–5970. https://doi.org/10.1021/es100679f.

Gounani, Z., Asadollahi, M.N., Pedersen, J.N., Lyngsø, J., Pedersen, J.S., Arpanaei, A., Meyer, R.L., 2019. Mesoporous silica nanoparticles carrying multiple antibiotics provide enhanced synergistic effect and improved biocompatibility. Colloids Surf. B: Biointerfaces 175, 498–508. https://doi.org/10.1016/j.colsurfb.2018.12.035.

Gu, J., Wang, T., Fan, G., Ma, J., Hu, W., Cai, X., 2016. Biocompatibility of artificial bone based on vancomycin loaded mesoporous silica nanoparticles and calcium sulfate composites. J. Mater. Sci. Mater. Med. 12 (14), 7651–7659. https://doi.org/10.1007/s10856-016-5671-z.

Guo, X., Cao, B., Wang, C., Lu, S., Hu, X., 2020. In vivo photothermal inhibition of methicillin-resistant *Staphylococcus aureus* infection by in situ templated formulation of pathogen-targeting phototheranostics. Nanoscale. 12 (14), 7651–7659. https://doi.org/10.1039/D0NR00181C.

Gupta, A., Mumtaz, S., Li, C.H., Hussain, I., Rotello, V.M., 2019. Combatting antibiotic-resistant bacteria using nanomaterials. Chem. Soc. Rev. 48 (2), 415–427. https://doi.org/10.1039/c7cs00748e.

Han, L., Wang, Z.M., Lu, X., Chao, L.D., Xie, C.M., Wang, K.F., Chen, X.I., Ding, Y.H., Weng, L.T., 2015. Mussel-inspired adhesive and transferable free-standing films by self-assembling dexamethasone encapsulated BSA nanoparticles and vancomycin immobilized oxidized alginate. Colloids Surf. B: Biointerfaces 126, 452–458. https://doi.org/10.1016/j.colsurfb.2014.12.050.

Han, L., Wang, M., Sun, H., Li, P., Wang, K., Ren, F., Lu, X., 2017. Porous titanium scaffolds with self-assembled micro/nano-hierarchical structure for dual functions of bone regeneration and anti-infection. J. Biomed. Mater. Res. 105 (12), 3482–3492. https://doi.org/10.1002/jbm.a.36178.

Harris, M., Ahmed, H., Barr, B., LeVine, D., Pace, L., Mohapatra, A., Morshed, B., Bumgardner, J.D., Jennings, J.A., 2017. Magnetic stimuli-responsive chitosan-based drug delivery biocomposite for multiple triggered release. Int. J. Biol. Macromol. 104 (Pt B), 1407–1414. https://doi.org/10.1016/j.ijbiomac.2017.03.141.

Hassan, N.M., Ranzoni, A., Phetsang, W., Blaskovich, M.A., Cooper, M.A., 2017. Surface ligand density of antibiotic-nanoparticle conjugates enhances target avidity and membrane permeabilization of vancomycin-resistant bacteria. Bioconjug. Chem. 28 (2), 353–361. https://doi.org/10.1021/acs.bioconjchem.6b00494.

Hassan, D., Omolo, C.A., Fasiku, V.O., Mocktar, C., Govender, T., 2020. Novel chitosan-based pH-responsive lipid-polymer hybrid nanovesicles (OLA-LPHVs) for delivery of vancomycin against methicillin-resistant *Staphylococcus aureus* infections. Int. J. Biol. Macromol. 147, 385–398. https://doi.org/10.1016/j.ijbiomac.2020.01.019.

Hassani Besheli, N., Mottaghitalab, F., Eslami, M., Gholami, M., Kundu, S.C., Kaplan, D. L., Farokhi, M., 2017. Sustainable release of vancomycin from silk fibroin nanoparticles for treating severe bone infection in rat tibia osteomyelitis model. ACS Appl. Mater. Interfaces 9 (6), 5128–5138. https://doi.org/10.1021/acsami.6b14912.

Heidary, M., Khosravi, A.D., Khoshnood, S., Nasiri, M.J., Soleimani, S., Goudarzi, M., 2018. Daptomycin. J. Antimicrob. Chemother. 73 (1), 1–11. https://doi.org/10.1093/jac/dkx349.

Hernandez, F.J., Hernandez, L.I., Kayruk, M., Arica, Y.M., Bayramoğlu, G., Borsa, B.A., Öktem, H.A., Schäfer, T., Özalp, V.C., 2014. NanoKeepers: stimuli responsive nanocapsules for programmed specific targeting and drug delivery. Chem. Commun. (Camb.) 50 (67), 9489–9492. https://doi.org/10.1039/C4CC04248D.

Hu, B., Cheng, Z., Liang, S., 2022. Advantages and prospects of stem cells in nanotoxicology. Chemosphere. 291 (Pt 2), 132861 https://doi.org/10.1016/j.chemosphere.2021.132861.

Hur, Y.E., Park, Y., 2016. Vancomycin-functionalized gold and silver nanoparticles as an antibacterial nanoplatform against methicillin-resistant *Staphylococcus aureus*. J. Nanosci. Nanotechnol. 16 (6), 6393–6399. https://doi.org/10.1166/jnn.2016.12393.

No time to wait: Securing the future from drug-resistant infections report to the secretary-general of the united nations, 2019. Interagency Coordination Group on Antimicrobial Resistance. https://www.who.int/publications/i/item/no-time-to-wait-securing-the-future-from-drug-resistant-infections (last accessed on 24th June 2021).

Javanbakht, T., Laurent, S., Stanicki, D., Wilkinson, K.J., 2016. Relating the surface properties of superparamagnetic iron oxide nanoparticles (SPIONs) to their bactericidal effect towards a biofilm of *Streptococcus mutans*. PLoS One 11 (4), e1054445. https://doi.org/10.1371/journal.pone.0154445.

Javed, R., Zia, M., Naz, S., Aisida, S.O., Ain, N.U., Ao, Q., 2020. Role of capping agents in the application of nanoparticles in biomedicine and environmental remediation: recent trends and future prospects. J. Nanobiotechnol. 18 (1), 172. https://doi.org/10.1186/s12951-020-00704-4.

Jefferson, K.K., Goldmann, D.A., Pier, G.B., 2005. Use of confocal microscopy to analyze the rate of vancomycin penetration through *Staphylococcus aureus* biofilms. Antimicrob. Agents Chemother. 49 (6), 2467–2473. https://doi.org/10.1128/AAC.49.6.2467-2473.2005.

Kalhapure, R.S., Mocktar, C., Sikwal, D.R., Sonawane, S.J., Kathiravan, M.K., Skelton, A., Govender, T., 2014. Ion pairing with linoleic acid simultaneously enhances encapsulation efficiency and antibacterial activity of vancomycin in solid lipid nanoparticles. Colloids Surf. B: Biointerfaces 117, 303–311. https://doi.org/10.1016/j.colsurfb.2014.02.045.

Kalhapure, R.S., Jadhav, M., Rambharose, S., Mocktar, C., Singh, S., Renukuntla, J., Govender, T., 2017a. pH-responsive chitosan nanoparticles from a novel twin-chain anionic amphiphile for controlled and targeted delivery of vancomycin. Colloids Surf. B: Biointerfaces 158, 650–657. https://doi.org/10.1016/j.colsurfb.2017.07.049.

Kalhapure, R.S., Sikwal, D.R., Rambharose, S., Mocktar, C., Singh, S., Bester, L., Oh, J.K., Renukuntla, J., Govender, T., 2017b. Enhancing targeted antibiotic therapy via pH responsive solid lipid nanoparticles from an acid cleavable lipid. Nanomedicine. 13 (6), 2067–2077. https://doi.org/10.1016/j.nano.2017.04.010.

Kang, S., Herzberg, M., Rodrigues, D.F., Elimelech, M., 2008. Antibacterial effects of carbon nanotubes: size does matter! Langmuir. 24 (13), 6409–6413. https://doi.org/10.1021/la800951v.

Karakeçili, A., Topuz, B., Korpayev, S., Erdek, M., 2019. Metal-organic frameworks for on-demand pH controlled delivery of vancomycin from chitosan scaffolds. Mater. Sci. Eng. C Mater. Biol. Appl. 105, 110098 https://doi.org/10.1016/j.msec.2019.110098.

Kaur, A., Preet, S., Kumar, V., Kumar, R., Kumar, R., 2019. Synergetic effect of vancomycin loaded silver nanoparticles for enhanced antibacterial activity. Colloids Surf. B: Biointerfaces 176, 62–69. https://doi.org/10.1016/j.colsurfb.2018.12.043.

Kavruk, M., Celikbicak, O., Ozalp, V.C., Borsa, B.A., Hernandez, F.J., Bayramoglu, G., Salih, B., Arica, M.Y., 2015. Antibiotic loaded nanocapsules functionalized with aptamer gates for targeted destruction of pathogens. Chem. Commun. (Camb.) 51 (40), 8492–8495. https://doi.org/10.1039/c5cc01869b.

Kędziora, A., Speruda, M., Krzyzewska, E., Rybka, J., Łukowiak, A., Bugla-Płoskońska, G., 2018. Similarities and differences between silver ions and silver in nanoforms as antibacterial agents. Int. J. Mol. Sci. 19, 444. https://doi.org/10.3390/ijms19020444.

Khalid, K., Tan, X., Mohd Zaid, H.F., Tao, Y., Lye Chew, C., Chu, D.T., Lam, M.K., Ho, Y. C., Lim, J.W., Chin Wei, L., 2020. Advanced in developmental organic and inorganic nanomaterial: a review. Bioengineered. 11 (1), 328–355. https://doi.org/10.1080/21655979.2020.1736240.

Kimna, C., Deger, S., Tamburaci, S., Tihminlioglu, F., 2019. Chitosan/montmorillonite composite nanospheres for sustained antibiotic delivery at post-implantation bone infection treatment. Biomed. Mater. 14 (4), 044101 https://doi.org/10.1088/1748-605X/ab1a04.

Kirk, R.G.W., 2018. Recovering the principles of human experimental technique. The 3Rs and the human essence of animal research. Sci. Technol. Hum. Values 43 (4), 622–648. https://doi.org/10.1177/0162243917726579.

Klein, E.Y., Van Boeckel, T.P., Martinez, E.M., Pant, S., Gandra, S., Levin, S.A., Goossens, H., Laxminarayan, R., 2018. Global increase and geographic convergence in antibiotic consumption between 2000 and 2015. Proc. Natl. Acad. Sci. U. S. A. 115, E3463–E3470. https://doi.org/10.1073/pnas.1717295115.

Kranjec, C., Morales Angeles, D., Torrissen Mårli, M., Fernández, L., García, P., Kjos, M., Diep, D.B., 2021. Staphylococcal biofilms: challenges and novel therapeutic perspectives. Antibiotics (Basel). 10 (2), 131. https://doi.org/10.3390/antibiotics10020131.

Kumar, P., Liu, B., Behl, G., 2019. A comprehensive outlook of synthetic strategies and applications of redox-responsive nanogels in drug delivery. Macromol. Biosci. 19 (8), e1900071 https://doi.org/10.1002/mabi.201900071.

Kvítek, L., Panáček, A., Soukupová, J., Kolář, M., Večeřová, R., Prucek, R., Holecová, M., Zbořil, R., 2008. Effect of surfactants and polymers on stability and antibacterial activity of silver nanoparticles (NPs). J. Phys. Chem. C 112 (15), 5825–5834. https://doi.org/10.1021/jp711616v.

Lai, H.Z., Chen, W.Y., Wu, C.Y., Chen, Y.C., 2015. Potent antibacterial nanoparticles for pathogenic bacteria. ACS Appl. Mater. Interfaces 7 (3), 2046–2054. https://doi.org/10.1021/am507919m.

Lallo da Silva, B., Caetano, B.L., Chiari-Andréo, B.G., Pietro, R.C.L.R., Chiavacci, L.A., 2019. Increased antibacterial activity of ZnO nanoparticles: influence of size and surface modification. Colloids Surf. B: Biointerfaces 177, 440–447. https://doi.org/10.1016/j.colsurfb.2019.02.013.

Lebreton, F., Cattoir, V., 2019. Resistance to glycopeptide antibiotics. In: Bonev, B.B., Brown, N.M. (Eds.), Bacterial Resistance to Antibiotics – From Molecules to Man. John Wiley & Sons, Ltd, pp. 51–80.

Lee, J.H., Kim, Y.G., Cho, M.H., Lee, J., 2014. ZnO nanoparticles inhibit *Pseudomonas aeruginosa* biofilm formation and virulence factor production. Microbiol. Res. 169 (12), 888–896. https://doi.org/10.1016/j.micres.2014.05.005.

Li, C., Zhang, X., Huang, X., Wang, X., Liao, G., Chen, Z., 2013. Preparation and characterization of flexible nanoliposomes loaded with daptomycin, a novel antibiotic, for topical skin therapy. Int. J. Nanomedicine 8, 1285–1292. https://doi.org/10.2147/IJN.S41695.

Li, L.L., Xu, J.H., Qi, G.B., Zhao, X., Yu, F., Wang, H., 2014. Core-shell supramolecular gelatin nanoparticles for adaptive and "on-demand" antibiotic delivery. ACS Nano 8 (5), 4975–4983. https://doi.org/10.1021/nn501040h.

Li, Y.J., Harroun, S.G., Su, Y.C., Huang, C.F., Unnikrishnan, B., Lin, H.J., Lin, C.H., Huang, C.C., 2016. Synthesis of self-assembled spermidine-carbon quantum dots effective against multidrug-resistant bacteria. Adv. Healthc. Mater. 5 (19), 2545–2554. https://doi.org/10.1002/adhm.201600297.

Li, Q., Pan, Y., Chen, T., Du, Y., Ge, H., Zhang, B., Xie, J., Yu, H., Zhu, M., 2018. Design and mechanistic study of a novel gold nanocluster-based drug delivery system. Nanoscale. 10 (21), 10166–10172. https://doi.org/10.1039/C8NR02189A.

Li, J., Nickel, R., Wu, J., Lin, F., van Lierop, J., Liu, S., 2019. A new tool to attack biofilms: driving magnetic iron-oxide nanoparticles to disrupt the matrix. Nanoscale. 11 (14), 6905–6915. https://doi.org/10.1039/c8nr09802f.

Liao, C., Li, Y., Tjong, S.C., 2020. Visible-light active titanium dioxide nanomaterials with bactericidal properties. Nanomaterials (Basel). 10 (1), 124. https://doi.org/10.3390/nano10010124.

Lin, S., Liu, X., Tan, L., Cui, Z., Yang, X., Yeung, K.W.K., Pan, H., Wu, S., 2017. Porous iron-carboxylate metal-organic framework: a novel bioplatform with sustained antibacterial efficacy and nontoxicity. ACS Appl. Mater. Interfaces 9 (22), 19248–19257. https://doi.org/10.1021/acsami.7b04810.

Liu, S., Zeng, T.H., Hofmann, M., Burcombe, E., Wei, J., Jiang, R., Kong, J., Chen, Y., 2011. Antibacterial activity of graphite, graphite oxide, graphene oxide, and reduced graphene oxide: membrane and oxidative stress. ACS Nano 5 (9), 6971–6980. https://doi.org/10.1021/nn202451x.

Liu, Z., Zhu, Y., Liu, X., Yeung, K.W.K., Wu, S., 2017. Construction of poly (vinyl alcohol)/poly (lactide-glycolide acid)/vancomycin nanoparticles on titanium for enhancing the surface self-antibacterial activity and cytocompatibility. Colloids Surf. B: Biointerfaces 151, 165–177. https://doi.org/10.1016/j.colsurfb.2016.12.016.

Liu, Y., Li, Z., Zou, S., Lu, C., Xiao, Y., Bai, H., Zhang, X., Mu, H., Zhang, X., Duan, J., 2020. Hyaluronic acid-coated ZIF-8 for the treatment of pneumonia caused by methicillin-resistant *Staphylococcus aureus*. Int. J. Biol. Macromol. 155, 103–109, 10.10167j.ijbiomac.2020.03.187.

Lopez-Chaves, C., Soto-Alvaredo, J., Montes-Bayon, M., Bettmer, J., Llopis, J., Sanchez-Gonzalez, C., 2018. Gold nanoparticles: distribution, bioaccumulation and toxicity. In vitro and in vivo studies. Nanomedicine. 14 (1), 1–12. https://doi.org/10.1016/j.nano.2017.08.011.

Lotfipour, F., Abdollahi, S., Jelvehgari, M., Valizadeh, H., Hassan, M., Milani, M., 2014. Study of antimicrobial effects of vancomycin loaded PLGA nanoparticles against enterococcus clinical isolates. Drug Res. (Stuttg). 64 (7), 348–352. https://doi.org/10.1055/s-0033-1358747.

Ma, K., Dong, P., Liang, M., Yu, S., Chen, Y., Wang, F., 2020. Facile assembly of multifunctional antibacterial nanoplatform leveraging synergistic sensitization between silver nanostructure and vancomycin. ACS Appl. Mater. Interfaces 12 (6), 6955–6965. https://doi.org/10.1021/acsami.9b22043.

MacCormack, T.J., Meli, M.V., Ede, J.D., Ong, K.J., Rourke, J.L., Dieni, C.A., 2021. Revisiting nanoparticle-assay interference: there's plenty of room at the bottom for misinterpretation. Comp. Biochem. Physiol. B Biochem. Mol. Biol. 255, 110601 https://doi.org/10.1016/j.cbpb.2021.110601.

Mada, P.K., Alam, M.U., 2021. Clostridium difficile. In: SteatPearls. https://www.ncbi.nlm.nih.gov/books/NBK431054/ (last accessed on 24th June 2021).

Maji, R., Omolo, C.A., Agrawal, N., Maduray, K., Hassan, D., Mokhtar, C., Mackhraj, I., Govender, T., 2019. pH-responsive lipid-dendrimer hybrid nanoparticles: An approach to target and eliminate intracellular pathogens. Mol. Pharm. 16 (11), 4594–4609. https://doi.org/10.1021/acs.molpharmaceut.9b00713.

Mamun, M.M., Sorinolu, A.J., Munir, M., Vejerano, E.P., 2021. Nanoantibiotics: Functions and properties at the nanoscale to combat antibiotic resistance. Front. Chem. 9, 687660 https://doi.org/10.3389/fchem.2021.687660.

Mann, R., Holmes, A., McNeilly, O., Cavaliere, R., Sotiriou, G.A., Rice, S.A., Gunawan, C., 2021. Evolution of biofilm-forming pathogenic bacteria in the presence of nanoparticles and antibiotic: adaptation phenomena and cross-resistance. J. Nanobiotechnol. 19 (1), 291. https://doi.org/10.1186/s12951-021-01027-8.

Marchianò, V., Matos, M., Serrano-Pertierra, E., Gutiérrez, G., Blanco-López, M.C., 2020. Vesicles as antibiotic carrier: State of art. Int. J. Pharm. 585, 119478 https://doi.org/10.1016/j.ijpharm.2020.119478.

Marcone, G.L., Binda, E., Berini, F., Marinelli, F., 2018. Old and new glycopeptide antibiotics: From product to gene and back in the post-genomic era. Biotechnol. Adv. 36 (2), 534–554. https://doi.org/10.1016/j.biotechadv.2018.02.009.

Martínez-Carmona, M., Gun'ko, Y., Vallet-Regí, M., 2018. ZnO nanostructures for drug delivery and theranostic applications. Nanomaterials (Basel) 8 (4), 268. https://doi.org/10.3390/nano8040268.

Martínez-Castañón, G., Niño-Martínez, N., Martínez-Gutierrez, F., Martínez-Mendoza, J., Ruiz, F., 2008. Synthesis and antibacterial activity of silver nanoparticles with different sizes. J. Nanopart. Res. 10, 1343–1348. https://doi.org/10.1007/s11051-008-9428-6.

Mas, N., Galiana, I., Mondragón, L., Aznar, E., Climent, E., Cabedo, N., Sancenón, F., Murguía, J.R., Martínez-Máñez, R., Marcos, M.D., Amorós, P., 2013. Enhanced efficacy and broadening of antibacterial action of drugs via the use of capped mesoporous nanoparticles. Chemistry. 19 (34), 11167–11171. https://doi.org/10.1002/chem.201302170.

Matica, M.A., Aachmann, F.L., Tøndervik, A., Sletta, H., Ostafe, V., 2019. Chitosan as a wound dressing starting material: antimicrobial properties and mode of action. Int. J. Mol. Sci. 20 (23), 5889. https://doi.org/10.3390/ijms20235889.

May, K.L., Grabowicz, M., 2018. The bacterial outer membrane is an evolving antibiotic barrier. Proc. Natl. Acad. Sci. U. S. A. 115 (36), 8852–8854. https://doi.org/10.1073/pnas.1812779115.

Mba, I.E., Nweze, E.I., 2021. Nanoparticles as therapeutic options for treating multidrug-resistant bacteria: research progress, challenges, and prospects. World J. Microbiol. Biotechnol. 37 (6), 108. https://doi.org/10.1007/s11274-021-03070-x.

Meeker, D.G., Jenkins, S.V., Miller, E.K., Beenken, K.E., Loughran, A.J., Powless, A., Muldoon, T.J., Galanzha, E.I., Zharov, V.P., Smeltzer, M.S., Chen, J., 2016. Synergistic photothermal and antibiotic killing of biofilm-associated *Staphylococcus aureus* using targeted antibiotic-loaded gold nanoconstructs. ACS Infect. Dis. 2 (4), 241–250. https://doi.org/10.1021/acsinfecdis.5b00117.

Meeker, D.G., Wang, T., Harrington, W.N., Zharov, V.P., Johnson, S.A., Jenkins, S.V., Oyibo, S.E., Walker, C.M., Mills, W.B., Shirtliff, M.E., Beenken, K.E., Chen, J., Smeltzer, M.S., 2018. Versatility of targeted antibiotic-loaded gold nanoconstructs for the treatment of biofilm-associated bacterial infections. Int. J. Hyperth. 34 (2), 209–219. https://doi.org/10.1080/02656736.2017.1392047.

Merkl, P., Long, S., McInerney, G.M., Sotiriou, G.A., 2021. Antiviral activity of silver, copper oxide and zinc oxide nanoparticle coatings against SARS-CoV-2. Nanomaterials (Basel). 11 (5), 1312. https://doi.org/10.3390/nano11051312.

Mhule, D., Kalhapure, R.S., Jadhav, M., Omolo, C.A., Rambharose, S., Mocktar, C., Singh, S., Waddad, A.Y., Ndesendo, V.M.K., Govender, T., 2018. Synthesis of an oleic acid based pH-responsive lipid and its application in nanodelivery of vancomycin. Int. J. Pharm. 550 (1-2), 149–159. https://doi.org/10.1016/j.ijpharm.2018.08.025.

Miller, W.R., Murray, B.E., Rice, L.B., Arias, C.A., 2016a. Vancomycin-resistant enterococci: therapeutic challenges in the 21st century. Infect. Dis. Clin. N. Am. 30 (2), 415–439. https://doi.org/10.1016/j.idc.2016.02.006.

Miller, W.R., Bayer, A.S., Arias, C.A., 2016b. Mechanism of action and resistance to Daptomycin in *Staphylococcus aureus* and Enterococci. Cold Spring Harb. Perspect. Med. 6 (11), a026997 https://doi.org/10.1101/cshperspect.a026997.

Mitchell, S.L., Hudson-Smith, N.V., Cahill, M.S., Reynolds, B.N., Frand, S.D., Green, C.M., Wang, C., Hang, M.N., Hernandez, R.T., Hamers, R.J., Feng, Z.V., Haynes, C.L., Carlson, E.E., 2019. Chronic exposure to complex metal oxide nanoparticles elicits rapid resistance in *Shewanella oneidensis* MR-1. Chem. Sci. 10 (42), 9768–9781. https://doi.org/10.1039/c9sc01942a.

Mohapatra, A., Harris, M.A., LeVine, D., Ghimire, M., Jennings, J.A., Morshed, B.I., Haggard, W.O., Bumgardner, J.D., Mishra, S.R., Fujiwara, T., 2018. Magnetic stimulus responsive vancomycin drug delivery system based on chitosan microbeads embedded with magnetic nanoparticles. J Biomed Mater Res B Appl Biomater 106 (6), 2169–2176. https://doi.org/10.1002/jbm.b.3401.

Montali, A., Berini, F., Brivio, M.F., Mastore, M., Saviane, A., Cappellozza, S., Marinelli, F., Tettamanti, G., 2020. A silkworm infection model for in vivo study of glycopeptide antibiotics. Antibiotics. 9, 300. https://doi.org/10.3390/antibiotics9060300.

Mora-Ochomogo, M., Lohans, C.T., 2021. β-Lactam antibiotic targets and resistance mechanisms: from covalent inhibitors to substrates. RSC Med. Chem. 12 (10), 1623–1639. https://doi.org/10.1039/d1md00200g.

Murei, A., Ayinde, W.B., Gitari, M.W., Samie, A., 2020. Functionalization and antimicrobial evaluation of ampicillin, penicillin and vancomycin with *Pyrenacantha grandiflora* Baill and silver nanoparticles. Sci. Rep. 10 (1), 11596. https://doi.org/10.1038/s41598-020-68290-x.

Naskar, A., Kim, K.S., 2019. Nanomaterials as delivery vehicles and components of new strategies to combat bacterial infections: advantages and limitations. Microorganisms. 7 (9), 356. https://doi.org/10.3390/microorganisms7090356.

Naskar, S., Kuotsu, K., Sharma, S., 2019. Chitosan-based nanoparticles as drug delivery systems: a review on two decades of research. J. Drug Target. 27 (4), 379–393. https://doi.org/10.1080/1061186X.2018.1512112.

Nguyen, T.T., Dung Nguyen, T.T., Vo, T.K., Tran, N.M., Nguyen, M.K., Van Vo, T., Van Vo, G., 2021. Nanotechnology-based drug delivery for central nervous system disorders. Biomed. Pharmacother. 143, 112117 https://doi.org/10.1016/j.biopha.2021.112117.

Niño-Martínez, N., Salas Orozco, M.F., Martínez-Castañón, G.A., Torres Méndez, F., Ruiz, F., 2019. Molecular mechanisms of bacterial resistance to metal and metal oxide nanoparticles. Int. J. Mol. Sci. 20, 2808. https://doi.org/10.3390/ijms20112808.

Nori, P., Cowman, K., Chen, V., Bartash, R., Szymczak, W., Madaline, T., Punjabi Katiyar, C., Jain, R., Aldrich, M., Weston, G., Gialanella, P., Corpuz, M., Gendlina, I., Guo, Y., 2021. Bacterial and fungal coinfections in COVID-19 patients hospitalized during the New York City pandemic surge. Infect. Control Hosp. Epidemiol. 42 (1), 84–88. https://doi.org/10.1017/ice.2020.368.

Okkeh, M., Bloise, N., Restivo, E., De Vita, L., Pallavicini, P., Visai, L., 2021. Gold nanoparticles: can they be the next magic bullet for multidrug-resistant bacteria? Nanomaterials (Basel). 11 (2), 312. https://doi.org/10.3390/nano11020312.

Omolo, C.A., Kalhapure, R.S., Agrawal, N., Jadhav, M., Rambharose, S., Mocktar, C., Govender, T., 2018. A hybrid of mPEG-b-PCL and G1-PEA dendrimer for enhancing delivery of antibiotics. J. Control. Release 290, 112–128. https://doi.org/10.1016/j.jconrel.2018.10.005.

Ortiz-Benítez, E.A., Velázquez-Guadarrama, N., Durán Figueroa, N.V., Quezada, H., Olivares-Trejo, J.J., 2019. Antibacterial mechanism of gold nanoparticles on *Streptococcus pneumoniae*. Metallomics 11 (7), 1265–1276. https://doi.org/10.1039/c9mt00084d.

Osorio, C., Garzón, L., Jaimes, D., Silva, E., Bustos, R.H., 2021. Impact on antibiotic resistance, therapeutic success, and control of side effects in therapeutic drug monitoring (TDM) of daptomycin: a scoping review. Antibiotics (Basel) 10 (3), 263. https://doi.org/10.3390/antibiotics10030263.

Parent, M., Magnaudeix, A., Delebassée, S., Sarre, E., Champion, E., Viana Trecant, M., Damia, C., 2016. Hydroxyapatite microporous bioceramics as vancomycin reservoir: antibacterial efficiency and biocompatibility investigation. J. Biomater. Appl. 31 (4), 488–498. https://doi.org/10.1177/0885328216653108.

Patra, J.K., Das, G., Fraceto, L.F., Ramos Campos, E.V., Rodriguez-Torres, M.P., Diaz-Torres, L.A., Grillo, R., Kumara Swamy, M., Sharma, S., Habtemariam, S., Shin, H.S., 2018. Nano based drug delivery systems: recent developments and future prospects. J. Nanobiotechnol. 16, 71. https://doi.org/10.1186/s12951-018-0392-8.

Pawar, V., Topkar, H., Srivastava, R., 2018. Chitosan nanoparticles and povidone iodine containing alginate gel for prevention and treatment of orthopedic implant associated infections. Int. J. Biol. Macromol. 115, 1131–1141. https://doi.org/10.1016/j.ijbiomac.2018.04.166.

Pei, Y., Mohamed, M.F., Seleem, M.N., Yeo, Y., 2017. Particle engineering for intracellular delivery of vancomycin to methicillin-resistant *Staphylococcus aureus* (MRSA)-infected macrophages. J. Control. Release 267, 133–143. https://doi.org/10.1016/j.jconrel.2017.08.007.

Pem, B., González-Mancebo, D., Moros, M., Ocaña, M., Becerro, A.I., Pavičić, I., Selmani, A., Babič, M., Horák, D., Vinković Vrček, I., 2018. Biocompatibility assessment of up-and down-converting nanoparticles: implications of interferences with in vitro assays. Methods Appl. Fluoresc. 7 (1), 1–15. https://doi.org/10.1088/2050-6120/aae9c8.

Perreault, F., de Faria, A.F., Nejati, S., Elimelech, M., 2015. Antimicrobial properties of graphene oxide nanosheets: why size matters. ACS Nano 9 (7), 7226–7236. https://doi.org/10.1021/acsnano.5b02067.

Petrarca, C., Clemente, E., Di Giampaolo, L., Mariani-Costantini, R., Leopold, K., Schindl, R., Lotti, L.V., Mangifesta, R., Sabbioni, E., Niu, Q., Bernardini, G., Di Gioacchino, M., 2014. Palladium nanoparticles induce disturbances in cell cycle entry and progression of peripheral blood mononuclear cells: paramount role of ions. J Immunol Res 2014, 295092. https://doi.org/10.1155/2014/295092.

Petrarca, C., Clemente, E., Amato, V., Pedata, P., Sabbioni, E., Bernardini, G., Iavicoli, I., Cortese, S., Niu, Q., Otsuki, T., Paganelli, R., Di Gioacchino, M., 2015. Engineered metal based nanoparticles and innate immunity. Clin. Mol. Allergy. 13 (1), 13. https://doi.org/10.1186/s12948-015-0020-1.

Pfalzgraff, A., Brandenburg, K., Weindl, G., 2018. Antimicrobial peptides and their therapeutic potential for bacterial skin infections and wounds. Front. Pharmacol. 9, 281. https://doi.org/10.3389/fphar.2018.00281.

Piacenza, E., Presentato, A., Zonaro, E., Lemire, J.A., Demeter, M., Vallini, G., Turner, R. J., Lampis, S., 2017. Antimicrobial activity of biogenically produced spherical Se-nanomaterials embedded in organic material against *Pseudomonas aeruginosa* and *Staphylococcus aureus* strains on hydroxyapatite-coated surfaces. Microb. Biotechnol. 10 (4), 804–818. https://doi.org/10.1111/1751-7915.

Piacenza, E., Presentato, A., Zonaro, E., Lampis, S., Vallini, G., Turner, R., 2018a. Selenium and tellurium nanomaterials. Phys. Sci. Rev. 3 (5), 20170100. https://doi.org/10.1515/psr-2017-0100.

Piacenza, E., Presentato, A., Turner, R.J., 2018b. Stability of biogenic metal(loid) nanomaterials related to the colloidal stabilization theory of chemical nanostructures. Crit. Rev. Biotechnol. 38 (8), 1137–1156. https://doi.org/10.1080/07388551.2018.1440525.

Pichavant, L., Carrié, H., Nguyen, M.N., Plawinski, L., Durrieu, M.C., Héroguez, V., 2016. Vancomycin functionalized nanoparticles for bactericidal biomaterial surfaces. Biomacromolecules. 17 (4), 1339–1346. https://doi.org/10.1021/acs.biomac.5b01727.

Pokropivny, V.V., Skorokhod, V.V., 2007. Classification of nanostructures by dimensionality and concept of surface forms engineering in nanomaterial science. Mater. Sci. Eng. C 27 (5-8), 990–993. https://doi.org/10.1016/j.msec.2006.09.023.

Pormohammad, A., Monych, N.K., Ghosh, S., Turner, D.L., Turner, R.J., 2021. Nanomaterials in wound healing and infection control. Antibiotics (Basel) 10 (5), 473. https://doi.org/10.3390/antibiotics10050473.

Posadowska, U., Brzychczy-Wloch, M., Pamula, E., 2016. Injectable gellan gum-based nanoparticles-loaded system for the local delivery of vancomycin in osteomyelitis treatment. J. Mater. Sci. Mater. Med. 27 (1), 9. https://doi.org/10.1007/s10856-015-5604-2.

Pourtalebi Jahromi, L., Ghazali, M., Ashrafi, H., Azadi, A., 2020. A comparison of models for the analysis of the kinetics of drug release from PLGA-based nanoparticles. Heliyon 6 (2), e03451. https://doi.org/10.1016/j.heliyon.2020.e03451.

Randall, C.P., Gupta, A., Jackson, N., Busse, D., O'neill, A.J., 2015. Silver resistance in Gram-negative bacteria: a dissection of endogenous and exogenous mechanisms. J. Antimicrob. Chemother. 70, 1037–1046. https://doi.org/10.1093/jac/dku523.

Rao, K., Young, V.B., 2015. Fecal microbiota transplantation for the management of *Clostridium difficile* infection. Infect. Dis. Clin. N. Am. 29 (1), 109–122. https://doi.org/10.1016/j.idc.2014.11.009.

Regiel-Futyra, A., Kus-Liśkiewicz, M., Sebastian, V., Irusta, S., Arruebo, M., Stochel, G., Kyzioł, A., 2015. Development of noncytotoxic chitosan-gold nanocomposites as efficient antibacterial materials. ACS Appl. Mater. Interfaces 7 (2), 1087–1099. https://doi.org/10.1021/am508094e.

Renwick, M., Mossialos, E., 2018. What are the economic barriers of antibiotics R&D and how we can overcome them? Expert Opin. Drug Discovery 13, 889–892. https://doi.org/10.1080/17460441.2018.1515908.

Robertson, J., Vlahović-Palčevski, V., Iwamoto, K., Högberg, L.D., Godman, B., Monnet, D.L., Garner, S., Weist, K., ESAC-Net Study Group, WHO Europe AMC Network Study Group, 2021. Variations in the consumption of antimicrobial medicines in the European region, 2014-2018: findings and implications from ESAC-net and WHO Europe. Front. Pharmacol. 12, 639207 https://doi.org/10.3389/fphar.2021.639207.

Romero-Vargas Castrillón, S., Perreault, F., Fonseca de Faria, A., Elimelech, M., 2015. Interaction of graphene oxide with bacterial cell membranes: insights from force spectroscopy. Environ. Sci. Technol. 2 (4), 112–117. https://doi.org/10.1021/acs.estlett.5b00066.

Sabbioni, E., Fortaner, S., Farina, M., Del Torchio, R., Olivato, I., Petrarca, C., Bernardini, G., Mariani-Costantini, R., Perconti, S., Di Giampaolo, L., Gornati, R., Di Gioacchino, M., 2014. Cytotoxicity and morphological transforming potential of cobalt nanoparticles, microparticles and ions in Balb/3T3 mouse fibroblasts: an in vitro model. Nanotoxicology. 8 (4), 455–464. https://doi.org/10.3109/17435390.2013.796538.

Sader, H.S., Flamm, R.K., Jones, R.N., 2013. Antimicrobial activity of daptomycin tested against Gram-positive pathogens collected in Europe, Latin America, and selected countries in the Asia-Pacific Region (2011). Diagn. Microbiol. Infect. Dis. 75 (4), 417–422. https://doi.org/10.1016/j.diagmicrobio.2013.01.001.

Safir, M.C., Bhavnani, S.M., Slover, C.M., Ambrose, P.G., Rubino, C.M., 2020. Antibacterial drug development: a new approach is needed for the field to survive and thrive. Antibiotics (Basel). 9 (7), 412. https://doi.org/10.3390/antibiotics9070412.

Saidykhan, L., Abu Bakar, M.Z., Rukayadi, Y., Kura, A.U., Latifah, S.Y., 2016. Development of nanoantibiotic delivery system using cockle shell-derived aragonite nanoparticles for treatment of osteomyelitis. Int. J. Nanomedicine 11, 661–673. https://doi.org/10.2147/IJN.S95885.

Salih, M., Omolo, C.A., Agrawal, N., Walvekar, P., Waddad, A.Y., Mocktar, C., Ramdhin, C., Govender, T., 2020. Supramolecular amphiphiles of Beta-cyclodextrin and Oleylamine for enhancement of vancomycin delivery. Int. J. Pharm. 574, 118881 https://doi.org/10.1016/j.ijpharm.2019.118881.

Salleh, A., Naomi, R., Utami, N.D., Mohammad, A.W., Mahmoudi, E., Mustafa, N., Fauzi, M.B., 2020. The potential of silver nanoparticles for antiviral and antibacterial applications: a mechanism of action. Nanomaterials (Basel) 10 (8), 1566. https://doi.org/10.3390/nano10081566.

Sánchez-López, E., Gomes, D., Esteruelas, G., Bonilla, L., Lopez-Machado, A.L., Galindo, R., Cano, A., Espina, M., Ettcheto, M., Camins, A., Silva, A.M., Durazzo, A., Santini, A., Garcia, M.L., Souto, E.B., 2020. Metal-based nanoparticles as antimicrobial agents: an overview. Nanomaterials (Basel). 10 (2), 292. https://doi.org/10.3390/nano10020292.

Sarkar, N., Sahoo, G., Das, R., Prusty, G., Swain, S.K., 2017. Carbon quantum dot tailored calcium alginate hydrogel for pH responsive controlled delivery of vancomycin. Eur. J. Pharm. Sci. 109, 359–371. https://doi.org/10.1016/j.ejps.2017.08.015.

Seedat, N., Kalhapure, R.S., Mocktar, C., Vepuri, S., Jadhav, M., Soliman, M., Govender, T., 2016. Co-encapsulation of multi-lipids and polymers enhances the performance of vancomycin in lipid-polymer hybrid nanoparticles: in vitro and in silico studies. Mater. Sci. Eng. C Mater. Biol. Appl. 61, 616–630. https://doi.org/10.1016/j.msec.2015.12.053.

Seitkalieva, M.M., Samoylenko, D.E., Lotsman, K.A., Rodygin, K.S., Ananikov, V.P., 2021. Metal nanoparticles in ionic liquids: synthesis and catalytic applications. Coord. Chem. Rev. 445, 213982 https://doi.org/10.1016/j.ccr.2021.213982.

Serri, A., Mahboubi, A., Zarghi, A., Moghimi, H.R., 2018. PAMAM-dendrimer enhanced antibacterial effect of vancomycin hydrochloride against Gram-negative bacteria. J. Pharm. Pharm. Sci. 22 (1), 10–21. https://doi.org/10.18433/jpps29659.

Shafique, M., Luo, X., 2019. Nanotechnology in transportation vehicles: an overview of its applications, environmental, health and safety concerns. Materials (Basel). 12 (15), 2493. https://doi.org/10.3390/ma12152493.

Shah, S., Gaikwad, S., Nagar, S., Kulshrestha, S., Vaidya, V., Nawani, N., Pawar, S., 2019. Biofilm inhibition and anti-quorum sensing activity of phytosynthesized silver nanoparticles against the nosocomial pathogen *Pseudomonas aeruginosa*. Biofouling 35 (1), 34–49. https://doi.org/10.1080/08927014.2018.1563686.

Sharipova, A., Swain, S.K., Gotman, I., Starosvetsky, D., Psakhie, S.G., Unger, R., Gutmanas, E.Y., 2018. Mechanical, degradation and drug-release behavior of nano-grained Fe-Ag composites for biomedical applications. J. Mech. Behav. Biomed. Mater. 86, 240–249. https://doi.org/10.1016/j.jmbbm.2018.06.037.

Shimizu, N., Otsuka, K., Sawada, H., Maejima, T., Shirotake, S., 2014. Bacteriolysis by vancomycin-conjugated acryl nanoparticles and morphological component analysis. Drug Dev. Ind. Pharm. 40 (6), 813–818. https://doi.org/10.3109/03639045.2013.788012.

Shkodenko, L., Kassirov, I., Koshel, E., 2020. Metal oxide nanoparticles against bacterial biofilms: perspectives and limitations. Microorganisms. 8 (10), 1545. https://doi.org/10.3390/microorganisms8101545.

Shvedova, A., Pietroiusti, A., Kagan, V., 2016. Nanotoxicology ten years later: lights and shadows. Toxicol. Appl. Pharmacol. 299, 1–2. https://doi.org/10.1016/j.taap.2016.02.014.

Sikwal, D.R., Kalhapure, R.S., Rambharose, S., Vepuri, S., Soliman, M., Mocktar, C., Govender, T., 2016. Polyelectrolyte complex of vancomycin as a nanoantibiotic: preparation, in vitro and in silico studies. Mater. Sci. Eng. C Mater. Biol. Appl. 63, 489–498. https://doi.org/10.1016/j.msec.2016.03.019.

Silva, N.C., Silva, S., Sarmento, B., Pintado, M., 2015. Chitosan nanoparticles for daptomycin delivery in ocular treatment of bacterial endophthalmitis. Drug Deliv. 22 (7), 885–893. https://doi.org/10.3109/10717544.2013.858195.

Simon, A., Moreira, M.L.A., Costa, I.F.J.B., de Sousa, V.P., Rodrigues, C.R., da Rocha, E., Lima, L.M.T., Sisnande, T., do Carmo, F.A., Leal, I.C.R., Dos Santos, K.R.N., da Silva, L.C.R.P., Cabral, L.M., 2020. Vancomycin-loaded nanoparticles against vancomycin intermediate and methicillin resistant *Staphylococcus aureus* strains. Nanotechnology. 31 (37), 375101 https://doi.org/10.1088/1361-6528/ab97d7.

Siriam, A., Kalanxhi, E., Kapoor, G., Craig, J., Balasubramanian, R., Brar, S., Criscuolo, N., Hamilton, A., Klein, E., Tseng, K., Van Boeckel, T., Laxminarayan, R., 2021. State of the world's antibiotics 2021: A global analysis of antimicrobial resistance and its drivers. https://cddep.org/wp-content/uploads/2021/02/The-State-of-the-Worlds-Antibiotics-in-2021.pdf (last accessed on 24th June 2021).

Sonawane, S.J., Kalhapure, R.S., Rambharose, S., Mocktar, C., Vepuri, S.B., Soliman, M., Govender, T., 2016. Ultra-small lipid-dendrimer hybrid nanoparticles as a promising strategy for antibiotic delivery: in vitro and in silico studies. Int. J. Pharm. 504 (1-2), 1–10. https://doi.org/10.1016/j.ijpharm.2016.03.021.

Sonawane, S.J., Kalhapure, R.S., Jadhav, M., Rambharose, S., Mocktar, C., Govender, T., 2020. AB2-type amphiphilic block copolymer containing a pH-cleavable hydrazone linkage for targeted antibiotic delivery. Int. J. Pharm. 575, 118948 https://doi.org/10.1016/j.ijpharm.2019.118948.

Stogios, P.J., Savchenko, A., 2020. Molecular mechanisms of vancomycin resistance. Protein Sci. 29, 654–669. https://doi.org/10.1002/pro.3819.

Suchý, T., Šupová, M., Klapková, E., Horný, L., Rýglová, Š., Žaloudková, M., Braun, M., Sucharda, Z., Ballay, R., Veselý, J., Chlup, H., Denk, F., 2016. The sustainable release of vancomycin and its degradation products from nanostructured collagen/hydroxyapatite composite layers. J. Pharm. Sci. 105 (3), 1288–1294. https://doi.org/10.1016/S0022-3549(15)00175-6.

Suchý, T., Šupová, M., Klapková, E., Adamková, V., Závora, J., Žaloudková, M., Rýglová, Š., Ballay, R., Denk, F., Pokorný, M., Sauerová, P., Hubálek Kalbáčová, M., Horný, L., Veselý, J., Voňavková, T., Průša, R., 2017. The release kinetics, antimicrobial activity and cytocompatibility of differently prepared collagen/hydroxyapatite/vancomycin layers: microstructure vs. nanostructure. Eur. J. Pharm. Sci. 100, 219–229. https://doi.org/10.1016/j.ejps.2017.01.032.

Suchý, T., Šupová, M., Sauerová, P., Hubálek Kalbáčová, M., Klapková, E., Pokorný, M., Horný, L., Závora, J., Ballay, R., Denk, F., Sojka, M., Vištejnová, L., 2019. Evaluation of collagen/hydroxyapatite electrospun layers loaded with vancomycin, gentamicin and their combination: comparison of release kinetics, antimicrobial activity and cytocompatibility. Eur. J. Pharm. Biopharm. 140, 50–59. https://doi.org/10.1016/j.ejpb.2019.04.021.

Sun, F., Oh, S., Kim, J., Kato, T., Kim, H.J., Lee, J., Park, E.Y., 2017. Enhanced internalization of macromolecular drugs into *Mycobacterium smegmatis* with the assistance of silver nanoparticles. J. Microbiol. Biotechnol. 27 (8), 1483–1490. https://doi.org/10.4014/jmb.1612.12041.

Tacconelli, E., Carrara, E., Savoldi, A., Harbarth, S., Mendelson, M., Monnet, D.L., Pulcini, C., Kahlmeter, G., Kluytmans, J., Carmeli, Y., Ouellette, M., Outterson, K., Patel, J., Cavaleri, M., Cox, E.M., Houchens, C.R., Grayson, M.L., Hansen, P., Singh, N., Theuretzbacher, U., Magrini, N., WHO Pathogens Priority List Working Group, 2018. WHO pathogens priority list working group. Discovery, research, and development of new antibiotics: the WHO priority list of antibiotic-resistant bacteria and tuberculosis. Lancet Infect. Dis. 18 (3), 318–327. https://doi.org/10.1016/S1473-3099(17)30753-3.

Tao, J., Zhang, Y., Shen, A., Yang, Y., Diao, L., Wang, L., Cai, D., Hu, Y., 2020. Injectable chitosan-based thermosensitive hydrogel/nanoparticle-loaded system for local delivery of vancomycin in the treatment of osteomyelitis. Int. J. Nanomedicine 15, 5855–5871. https://doi.org/10.2147/IJN.S247088.

Tawade, B.V., Apata, I.E., Pradhan, N., Karim, A., Raghavan, D., 2021. Recent advances in the synthesis of polymer-grafted low-K and high-K nanoparticles for dielectric and electronic applications. Molecules. 26 (10), 2942. https://doi.org/10.3390/molecules26102942.

Tirumala, M.G., Anchi, P., Raja, S., Rachamalla, M., Godugu, C., 2021. Novel methods and approaches for safety evaluation of nanoparticle formulations: a focus towards in vitro models and adverse outcome pathways. Front. Pharmacol. 12, 612659 https://doi.org/10.3389/fphar.2021.612659.

Tong, C., Li, L., Xiao, F., Fan, J., Zhong, X., Liu, X., Liu, B., Wu, Z., Zhou, J., 2019. Daptomycin and AgNP co-loaded rGO nanocomposites for specific treatment of Gram-positive bacterial infection in vitro and in vivo. Biomater. Sci. 7 (12), 5097–5111. https://doi.org/10.1039/C9BM01229J.

Troisi, M., Andreano, E., Sala, C., Kabanova, A., Rappuoli, R., 2020. Vaccines as remedy for antimicrobial resistance and emerging infections. Curr. Opin. Immunol. 65, 102–106. https://doi.org/10.1016/j.coi.2020.09.003.

Turner, R.J., 2017. Metal-based antimicrobial strategies. Microb. Biotechnol. 10 (5), 1062–1065. https://doi.org/10.1111/1751-7915.12785.

Ucak, S., Sudagidan, M., Borsa, B.A., Mansuroglu, B., Ozalp, V.C., 2020. Inhibitory effects of aptamer targeted teicoplanin encapsulated PLGA nanoparticles for *Staphylococcus aureus* strains. World J. Microbiol. Biotechnol. 36, 69. https://doi.org/10.1007/s11274-020-02845-y.

Uhl, P., Pantze, S., Storck, P., Parmentier, J., Witzigmann, D., Hofhaus, G., Huwyler, J., Mier, W., Fricker, G., 2017. Oral delivery of vancomycin by tetraether lipid liposomes. Eur. J. Pharm. Sci. 108, 111–118. https://doi.org/10.1016/j.ejps.2017.07.013.

Valdez-Salas, B., Beltran-Partida, E., Cheng, N., Salvador-Carlos, J., Valdez-Salas, E.A., Curiel-Alvarez, M., Ibarra-Wiley, R., 2021. Promotion of surgical masks antimicrobial activity by disinfection and impregnation with disinfectant silver nanoparticles. Int. J. Nanomedicine 16, 2689–2702. https://doi.org/10.2147/IJN.S301212.

Van Bambeke, F., 2015. Lipoglycopeptide antibacterial agents in Gram-positive infections: a comparative review. Drugs. 75 (18), 2073–2095. https://doi.org/10.1007/s40265-015-0505-8.

Van Giau, V., An, S.S.A., Hulme, J., 2019. Recent advances in the treatment of pathogenic infections using antibiotics and nano-drug delivery vehicles. Drug. Des. Devel. Ther. 13, 327–343. https://doi.org/10.2147/DDDT.S190577.

Vasileiadis, S., Puglisi, E., Trevisan, M., Scheckel, K.G., Langdon, K.A., McLaughlin, M.J., Lombi, E., Donner, E., 2015. Changes in soil bacterial communities and diversity in response to long-term silver exposure. FEMS Microbiol. 91 (10), fiv114. https://doi.org/10.1093/femsec/fiv114.

Vrancianu, C.O., Gheorghe, I., Dobre, E.G., Barbu, I.C., Cristian, R.E., Popa, M., Lee, S.H., Limban, C., Vlad, I.M., Chifiriuc, M.C., 2020. Emerging strategies to combat β-lactamase producing ESKAPE pathogens. Int. J. Mol. Sci. 21 (22), 8527. https://doi.org/10.3390/ijms21228527.

Vranic, S., Shimada, Y., Ichihara, S., Kimata, M., Wu, W., Tanaka, T., Boland, S., Tran, L., Ichihara, G., 2019. Toxicological evaluation of SiO_2 nanoparticles by zebrafish embryo toxicity test. Int. J. Mol. Sci. 20 (4), 882. https://doi.org/10.3390/ijms20040882.

Wan, Y., Zhang, D., Wang, Y., Qi, P., Wu, J., Hou, B., 2011. Vancomycin-functionalised Ag@TiO_2 phototoxicity for bacteria. J. Hazard. Mater. 186 (1), 306–312. https://doi.org/10.1016/j.jhazmat.2010.10.110.

Wang, C., Zhang, K., Zhou, Z., Li, Q., Shao, L., Hao, R.Z., Xiao, R., Wang, S., 2017a. Vancomycin-modified Fe_3O_4@SiO_2@Ag microflowers as effective antimicrobial agents. Int. J. Nanomedicine 12, 3077–3094. https://doi.org/10.2147/IJN.S132570.

Wang, L., Hu, C., Shao, L., 2017b. The antimicrobial activity of nanoparticles: present situation and prospects for the future. Int. J. Nanomedicine 12, 1227–1249. https://doi.org/10.2147/IJN.S121956.

Wang, S.G., Chen, Y.C., Chen, Y.C., 2018. Antibacterial gold nanoparticle-based photothermal killing of vancomycin-resistant bacteria. Nanomedicine (London) 13 (12), 1405–1416. https://doi.org/10.2217/nnm-2017-0380.

Wang, H., Song, Z., Li, S., Wu, Y., Han, H., 2019. One stone with two birds: functional gold nanostar for targeted combination therapy of drug-resistant *Staphylococcus aureus* infection. ACS Appl. Mater. Interfaces 11 (36), 32659–32669. https://doi.org/10.1021/acsami.9b09824.

Wang, J., Zhang, J., Liu, K., He, J., Zhang, Y., Chen, S., Ma, G., Cui, Y., Wang, L., Gao, D., 2020a. Synthesis of gold nanoflowers stabilized with amphiphilic daptomycin for enhanced photothermal antitumor and antibacterial effects. Int. J. Pharm. 580, 119231 https://doi.org/10.1016/j.ijpharm.2020.119231.

Wang, S., Gao, Y., Jin, Q., Ji, J., 2020b. Emerging antibacterial nanomedicine for enhances antibiotic therapy. Biomater. Sci. 8, 6825–6839. https://doi.org/10.1039/D0BM00974A.

World Health Organization, 2015. Global action plan on antimicrobial resistance. https://www.who.int/publications/i/item/9789241509763 (last accessed on 19th January 2022).

World Health Organization, 2019a. Critically Important Antimicrobials for Human Medicine (WHO CIA List), 6th revision. https://www.who.int/publications/i/item/9789241515528 (last accessed on 24th June 2021).

World Health Organization, 2019b. Model list of essential medicines, 21st list 2019. https://www.who.int/publications/i/item/WHOMVPEMPIAU2019.06 (last accessed on 24th June 2021).

Xiang, Y., Li, J., Liu, X., Cui, Z., Yang, X., Yeung, K.W.K., Pan, H., Wu, S., 2017. Construction of poly(lactic-co-glycolic acid)/ZnO nanorods/Ag nanoparticles hybrid coating on Ti implants for enhanced antibacterial activity and biocompatibility. Mater. Sci. Eng. C Mater. Biol. Appl. 79, 629–637. https://doi.org/10.1016/j.msec.2017.05.115.

Xiang, Y., Liu, X., Mao, C., Liu, X., Cui, Z., Yang, X., Yeung, K.W.K., Zheng, Y., Wu, S., 2018. Infection-prevention on Ti implants by controlled drug release from folic acid/ZnO quantum dots sealed titania nanotubes. Mater. Sci. Eng. C Mater. Biol. Appl. 85, 214–224. https://doi.org/10.1016/j.msec.2017.12.034.

Xie, X., Mao, C., Liu, X., Tan, L., Cui, Z., Yang, X., Zhu, S., Li, Z., Yuan, X., Zheng, Y., Wai, K., Yeung, K., Chu, P.K., Wu, S., 2018. Tuning the bandgap of photo-sensitive polydopamine/Ag_3PO_4/graphene oxide coating for rapid, noninvasive disinfection of implants. ACS Cent. Sci. 4, 724–738. https://doi.org/10.1021/acscentsci.8b00177.

Xu, M., Hu, Y., Xiao, Y., Zhang, Y., Sun, K., Wu, T., Lv, N., Wang, W., Ding, W., Li, F., Qiu, B., Li, J., 2020. Near-infrared-controlled nanoplatform exploiting photothermal promotion of peroxidase-like and OXD-like activities for potent antibacterial and anti-biofilm therapies. ACS Appl. Mater. Interfaces 12 (45), 50260–50274. https://doi.org/10.1021/acsami.0c14451.

Yan, Z., Shi, P., Ren, J., Qu, X., 2015. A "sense-and-treat" hydrogel used for treatment of bacterial infection on the solid matrix. Small. 11 (41), 5540–5541. https://doi.org/10.1002/smll.201501958.

Yang, Z., Wang, Y., Zhang, D., 2017. A novel multifunctional electrochemical platform for simultaneous detection, elimination, and inactivation of pathogenic bacteria based on the Vancomycin-functionalised AgNPs/3D-ZnO nanorod arrays. Biosens. Bioelectron. 98, 248–253. https://doi.org/10.1016/j.bios.2017.06.058.

Yim, G., Thaker, M.N., Koteva, K., Wright, G., 2014. Glycopeptide antibiotic biosynthesis. J. Antibiot. (Tokyo). 67 (1), 31–41. https://doi.org/10.1038/ja.2013.117.

Yousry, C., Fahmy, R.H., Essam, T., El-Laithy, H.M., Elkheshen, S.A., 2016. Nanoparticles as tool for enhanced ophthalmic delivery of vancomycin: a multidistrict-based microbiological study, solid lipid nanoparticles formulation and evaluation. Drug Dev. Ind. Pharm. 42 (11), 1752–1762. https://doi.org/10.3109/03639045.2016.1171335.

Yousry, C., Elkheshen, S.A., El-Laithy, H.M., Essam, T., Fahmy, R.H., 2017. Studying the influence of formulation and process variables on Vancomycin-loaded polymeric nanoparticles as potential carrier for enhanced ophthalmic delivery. Eur. J. Pharm. Sci. 100, 142–154. https://doi.org/10.1016/j.ejps.2017.01.013.

Yu, J., Chu, X., Cai, Y., Tong, P., Yao, J., 2014. Preparation and characterization of antimicrobial nano-hydroxyapatite composites. Mater. Sci. Eng. C Mater. Biol. Appl. 37, 54–59. https://doi.org/10.1016/j.msec.2013.12.038.

Yu, C.H., Chen, G.Y., Xia, M.Y., Xie, Y., Chi, Y.Q., He, Z.Y., Zhang, C.L., Zhang, T., Chen, Q.M., Peng, Q., 2020. Understanding the sheet size-antibacterial activity relationship of graphene oxide and the nano-bio interaction-based physical mechanisms. Colloids Surf. B: Biointerfaces 191, 111009. https://doi.org/10.1016/j.colsurfb.2020.111009.

Yushchuk, O., Ostash, B., Truman, A.W., Marinelli, F., Fedorenko, V., 2020a. Teicoplanin biosynthesis: unravelling the interplay of structural, regulatory, and resistance genes. Appl. Microbiol. Biotechnol. 104 (8), 3279–3291. https://doi.org/10.1007/s00253-020-10436-y.

Yushchuk, O., Binda, E., Marinelli, F., 2020b. Glycopeptide antibiotic resistance denes: distribution and function in the producer actinomycetes. Front. Microbiol. 11, 1173. https://doi.org/10.3389/fmicb.2020.01173.

Zakeri-Milani, P., Loveymi, B.D., Jelvehgari, M., Valizadeh, H., 2013. The characteristics and improved intestinal permeability of vancomycin PLGA-nanoparticles as colloidal drug delivery system. Colloids Surf. B: Biointerfaces 103, 174–181. https://doi.org/10.1016/j.colsurfb.2012.10.021.

Zhang, Y., Liang, R.J., Xu, J.J., Shen, L.F., Gao, J.Q., Wang, X.P., Wang, N.N., Shou, D., Hu, Y., 2017. Efficient induction of antimicrobial activity with vancomycin nanoparticle-loaded poly(trimethylene carbonate) localized drug delivery system. Int. J. Nanomedicine 12, 1201–1214. https://doi.org/10.2147/IJN.S127715.

Zhang, X., Song, J., Klymov, A., Zhang, Y., de Boer, L., Jansen, J.A., van den Beucken, J. J., Yang, F., Zaat, S.A., Leeuwenburgh, S.C., 2018. Monitoring local delivery of vancomycin from gelatin nanospheres in zebrafish larvae. Int. J. Nanomedicine 13, 5377–5394. https://doi.org/10.2147/IJN.S168959.

Zhang, W., Taheri-Ledari, R., Hajizadeh, Z., Zolfaghari, E., Ahghari, M.R., Maleki, A., Hamblin, M.R., Tian, Y., 2020. Enhanced activity of vancomycin by encapsulation in hybrid magnetic nanoparticles conjugated to a cell-penetrating peptide. Nanoscale. 12 (6), 3855–3870. https://doi.org/10.1039/C9NR09687F.

Zhao, Y., Tian, Y., Cui, Y., Liu, W., Ma, W., Jiang, X., 2010. Small molecule-capped gold nanoparticles as potent antibacterial agents that target Gram-negative bacteria. J. Am. Chem. Soc. 132 (35), 12349–12356. https://doi.org/10.1021/ja1028843.

Zhao, Z., Yan, R., Yi, X., Li, J., Rao, J., Guo, Z., Yang, Y., Li, W., Li, Y.Q., Chen, C., 2017. Bacteria-activated theranostic nanoprobes against methicillin-resistant *Staphylococcus aureus* infection. ACS Nano 11 (5), 4428–4438. https://doi.org/10.1021/acsnano.7b00041.

Zheng, K., Setyawati, M.I., Lim, T.P., Leong, D.T., Xie, J., 2016. Antimicrobial cluster bombs: silver nanoclusters packed with daptomycin. ACS Nano 10 (8), 7934–7942. https://doi.org/10.1021/acsnano.6b03862.

Zheng, K., Setyawati, M.I., Leong, D.T., Xie, J., 2017. Antimicrobial gold nanoclusters. ACS Nano 11 (7), 6904–6910. https://doi.org/10.1021/acsnano.7b02035.

Zheng, Y., Liu, W., Chen, Y., Li, C., Jiang, H., Wang, X., 2019. Conjugating gold nanoclusters and antimicrobial peptides: from aggregation-induced emission to antibacterial synergy. J. Colloid Interface Sci. 546, 1–10. https://doi.org/10.1016/j.jcis.2019.03.052.

Zhou, Z., Peng, S., Sui, M., Chen, S., Huang, L., Xu, H., Jiang, T., 2018. Multifunctional nanocomplex for surface-enhanced Raman scattering imaging and near-infrared photodynamic antimicrobial therapy of vancomycin-resistant bacteria. Colloids Surf. B: Biointerfaces 161, 394–402. https://doi.org/10.1016/j.colsurfb.2017.11.005.

Ziglam, H.M., Finch, R.G., 2001. Limitations of presently available glycopeptides in the treatment of Gram-positive infection. Clin. Microbiol. Infect. 4, 53–65. https://doi.org/10.1046/j.1469-0691.2001.00059.x.

Zou, Z., Sun, J., Li, Q., Pu, Y., Liu, J., Sun, R., Wang, L., Jiang, T., 2020. Vancomycin modified copper sulfide nanoparticles for photokilling of vancomycin-resistant enterococci bacteria. Colloids Surf. B: Biointerfaces 189, 110875. https://doi.org/10.1016/j.colsurfb.2020.110875.

Zurawski, D.V., McLendon, M.K., 2020. Monoclonal antibodies as an antibacterial approach against bacterial pathogens. Antibiotics. 9 (4), 155. https://doi.org/10.3390/antibiotics9040155.